

**BACK-CALCULATING EMISSION RATES FOR
AMMONIA AND PARTICULATE MATTER FROM AREA
SOURCES USING DISPERSION MODELING**

A Thesis

by

JACQUELINE ELAINE PRICE

Submitted to the Office of Graduate Studies of
Texas A&M University
in partial fulfillment of the requirements for the degree of

MASTER OF SCIENCE

August 2004

Major Subject: Biological and Agricultural Engineering

**BACK-CALCULATING EMISSION RATES FOR
AMMONIA AND PARTICULATE MATTER FROM AREA
SOURCES USING DISPERSION MODELING**

A Thesis

by

JACQUELINE ELAINE PRICE

Submitted to Texas A&M University
in partial fulfillment of the requirements
for the degree of

MASTER OF SCIENCE

Approved as to style and content by:

Ronald E. Lacey
(Chair of Committee)

N. Andy Cole
(Member)

Bryan W. Shaw
(Member)

Gerald Riskowski
(Head of Department)

August 2004

Major Subject: Biological and Agricultural Engineering

ABSTRACT

Back-Calculating Emission Rates for Ammonia and Particulate Matter from Area Sources Using Dispersion Modeling. (August 2004)

Jacqueline Elaine Price, B.S., Texas A&M University

Chair of Advisory Committee: Dr. Ronald E. Lacey

Engineering directly impacts current and future regulatory policy decisions. The foundation of air pollution control and air pollution dispersion modeling lies in the math, chemistry, and physics of the environment. Therefore, regulatory decision making must rely upon sound science and engineering as the core of appropriate policy making (objective analysis in lieu of subjective opinion).

This research evaluated particulate matter and ammonia concentration data as well as two modeling methods, a backward Lagrangian stochastic model and a Gaussian plume dispersion model. This analysis assessed the uncertainty surrounding each sampling procedure in order to gain a better understanding of the uncertainty in the final emission rate calculation (a basis for federal regulation), and it assessed the differences between emission rates generated using two different dispersion models.

First, this research evaluated the uncertainty encompassing the gravimetric sampling of particulate matter and the passive ammonia sampling technique at an animal feeding operation. Future research will be to further determine the wind velocity profile as well

as determining the vertical temperature gradient during the modeling time period. This information will help quantify the uncertainty of the meteorological model inputs into the dispersion model, which will aid in understanding the propagated uncertainty in the dispersion modeling outputs.

Next, an evaluation of the emission rates generated by both the Industrial Source Complex (Gaussian) model and the WindTrax (backward-Lagrangian stochastic) model revealed that the calculated emission concentrations from each model using the average emission rate generated by the model are extremely close in value. However, the average emission rates calculated by the models vary by a factor of 10. This is extremely troubling.

In conclusion, current and future sources are regulated based on emission rate data from previous time periods. Emission factors are published for regulation of various sources, and these emission factors are derived based upon back-calculated model emission rates and site management practices. Thus, this factor of 10 ratio in the emission rates could prove troubling in terms of regulation if the model that the emission rate is back-calculated from is not used as the model to predict a future downwind pollutant concentration.

I dedicate this thesis to my family, my future husband Durward and his family, and my close friends. The love and support that each of you provides continue to encourage me to always strive to do my best each and every day.

ACKNOWLEDGMENTS

I would like to thank my committee members for providing me guidance throughout the past couple of years, while allowing me to venture into a new area beyond your initial knowledge base. Dr. Lacey, Dr. Shaw, and Dr. Cole, it has been such a pleasure working with you, and I look forward to many more opportunities in the future! Dr. Lacey, in particular, thank you for giving me an opportunity to work with you and the CAAQES crew. It has been such a pleasure!

I would also like to thank the rest of the “Air Crew”. You all have made even the most frustrating times, the most pleasant. You definitely know how to make me laugh! I will never forget our crazy times in the office, lunches, sampling trip *adventures*, and conference presentations (we even went out of the country!). In particular, I would like to thank Dr. Parnell, Ling, John, Cale, and Barry. There is no way I would have ever finished without each of you. God bless you all in all that you do! I know that each of you guys will have such a positive impact on agricultural air quality. I would also like to thank Josh and Cassie for bringing me into the department and showing me how we can impact the University in all that we do.

I would like to thank Dr. Riskowski for his continued support of my research, education, and service to the University. Furthermore, I would like to thank the staff: Violet, Susie, Leo, David, Sonia, Jeana, Lisa, Amy, and Paula. You all are an amazing bunch!

Finally, I would like to extend a huge thanks to my family and friends. To my parents, Martha and J.B. You both have been a living example to me by showing me that you can do anything that you want to, as long as you put your mind to it. I know that I have said it before, but thank you for showing me how to fly! To my brother, Johnny. You are awesome! You have always been my sidekick, and it has been great getting to spend another couple of years in the same town together. To my future husband, Durward. You never cease to make me smile, and you have always been there for me the past 5 years. It is your encouragement and prayers each and every day that have continued to support me in all that I do. To my close friends through the years. You all have always been there for me through it all – the calm and the crazy times! I cannot thank any of you enough. You have shown me the true value of a friendship. To my softball/church/choir buds. Thanks for keeping me sane throughout these past two years of graduate school. You guys have shown me not only the value of a friend as well, but also faith in action. To the Christ UMC youth. You guys are the most amazing young people that I have ever met! Thank you for the last couple of years. Continue to strive for the truth in all that you do!

TABLE OF CONTENTS

	Page
ABSTRACT	iii
DEDICATION	v
ACKNOWLEDGMENTS	vi
TABLE OF CONTENTS	viii
LIST OF FIGURES	x
LIST OF TABLES	xii
CHAPTER	
I INTRODUCTION	1
II RESEARCH OBJECTIVES	4
III LITERATURE REVIEW	5
Regulatory Policy	5
Particulate Matter	9
Ammonia	11
Analysis of Uncertainty	14
Wind Speed and Wind Direction Variability	16
Air Pollution Dispersion Modeling	17
Gaussian Dispersion Modeling	18
Backward Lagrangian Stochastic (bLS) Modeling	19
IV ANALYSIS OF UNCERTAINTY	26
Primary Systematic Uncertainty Determination	26
Uncertainty Propagation Calculation	27
Particulate Matter – Results and Discussion	29
Sensitivity Coefficient Determination	33
Sensitivity & Uncertainty Analysis	35
Ammonia – Uncertainty Discussion	45
V WIND VELOCITY UNCERTAINTY	49

CHAPTER	Page
VI DISPERSION MODELING	53
Receptor Layouts	54
Model Inputs Defined	55
Gaussian Plume Dispersion Modeling	57
Backward Lagrangian Stochastic (bLS) Model	61
Pre-modeling Tests	62
Determination of the Area Emission Rate	64
Model Output Discussion	76
VII CONCLUSIONS AND FUTURE RESEARCH	79
REFERENCES	83
Supplemental Sources Consulted	89
APPENDIX A	90
APPENDIX B	99
APPENDIX C	114
APPENDIX D	118
APPENDIX E	122
APPENDIX F	134
VITA	146

LIST OF FIGURES

FIGURE	Page
3.1 Illustration of Total Error, δ	15
4.1 Determining the Uncertainty for an Experiment	27
4.2 Breakdown of Gravimetric Sampling Equations	30
4.3 TAMU – $Q \approx 0.000278 \text{ m}^3\text{s}^{-1}$ (0.6 cfm) – Uncertainty Analysis	38
4.4 TAMU – $Q \approx 0.0184 \text{ m}^3\text{s}^{-1}$ (39 cfm) – Uncertainty Analysis	39
4.5 TAMU – $Q \approx 0.0236 \text{ m}^3\text{s}^{-1}$ (50 cfm) – Uncertainty Analysis	40
4.6 TAMU – $Q \approx 0.0283 \text{ m}^3\text{s}^{-1}$ (60 cfm) – Uncertainty Analysis	41
4.7 High Volume Sampling Setup	42
4.8 Low Volume Sampling Setup	42
4.9 UC Davis Passive Ammonia Sampler	45
5.1 Tower with Co-located Anemometers and Receptors	50
5.2 Measured Wind Speed as a Function of Time at Various Heights	51
6.1 Ammonia Passive Sampler Feedyard Layout	54
6.2 ISC Layout Screen Shot	58
6.3 WindTrax Toolbar	66
6.4 Project Tower Screen Shot	67
6.5 Input Data Screen Shot	68
6.6 Input Data File Screen Shot	69
6.7 Screen Shot of the BLS Prior to Running the Model	70
6.8 Examples of the BLS Model During 2 Different Runs	72

FIGURE	Page
B.1 Ammonia Diagrams	100
B.2 Ammonia Volatilization Equilibria	105
B.3 Graphical Representation of the NO_x/NH_3 Problem near Los Angeles	111

LIST OF TABLES

TABLE		Page
4.1	Instrument Specifications for Gravimetric PM Sampling	34
4.2	Total Uncertainty for Gravimetric Sampling	43
4.3	Gravimetric Sensitivity Analysis for Uncertainty Propagation.....	44
6.1	SRDT Method for Estimating Stability Class	56
6.2	Average Calculated Emission Rates Using ISC-ST3	60
6.3	Average Calculated Emission Rates Using WindTrax	75
6.4	Overall Comparison of Summary Model Outputs	77
B.1	Relative Contribution of Ammonia Sources	103

CHAPTER I

INTRODUCTION

As part of the Clean Air Act Amendments in July, 1970, the White House and Congress established the Environmental Protection Agency (EPA) in response to the growing public demand for cleaner water, air and land (Sullivan, 2001). The Clean Air Act and the subsequent amendments assigned the Environmental Protection Agency the responsibility of formulating environmental rules and regulations (refer to 40 Code of Federal Regulations (CFR) Parts 50, 51, 53, 55, 60, 61, 63, 70, and 71). These delegated rulemaking activities include developing health based air quality standards (the National Ambient Air Quality Standards (NAAQS)) for criteria pollutants, creating Maximum Achievable Control Technologies (MACTs) for hazardous air pollutants from major pollution sources, and developing New Source Performance Standards (NSPSs) for facilities that contribute significantly to air pollution in a continued effort to protect the public health, the public welfare, and the environment (40 CFR Part 50, 51, 53, 55, 60, 61, 63, 70, 71). While the EPA establishes these minimum national air quality standards, states are delegated the responsibility of ensuring stationary source compliance with these standards. States can implement standards that are stricter than the federal standards, but they cannot implement less stringent standards.

This thesis follows the style and format of the *Transactions of the ASAE*.

Engineering directly impacts these current and future regulatory policy decisions. Literature defines engineering as the application of science to determine the most economical and feasible solution to a problem impacting the public (Parnell, 2000). The foundation of air pollution control and air pollution dispersion lies in the math, chemistry, and physics of the environment. Furthermore, regulatory decision making depends on this science put into practical application, which precisely defines engineering. Therefore, as an engineer, it is crucial to understand how data affect the environment as well as the industry in the surrounding world. Any engineer directly or indirectly working on projects relating to the regulation of air pollution must have a working knowledge of the regulatory process in terms of air pollution along with an understanding of recent air pollution litigation decisions. Environmental regulatory decisions depend upon sound science and engineering practice (Parnell, 2000).

Numerous groups impact the regulation of air pollution including regulated industries, regulating agencies (the EPA as well as State Air Pollution Regulatory Agencies), scientists, engineers, the public, and special interest groups. However, regulatory decision making must rely upon sound science and engineering as the core of appropriate policy making (objective analysis in lieu of subjective opinion). Some stakeholder groups attempt to make public statements based upon poor science and engineering in order to manipulate public opinion and bias current and future air pollution regulatory decisions. The regulatory agencies have to continue to keep their goals in sight: to protect the public health and welfare in the most economically feasible

way. The only way to accomplish this is to rely upon the expertise of engineers, who apply sound science, while considering feasibility, when engaging in regulatory policy actions.

This research focuses on the emission rate determination procedure used in the permitting and regulation of facilities under the Clean Air Act. Using gathered pollutant concentration data, a defined mathematical model (dispersion modeling) can be used to back-calculate the emission rate of a pollutant from a given source. Using this generated source pollutant emission rate and the meteorological conditions, future estimates of pollutant concentrations downwind of a source can be predicted. These modeled downwind concentrations are the basis for which these facilities are regulated.

Additionally, this research specifically evaluates particulate matter and ammonia concentration data as well as two modeling methods, a backward Lagrangian stochastic model and a Gaussian plume dispersion model. This analysis evaluates the uncertainty surrounding each sampling procedure in order to gain a better understanding of the uncertainty in the final emission rate calculation (a basis for federal regulation), and it assesses the differences between emission rates generated using two different dispersion models.

CHAPTER II

RESEARCH OBJECTIVES

This research seeks to gain a better understanding of the uncertainty in the output of dispersion modeling and the uncertainty inherent in the model inputs. Thus, the three main objectives directly relate to the fundamental issue of agricultural air quality policy formation and regulation:

1. Determine the uncertainty surrounding the wet chemistry measurement of ammonia (NH_3) concentration and the gravimetric measurement of particulate matter (PM) concentration and identify the most critical measurements and their implications on the calibration, operation, and design of these NH_3 and PM samplers using a sensitivity analysis.
2. Evaluate the wind speed profile at a confined animal feeding operation site during multiple periods of particulate matter concentration sampling.
3. Compare the back-calculated NH_3 emission rates resulting from two different dispersion models (Gaussian Model and Backward Lagrangian Stochastic Model) used for predicting the downwind concentration of NH_3 from a confined animal feeding operation.

CHAPTER III

LITERATURE REVIEW

Currently, all industries, including agricultural operations, must come into compliance with the regulatory health-based standards known as the National Ambient Air Quality Standards (NAAQS). Uncertainty surrounds the measurement of these constituents as well as the development of the standards, and this uncertainty has a direct impact on agency policies and procedures to enforce these standards. Thus, quantifying measurement uncertainty is crucial in understanding the reliability of pollutant concentration measurements for the purpose of air quality regulation. With an understanding of measurement uncertainty in the quantification of emissions, a better estimate of the level of compliance of a source can be obtained.

Regulatory Policy

Pollutant emission rate determination is the fundamental basis of regulatory air quality management. Emission rates are expressed as a mass emitted per unit time and serves as the foundation for the determination of emission factors for a specific source. These emission factors depend upon the physical conditions of the source as well as the conditions of the specific operation. The emission rates, and subsequent determined emission factors, provide the foundation for the permitting and control programs at federal, state, and local levels; the development of abatement strategies; and the

determination of the effects of pollutants and strategies for mitigating these effects (Lacey et al., 2002). The EPA provides a specific definition for an emission factor in the *Compilation of Air Pollutant Emission Factors, AP-42* and the *Supplement* to this work (US EPA, 1995; US EPA, 2000b):

An emission factor is a representative value that attempts to relate the quantity of a pollutant released to the atmosphere with an activity associated with the release of that pollutant. These factors are usually expressed as the weight of pollutant divided by a unit weight, volume, distance, or duration of the activity emitting the pollutant (e. g., kilograms of particulate emitted per megagram of coal burned). Such factors facilitate estimation of emissions from various sources of air pollution. In most cases, these factors are simply averages of all available data of acceptable quality, and are generally assumed to be representative of long-term averages for all facilities in the source category (i.e., a population average).

Particulate matter is regulated as part of the NAAQS under the Clean Air Act and subsequent Clean Air Act Amendments. Currently, ammonia (NH_3) is not regulated under this same act, but it is regulated under the Comprehensive Environmental Response, Compensation and Liability Act (also known as CERCLA). Passed in 1980, this federal act gave the EPA authority to directly respond to any hazardous substance releases that could endanger the public health, public welfare, or the environment.

The EPA must review the scientific data upon which these standards are based and amend these standards every five years, if necessary. Typically, the EPA exceeds this five year mark for review and revision (Sullivan, 2001). In addition, the EPA is responsible for designating non-attainment areas where air quality standards have not been met, as defined in Title 1 § 107(d)(1)(A)(i) of the Clean Air Act. An area is in *non-attainment* if it does not meet the primary or secondary ambient air quality standards for a pollutant or multiple pollutants. An area can also be classified as *non-attainment* if it contributes to the failure of another area to meet the primary or secondary ambient air quality standards. Additionally, the EPA is responsible for overseeing the state air pollution regulation as well as approving the State Implementation Plans (SIPs) submitted by State Air Pollution Regulatory Agencies (SAPRAs). This advisory position over SAPRAs is enforced through judicial action if necessary.

Thus, states are delegated the responsibility of ensuring stationary source compliance with the standards set by the EPA. State legislatures delegate state regulatory authority to their respective SAPRA, and, in turn, these SAPRAs create rules and regulations, as well as permit and enforce permitted facilities (Schoenbaum et al., 2002). States are required to create and submit SIPs to attain and maintain the standards set by the EPA (Sullivan, 2001). Failing to create a SIP could result in a state's loss of federal highway funds and/or local control of the regulatory process. SIPs must be revised to comply with federal regulatory changes and technical advancements, and they must contain imposable emission limitations, control measures (including economic incentives), and

schedules for compliance. Additionally, SAPRAs are in charge of permitting facilities (preconstruction and Title V operating permits) and bringing administrative enforcement actions against violators.

SIPs contain implementation plans that consist of preconstruction permits and operating permits (Title V). The preconstruction permit requirement applies to all major new sources and major modifications of an existing source (Schoenbaum et al., 2002). Part of the preconstruction permit is the Prevention of Significant Deterioration (PSD) of air quality in regions where the NAAQS have been met with additional provisions for non-attainment areas. Currently, only major sources, which are generally large industrial sources, are required to have a Title V permit as further discussed in the Code of Federal Regulation (40 CFR Parts 70 and 71). A major source is defined as a source emitting more than 100 tons per year of any pollutant (Title V thresholds) in an attainment area (40 CFR Part 70, 1999; 40 CFR Part 71, 1996). In a non-attainment area, PM₁₀ has a threshold of only 70 tons per year. However, in places of extreme non-attainment, the PM₁₀ threshold can be as low as 10 tons per year (Schoenbaum et al., 2002).

Major sources, as defined by EPA regulations, pay an annual permit fee based on total emissions of regulated pollutants, which is determined using dispersion modeling.

Permits contain information such as emission limitations and standards enforceable by the SAPRA, a compliance schedule, and requirements for reporting emissions. These permits can act as a shield for the permitted source because of the assumption that

facilities in compliance with the permit are essentially in compliance with the applicable provisions of the Clean Air Act.

Thus, engineering and scientific input is extremely important in ensuring that applicable data is used during the permitting process. The degree of uncertainty in the data is critical because these data are the basis for comparison for regulation. Permit exceedances result in fines on the violating company/person. Fees incurred by this Title V permitting procedure and fines from exceedances fund environmental activities of the state and federal governments.

Particulate Matter

The US EPA established these ambient air standards for certain pollutants seen as harmful to public health and the environment as required by the Clean Air Act. The NAAQS include primary and secondary standards for six criteria pollutants: Ozone (O₃), Particulate Matter (PM), Carbon Monoxide (CO), Sulfur Dioxide (SO₂), Nitrogen Oxides (NO_x), and Lead (Pb). These standards are ambient standards based off potential health effects to human exposure (primary standards) as well as the protection of human welfare and the environment (secondary standards such as visibility, crops, animals, and buildings). Consequently, the EPA regulates based upon these ambient air standards.

Gravimetric measurement of particulate matter (PM) concentration in ambient environments is the basis for regulation of PM fractions under the Clean Air Act. Currently, concentrations of pollutants are measured at the property line and compared to the NAAQS for regulation. However, the property line does not necessarily represent ambient conditions, and the NAAQS were not intended to be regulatory law but health based standards. Additionally, ambient conditions include emissions as a whole, so as to not distinguish between sources of the pollutant. Models link emissions with ambient pollutant concentrations. An understanding of the transport and modeling of pollutants, such as PM and Ammonia, and the inherent error is essential for appropriate regulatory decisions and determination of source compliance with the law.

Particulate matter emissions have been extensively researched (Goodrich et al., 2003; Wanjura et al., 2003; Puxbaum et al., 1993). This research lays the foundation for understanding the dispersion of other species. PM is typically fairly unreactive in the atmosphere (compared to gaseous emissions), so chemical reaction components of transport processes can be reasonably ignored. Thus, PM is one of the more simplified species modeled for regulatory purposes, and an understanding of the transport and modeling of PM can provide a foundation for understand the transport of more complex aerosol processes.

Ammonia

Ammonia (NH_3) emissions serve as crucial elements of atmospheric models because ammonia is one of the most prevalent gaseous bases found in the planetary boundary layer (PBL). Ammonia concentrations affect the overall acidity of precipitation, cloud water, and atmospheric aerosols (Aneja et al., 2001). Typically, ammonia reacts with acidic species to form ammonium sulfate ($(\text{NH}_4)_2\text{SO}_4$), ammonium nitrate (NH_4NO_3), ammonium chloride (NH_4Cl), ammonium and the hydroxyl radical (NH_4^+ and OH^-), or it may be deposited to the earth's surface by either dry or wet deposition processes (Seinfeld and Pandis, 1998).

Ammonia atmospheric aerosols have the attention of the EPA and other regulatory agencies because these aerosols are thought to comprise a large part of secondary $\text{PM}_{2.5}$, which is a classification for particulate matter with an aerodynamic equivalent diameter less than or equal to a nominal $2.5 \mu\text{m}$ (Makar et al., 2003; Gupta et al., 2003; Aneja et al., 2001; Yamamoto et al., 1998; Battye et al., 1994). Secondary pollutants result from the chemical reaction among two or more pollutants. Researchers have shown that a large percentage of $\text{PM}_{2.5}$ penetrates human respiratory systems and deposits in the lungs and alveolar region, subsequently endangering the public health (Hinds, 1999; Aneja et al., 2001). Additionally, these atmospheric aerosols have the potential to significantly influence global warming and ozone depletion and to cause major environmental damage when redeposited on land and water (MAFF, 1998).

Currently, neither the EPA nor the Texas Commission of Environmental Quality (TCEQ) regulates ammonia as a criteria pollutant. However, ammonia concentration levels are monitored by Effects Screening Levels (ESLs). If airborne ammonia concentration ESLs are not exceeded, then negative health effects and/or welfare effects would not be anticipated (TNRCC, 2001). However, ammonia emissions are now being considered as an air quality concern. Literature notes that agricultural operations account for a considerable amount of the anthropogenic ammonia emitted (Battye et al., 1994; Aneja et al., 2003; Arogo et al., 2001). Subsequently, ammonia emissions from agricultural operations have drawn attention from the regulators and the agricultural industry as well as the general public outside of the agricultural industry. An understanding of the transport and modeling of NH_3 and the inherent error surrounding the modeling process is essential for appropriate regulatory decisions and determination of source compliance with future regulatory policy.

Approximately 80% of Ammonia emissions result from nitrogen emissions from certain farm animals, such as cattle, calves, poultry, hogs, and pigs. These animals ingest a large amount of nitrogen containing substances in their feed. This intake subsequently produces ammonia through the bacterial activity involving their excreted organic nitrogen substrates (Arogo et al., 2001). Ammonia emissions are sensitive to fluctuations in factors such as the diet of the animals, atmospheric temperature and humidity, waste-handling practices, wind speed, and other source and surface

characteristics. Because of the many uncertainties surrounding these factors, obtaining accurate ammonia emissions estimates becomes quite challenging (Aneja et al., 2003).

An important component to understanding the impact of ammonia atmospheric aerosols is understanding the volatilization of ammonia and the chemical reactions of ammonia and other species in the atmosphere. Typically, ammonia reacts with acidic species to form ammonium sulfate ((NH₄)₂SO₄), ammonium nitrate (NH₄NO₃), ammonium chloride (NH₄Cl), ammonium and the hydroxyl radical (NH₄⁺ and OH⁻), and specifics concerning the properties, sources, and potential impact of ammonia emissions is continued in Appendix B.

In order to determine ESL exceedances, ammonia emissions must be quantified appropriately. Gas sampling from an industrial process can be easily performed by directly sampling from the stack exhaust. However, it is much more challenging to quantify gaseous emissions from an area source. One option is to utilize atmospheric dispersion modeling to back-calculate pollutant emission rates indirectly. Literature notes that the backward modeling approach offers a lot in terms of ease of calculations, efficiency, and flexibility (Flesch et al., 1995).

Analysis of Uncertainty

A measurement of a variable can only provide a deterministic estimate of the quantity being measured; thus, it can only be considered complete when supplemented by a quantitative statement of the inaccuracies surrounding the measurement. Therefore, proper experimental planning and design requires an understanding of the errors inherent in these measurements so that the experimenter can have some degree of certainty in the final measurements and calculations. While these PM and NH₃ measurements seem straightforward, uncertainty will affect the data, resulting in a larger uncertainty in the resulting concentration calculation.

Uncertainty can be defined as the statistical representation of the reliability associated with a specific set of measurements (Yegnan et al., 2002). Uncertainty can also be described as the possible set of values on a given measurement and can be considered a statistical variable (Kline, 1985). The term *error* takes on a slightly different definition. *Total error*, δ , is the difference between the measured value and the true value of the quantity being measured. It can also be thought of as the sum of the *systematic error* and the *random error*, $\delta = \beta + \epsilon$, where β is the systematic error and ϵ is the random error (ANSI/ASME, 1998). This is illustrated by Figure 3.1.

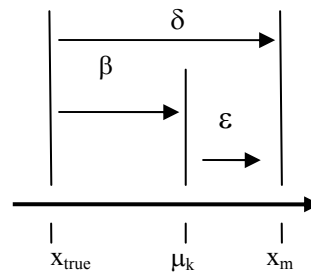


Figure 3.1. Illustration of Total Error, δ

Systematic error, β , also known as fixed error or bias, is defined as the constant element of the total error, δ ; therefore, this value remains constant for each measurement.

Random error, ϵ , also known as repeatability error, precision error, or uncertainty, is the random element of the total error. Each measurement takes on a different value for this part of the total error measurement (ANSI/ASME, 1998). Thus, the term error refers to the sum of a fixed quantity and a variable quantity and cannot be considered a statistical variable.

Many of the current methods of estimating the uncertainty surrounding experimental results are based upon an analysis by Kline and McClintock (1953). With the goal in mind of determining the effect of each potential measurement error, they proposed a process which considers the impact of these individual uncertainties, commonly referred to as the propagation of uncertainty (Kline and McClintock, 1953). This process involves a first or second order Taylor series approximation to estimate the uncertainty in various circumstances. In general, a first order analysis process, as defined later in the

Chapter IV of this thesis, is sufficient to quantify uncertainty. Each uncertainty from the individual independent variables propagate through a data reduction equation into a resulting overall estimate of uncertainty (Coleman & Steele, 1999).

Wind Speed and Wind Direction Variability

Accurate meteorological data is essential for valid dispersion modeling estimates to be made. These data include wind speed, wind direction, solar radiation, and ambient air temperature measurements at various time intervals at the same site where concentration data have been taken or where concentration data will be predicted. These data define the atmospheric stability class and directly impact concentration values at established or modeled receptors (US EPA, 2000a). Instantaneous wind velocity measurements are not used in the dispersion modeling process, but regulatory agencies require one hour vector averages of the wind speed and wind direction for the modeled period of time. Thus, because of continuously changing wind conditions, there is variation inherent in the wind profile measurements used to calculate hourly vector averages for use in dispersion modeling.

There has been some research done within the Center for Agricultural Air Quality Engineering and Science on the variability of the wind speed and direction at a single height (Fritz, 2002). However, while on sampling trips, researchers have noticed an extreme particulate matter peak in the evening hours around 2200. This has perplexed

researchers and various hypotheses have been formed as to why this phenomena occurs. One hypothesis has to do with the reduction of wind speed during the late evening hours with the possibility of an evening low inversion. Thus, there has been a keen interest in collecting data on the wind speed and direction profile co-located with total suspended particulate matter samplers on a tower located downwind from an emitting source in order to estimate the wind velocity profile at the sampling location.

Air Pollution Dispersion Modeling

Modeling of air pollutants plays an important role in the regulatory process by mathematically and scientifically describing the causal relationship between pollutant emissions and corresponding atmospheric concentrations (Bultjes, 2003). Dispersion models provide a means to mathematically simulate the transport of gases and particles through the atmosphere. Estimates of pollutant concentrations downwind of a source can be established from the pollutant emission rate and the meteorological conditions using a defined mathematical model. Part of the state regulatory process consists of a preconstruction permit, which includes demonstrating compliance with air quality standards for all regulated pollutants. Dispersion modeling provides a scientific method for the regulatory agency to measure air quality compliance of a future source (one that has not been constructed). Additionally, dispersion modeling can be utilized to quantify the impact of the change in an abatement strategy of an existing source (Bultjes, 2003).

Gaussian Dispersion Modeling

Currently, the EPA has approved Industrial Source Complex – Short Term 3 (ISC-ST3) as the short range dispersion model used to model low level sources, such as animal feeding operations (40 CFR part 51, 1999). This model is based on a double reflected Gaussian dispersion model, which describes the horizontal and vertical concentration distributions with the assumptions of continuous emissions, conservation of mass, steady-state conditions, and normal distribution of crosswind and vertical concentrations of pollutants (Cooper and Alley, 2002). The Gaussian dispersion model utilizes the experimentally determined Pasquill-Gifford horizontal and vertical plume spread parameters, σ_y and σ_z as seen in equation 3.1 below.

$$C_{10} = \frac{Q}{2\pi u \sigma_y \sigma_z} \exp\left(-\frac{1}{2} \frac{y^2}{\sigma_y^2}\right) \left\{ \exp\left(-\frac{1}{2} \frac{(z-H)^2}{\sigma_z^2}\right) + \exp\left(-\frac{1}{2} \frac{(z+H)^2}{\sigma_z^2}\right) \right\} \quad (3.1)$$

where C_{10} is the 10 minute concentration ($\mu\text{g}/\text{m}^3$), Q is the emission rate ($\mu\text{g}/\text{s}$), u is the one hour average wind speed at stack height (m/s), y is the horizontal distance from the centerline of the plume (m), z is the height of the receptor with respect to the ground level (m), and H is the effective stack height (m) (Cooper and Alley, 2002). Using measured concentration values as well as meteorological data from the concentration sampling period, a pollutant emission rate can be back-calculated through equation 3.1.

Literature notes that there are at least three situations in which atmospheric behavior is poorly modeled by Gaussian modeling (Trinity Consultants, 2000). First, surface releases are a challenge because single wind speed and published dispersion parameters cannot accurately simulate the rapid changes in wind speed and turbulent eddy sizes. Next, atmospheric behavior is not accurately represented when horizontal and vertical dispersion independence exists. Finally, in an unstable atmosphere (convective conditions), a non-Gaussian vertical distribution of concentration results from a few updrafts of significant magnitude and number of smaller downdrafts, causing one of the model assumptions to be invalid.

Backward Lagrangian Stochastic (bLS) Modeling

Lagrangian stochastic (LS) models, also known as random-flight models, determine particle trajectories in attempt to imitate turbulent dispersion. By simulating individual parcels of air, the LS model predicts the path followed by each parcel to reach a receptor (Seinfeld and Pandis, 1998).

The bLS model is based on the forward LS model, which is the generalized Langevin equation under the assumption that the position of a particle evolves jointly as a Markov process with the velocity (Flesch et al., 1995). This model by Flesch, which is simulated by the WindTrax software, accounts for the location of particle impact with the ground and the subsequent reflection of these particles back into the atmosphere.

The model uses this information to define the ratio of the modeled concentration to the emission rate $(C/Q)_{sim}$ as seen in equation 3.2 below (Flesch et al., 2004a).

$$(C/Q)_{sim} = \frac{1}{N} \sum \left| \frac{2}{w_0} \right| \quad (3.2)$$

where N is the number of particles and w_0 are the vertical touchdown velocities at the particle's impact with the ground. The bLS model requires the specification of wind statistics for the surface layer. These can be calculated using established Monin-Obukhov similarity theory (MOST) based formulas (Flesch et al., 2004a). The MOST approach asserts that the average gradient and turbulent features of a stratified surface layer only rely upon the height, the kinematic heat flux, the buoyancy variable, and the kinematic surface stress (Arya, 2001).

The bLS approach is based on simulating atmospheric diffusion at a specific location, and its validity hinges upon the fundamental diffusion and subsequent Lagrangian models. The air parcels simulated by the Lagrangian model are vertical columns of air that extend from the ground up to some height H (Seinfeld and Pandis, 1998). An underlying assumption in the Lagrangian trajectory model is that, when applied to reacting species, it is only applicable to linearly reactive species (Lamb and Seinfeld, 1973). An additional underlying assumption is that the chemical reactions that occur are independent of particle displacement and are not determined by the frequency of the

collisions of particles (Lamb and Seinfeld, 1973). First the three-dimensional wind field, which is defined by $u_x(x, y, z)$, $u_y(x, y, z)$, and $u_z(x, y, z)$, is used to calculate the backward trajectories of the air parcels from equation 3.3 (Seinfeld and Pandis, 1998):

$$\frac{d\bar{s}(t)}{dt} = \bar{u}(t) \quad (3.3)$$

where the location of the air parcel at time t is $\bar{s}(t)$ and $\bar{u}(t)$ is the wind velocity vector (defined by u_x, u_y, u_z). If this equation is integrated from t to t_o , then the location of the air parcel at any given time t on the backward trajectory of the particle, which is defined by $\bar{s}(t)$, can be calculated straightforwardly as:

$$\bar{s}_0 - \bar{s}(t) = \int_t^{t_o} \bar{u}(\tau) d\tau \quad (3.4)$$

assuming that at a time t_o the trajectory ends at the location \bar{s}_0 . Following the calculation of the trajectory path $\bar{s}(t)$, corresponding emission fluxes can be determined by interpolating the emission field $E(x, y, z, t)$ and defining flux along the trajectory path, $E_t(t)$ as (Seinfeld and Pandis, 1998):

$$E_t(t) = E(\bar{s}(t), t) \quad (3.5)$$

The basic diffusion equation is built upon the basic continuity assumption

$$\begin{aligned}
 & \frac{\partial c_i}{\partial t} + u_x \frac{\partial c_i}{\partial x} + u_y \frac{\partial c_i}{\partial y} + u_z \frac{\partial c_i}{\partial z} \\
 &= \frac{\partial}{\partial x} \left(K_{xx} \frac{\partial c_i}{\partial x} \right) + \frac{\partial}{\partial y} \left(K_{yy} \frac{\partial c_i}{\partial y} \right) + \frac{\partial}{\partial z} \left(K_{zz} \frac{\partial c_i}{\partial z} \right) \\
 &+ R_i(c_1, c_2, \dots, c_n) + E_i(x, y, z, t) - S_i(x, y, z, t)
 \end{aligned} \tag{3.6}$$

for $i = 1, 2, \dots, N$, where c_i denotes the theoretical mean concentration of species i , K represents the corresponding eddy diffusivity components, R_i is the chemical generation of species i , E_i describes the emission flux, S_i is the removal flux, and u represents the mean value for each of the wind velocity components. Equation 3.6 can be simplified to correspond to a coordinate system that moves horizontally with velocities equal to the wind speed. Thus, the particle moves at a velocity equal to that of the wind speed, and no material exchange exists between the parcel and its surroundings by advection (Seinfeld and Pandis, 1998). Thus, the diffusion equation can be simplified to

$$\begin{aligned}
 \frac{\partial c_i}{\partial t} + u_z \frac{\partial c_i}{\partial z} &= \frac{\partial}{\partial x} \left(K_{xx} \frac{\partial c_i}{\partial x} \right) + \frac{\partial}{\partial y} \left(K_{yy} \frac{\partial c_i}{\partial y} \right) + \frac{\partial}{\partial z} \left(K_{zz} \frac{\partial c_i}{\partial z} \right) \\
 &+ R_i(c_1, c_2, \dots, c_n) + E_{t,i}(t) - S_i(t)
 \end{aligned} \tag{3.7}$$

The diffusion equation can be further simplified in the local model by comparing the vertical advective transport, which is described by the term $u_z \frac{\partial c_i}{\partial z}$, to the vertical turbulent dispersion, which is described by the term $\frac{\partial}{\partial z} \left(K_{zz} \frac{\partial c_i}{\partial z} \right)$ in the diffusion equation (Seinfeld and Pandis, 1998). This assumption can be written as:

$$\left| u_z \frac{\partial c_i}{\partial z} \right| \ll \frac{\partial}{\partial z} \left(K_{zz} \frac{\partial c_i}{\partial z} \right) \quad (3.8)$$

Thus, the $u_z \frac{\partial c_i}{\partial z}$ term can be neglected in the diffusion equation. Next, assuming that horizontal concentration gradients contribute negligibly to the overall mass balance of the system, the horizontal turbulent dispersion terms can be neglected (Seinfeld and Pandis, 1998). Note, this assumption contributes a very small error in an area with homogenous emissions (uniform emission across the source); however, the error from this assumption becomes quite important in an area dominated by a few strong point sources (Seinfeld and Pandis, 1998). These two assumptions can be stated as:

$$\frac{\partial}{\partial x} \left(K_{xx} \frac{\partial c_i}{\partial x} \right) \cong 0, \quad \frac{\partial}{\partial z} \left(K_{zz} \frac{\partial c_i}{\partial z} \right) \cong 0 \quad (3.9)$$

The third, and final, simplifying assumption to the diffusion equation is to neglect the wind shear. The Lagrangian model assumes that the air column being modeled remains intact during transport, thus assuming that

$$u_x(x, y, z, t) \cong u_x(x, y, t) \quad (3.10)$$

and

$$u_x(x, y, z, t) \cong u_x(x, y, t) \quad (3.11)$$

Literature notes that this assumption is critical to the validity of the trajectory model (Liu and Seinfeld, 1975). Additionally, literature notes that this provides a major source of error in some of the trajectory model calculations, in particular those models that utilize long transport times.

With these three assumptions, the one dimensional Lagrangian trajectory model, a simplification of the initial diffusion equations, can be written as

$$\frac{\partial c_i}{\partial t} = \frac{\partial}{\partial z} \left(K_{zz} \frac{\partial c_i}{\partial z} \right) + R_i(c_1, c_2, \dots, c_n) + E_{t,i}(t) - S_i(t) \quad (3.12)$$

Assuming that the source is continuously emitting and homogenous turbulence, a Gaussian plume becomes the solution to the Lagrangian equation. However, even in nonstationary and inhomogenous turbulence, the Gaussian equation can give an estimate of reasonable order of magnitude in practical circumstances (Lamb and Seinfeld, 1973).

The backward – Lagrangian model used by Flesch et al. (2004b) is based on the simplified Lagrangian equation and of assumptions. However, literature from these scientists notes that the backward model accounts for particle reflection from the surface, as does the Gaussian model used in this evaluation, which leads to false particle gradients at the surface (Flesch et al., 1995). To reduce this error potential, the time scale on the model is reduced, thus reducing the maximum source to receptor distance of the model. Research has shown that the backward model is about 50 times faster than the forward LS model when predicting concentrations from a substantial area source at a short range (Flesch et al., 1995). The bLS model utilizes touchdown catalogs to determine the source of the particles arriving to a receptor location.

The touchdown catalogs are independent of the average wind speed and concentration data, so, the model can be initially run without knowledge of the source geometry (Flesch et al., 2004b). Inherent in the bLS model are the same essential assumptions of the LS model: horizontally homogenous flow and a spatially uniform emission rate of the species being modeled (Flesch et al., 2004a).

CHAPTER IV

ANALYSIS OF UNCERTAINTY

The impact of individual uncertainties for each primary measurement in an experiment on the total uncertainty of the experiment must be approximated. This idea is commonly referred to as the law of propagation of uncertainty (ISO, 1995). The uncertainties from the individual independent variables propagate through a data reduction equation resulting in an overall estimate of uncertainty as demonstrated in Figure 4.1 (Coleman and Steele, 1999).

Primary Systematic Uncertainty Determination

Typically, manufacturers specify the accuracy of their respective measurement instrument, and this information is used in this analysis as the value for the uncertainty of the measuring device. This accuracy specification takes into account various factors such as linearity, gain, and zero errors (Coleman & Steele, 1999). All of the uncertainty values used in this discussion except for that of the pressure drop across the orifice meter (ΔP_a) were obtained from specifications on the manufacturers' data sheets.

Uncertainty Propagation Calculation

With the individual uncertainties now determined, the propagated systematic uncertainty can be calculated.

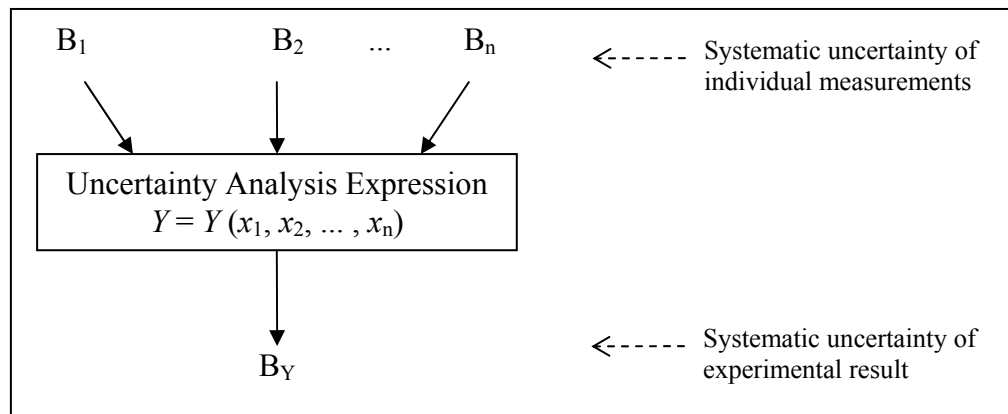


Figure 4.1. Determining the Uncertainty for an Experiment.
(adapted from Coleman and Steele, 1999)

Assuming that all individual uncertainties are at the same confidence level (95% confidence interval or 20:1 odds in this instance), let Y be a function of independent variables $x_1, x_2, x_3, \dots, x_n$. Therefore, the data reduction equation for determining Y from each x_i is

$$Y = Y(x_1, x_2, \dots, x_n) \quad (4.1)$$

Furthermore, let ω be defined as the uncertainty in the result and $\omega_1, \omega_2, \dots, \omega_n$ as the uncertainties in each of the above independent variables. Given the same confidence interval on each of the independent (uncorrelated) variables, the resulting uncertainty of Y , ω_Y , can be calculated as the positive square root of the estimated variance, ω_y^2 , from the following equation (Holman, 2001)

$$\omega_Y = +\sqrt{\omega_y^2} \quad (4.2)$$

where the variance, ω_y^2 , is calculated by

$$\omega_y^2 = \left(\frac{\delta Y}{\delta x_1} \omega_1\right)^2 + \left(\frac{\delta Y}{\delta x_2} \omega_2\right)^2 + \dots + \left(\frac{\delta Y}{\delta x_n} \omega_n\right)^2 \quad (4.3)$$

or

$$\omega_y^2 = (\theta_1 \omega_1)^2 + (\theta_2 \omega_2)^2 + \dots + (\theta_n \omega_n)^2 \quad (4.4)$$

where θ , the *sensitivity coefficient*, is defined as

$$\theta_i = \frac{\delta Y}{\delta x_i} \quad (4.5)$$

Particulate Matter – Results and Discussion

The concentration of particulate matter (PM) in the air can be measured by gravimetric means, where the PM in the air is captured on a filter and then weighed. The process of measuring particulate matter concentration has uncertainty associated with it. Particulate matter concentration is a function of the mass of PM collected in a known volume of air using the equation

$$C = \frac{W}{V} \quad (4.6)$$

where C is the concentration, W is the mass of PM_{10} collected on the filter, and V is the total volume of air through the system during the time of sampling. Both W and V are calculated quantities from other measurements. Therefore, these quantities must be reduced to basic measurements as seen in Figure 4.2 that follows. This analysis evaluates the process of determining the concentration of PM on the filter.

$$\begin{aligned}
 C &= \frac{W}{V} \\
 &\rightarrow W = W_f - W_i \\
 &\rightarrow V = Q * \Theta \\
 &\quad \rightarrow Q = 5.976 * k * (D_0)^2 * \sqrt{\frac{\Delta P_a}{\rho_a}} \\
 &\quad \rightarrow \rho_a = \left[\frac{P_a - RH * P_s}{0.37 * (460 + T)} \right] + \left[\frac{RH * P_s}{0.596 * (460 + T)} \right] \\
 &\quad \rightarrow k = \frac{Q_{LFE}}{5.976 * (D_0)^2 * \sqrt{\frac{\Delta P_c}{\rho_c}}} \\
 &\quad \rightarrow \rho_c = \left[\frac{P_c - RH * P_s}{0.37 * (460 + T)} \right] + \left[\frac{RH * P_s}{0.596 * (460 + T)} \right]
 \end{aligned}$$

Figure 4.2. Breakdown of Gravimetric Sampling Equations.

First, the mass of TSP on the filter, W , is necessary. Assuming a lognormal particle size distribution of the PM in the air with a typical rural dust mass median diameter of $20 \mu\text{m}$ and GSD of 2.0, the mass of PM_{10} on the filter equals approximately 16% of the total suspended particulate matter (TSP) measured (Wang, 2000). The TSP can be defined as the total amount of particulate suspended in the volume of air sampled. PM_{10} refers to the particulate matter with an aerodynamic equivalent diameter less than or equal to 10 microns, and it is a quantity regulated under the NAAQS. Therefore, the mass of the TSP on the filter is calculated by equation 4.7.

$$W = (W_f - W_i) \quad (4.7)$$

where W_f is the weight of the filter and TSP after the sampling period and W_i is the weight of the filter before the sampling period. These filters are weighed three times before and after sampling under controlled environmental conditions (relative humidity and temperature have an impact on the accuracy of the weight), and the mean of each of these three measurements is used. Both W_f and W_i are primary measured quantities, so no further reduction is necessary.

The total volume of air in ft^3 , V , used during the sampling time is determined by

$$V = Q * \Theta \quad (4.8)$$

where Q is the volumetric flow rate in cfm and θ is the elapsed time of the test in minutes. The elapsed time of the test, θ , is a measured quantity; however, Q is not. So, Q must be evaluated further. Each gravimetric sampler uses a fan or pump to draw air downward through the filter. The fan/pump setup includes an orifice meter in the line to the sampler in order to calculate the volumetric flow rate of air through the tube. The volumetric flow rate in cfm, Q , is calculated from the pressure drop across an orifice meter as in equation 4.9 that follows, which is derived from Bernoulli's equation (Sorenson and Parnell, 1991)

$$Q = 5.976 * k * (D_0)^2 * \sqrt{\frac{\Delta P_a}{\rho_a}} \quad (4.9)$$

where k is a calibration constant for the orifice meter, ΔP_a is the measured pressure drop across the orifice meter in inches of water using a transducer output to a data logger to record the instantaneous pressure drop across the orifice meter, ρ_a is the mean air density in $\text{lbs}\cdot\text{ft}^{-3}$, and D_0 is the diameter of the orifice in inches determined by the end mill specifications. In the case of the ΔP_a reading from the Hobo instrument, the uncertainty in both the pressure transducer and the Hobo data logger must be accounted for.

For field sampling measurements, the gas used is air where the air density in $\text{lbs}\cdot\text{ft}^{-3}$ can be estimated by (Cooper and Alley, 2002)

$$\rho_a = \left[\frac{P_a - RH * P_s}{0.37 * (460 + T)} \right] + \left[\frac{RH * P_s}{0.596 * (460 + T)} \right] \quad (4.10)$$

where P_s is the saturated vapor pressure in $\text{lbs}\cdot\text{in}^{-2}$ at T , T is the dry bulb temperature of the air in degrees Fahrenheit, and RH is the relative humidity fraction of the air. In three of the four examples that follow, the value of k is determined against a laminar flow element (LFE) of greater precision and accuracy than the orifice meter, where the value of k is given by

$$k = \frac{Q_{LFE}}{5.976 * (D_0)^2 * \sqrt{\frac{\Delta P_c}{\rho_c}}} \quad (4.11)$$

where Q_{LFE} is the flow given by the LFE ($\text{ft}^3 \cdot \text{min}^{-1}$), ρ_c is the density of the air during calibration ($\text{lbs} \cdot \text{ft}^{-3}$), and ΔP_c is the pressure drop across the orifice meter during calibration in inches of water. In the low volume example, the reading from a mass flow meter ($Q_{\text{massflowmeter}}$) is used in lieu of Q_{LFE} in equation 4.11 (to determine the k value). The density of the air during calibration, ρ_c , is calculated using the same equation as ρ_a , (equation 4.10). In the case of the ΔP_c reading from the Hobo instrument, the uncertainty in both the pressure transducer and the Hobo data logger must be accounted for.

Sensitivity Coefficient Determination

In order to evaluate the effect of each primary measurement on the final concentration measurement, the sensitivity must be calculated with respect to each of these primary measurements. The sensitivity coefficient for each element of gravimetric sampling system is based on equation 4.5. In order to determine the sensitivity coefficients, the uncertainty of each instrument is necessary.

Table 4.1. Instrument Specifications for Gravimetric PM Sampling.

Parameter	Instrument	Reported Uncertainty
W_i, W_f	Sartorius SC2 (low volume)	$1 * 10^{-7}$ g
	Mettler Toledo AG balance (high volume)	$2 * 10^{-4}$ g
Θ (Time)	HOBO data logger	0.20 min
ΔP_a	Omega PX274 Pressure Transducer	0.075
	+ HOBO cord	0.1 mA + 3 %
D_o	End Mill Specs	0.025 in
T_a	HOBO Weather Station Temperature/RH Smart Sensor	0.8 °F
P_a	HOBO Weather Station Barometric Pressure Smart Sensor	1 %
RH_a	HOBO Weather Station Temperature/RH Smart Sensor	3 %
P_{sata}	Steam Tables	0.0001 psia
$Q_{massflowmeter}$	Aalborg GFC17 Mass Flowmeter	1.5 % FS
Q_{LFE}	Meriam Instruments Model 50MC2-2	0.344 cfm
ΔP_c	Digital Manometer – Dwyer Series 475 Mark III	0.5 % FS
T_c	Davis Perception II	1 °F
P_c	Davis Perception II	1 %
RH_c	Davis Perception II	5%
P_{satc}	Steam Tables	0.0001 psia

Table 4.1 specifies the instruments used for each measurement as well as the related uncertainty as provided in the manufacturer's specifications. These uncertainty values are assumed to be at a 95% confidence interval, which represents 2 standard deviations from the mean, also referred to as 20:1 odds. Literature identifies this as a Type B analysis in which the evaluation of uncertainty is based upon scientific judgment and manufacturers' specifications (NIST, 1994).

With this uncertainty information, the sensitivity coefficient for each variable in equations 4.6 – 4.11 is determined using partial differential equations as described by equation 4.5. These computed partial differentials can be found in Appendix C.

Sensitivity & Uncertainty Analysis

To determine the most sensitive input parameters with respect to the output particulate matter concentration, a sensitivity analysis must be performed on the uncorrelated primary measurements (Yegnan et al., 2002). The information obtained from the sensitivity analysis is used to obtain the uncertainty in the particulate matter concentration calculation. Additionally, this information helps identify the most influential sources of uncertainty. This proves to be important when the amount of uncertainty in the final computation needs to be reduced by identifying these influential sources of uncertainty.

This analysis evaluates the PM_{10} (particulate matter with an aerodynamic equivalent diameter less than or equal to 10 microns) concentrations in four situations: the high volume sampling technique ($Q \approx 0.0236 \text{ m}^3\text{s}^{-1}$ (50 cfm), which is the midpoint of the U.S. EPA defined appropriate operating flow rates; where $Q \approx 0.0184 \text{ m}^3\text{s}^{-1}$ (39 cfm) and $Q \approx 0.0283 \text{ m}^3\text{s}^{-1}$ (60 cfm), which are the upper and lower limit flow rates as defined by the U.S. EPA) and low volume sampling technique ($Q \approx 0.000278 \text{ m}^3\text{s}^{-1}$ (0.59 cfm)) used by the Texas A&M Center for Agricultural Air Quality Engineering & Science

(CAAQES). It is important to note that the sampling instrumentation used by CAAQES has less uncertainty and variability associated with each piece of instrumentation than the approved EPA sampling instrumentation.

Each portion of Table 4.2 provides a summary of the sensitivity of each independent parameter contributing to the final particulate matter concentration. This information is derived from a model in Microsoft Excel as provided in Appendix C. Using the process as defined earlier in this chapter, the sensitivities of each of the parameters are calculated based on equation 4.5. The uncertainty of each secondary measurement is determined by the propagation of the primary measurements as described by equations 4.3 and 4.4. These secondary uncertainties include not only the uncertainty in the concentration measurement (ω_C) but also the uncertainty in the mass on the filter (ω_W), the volume of air (ω_V), the volumetric flow rate of air (ω_Q), the density of the air during the sampling period (ω_{ρ_a}), the density of the air during the orifice meter calibration (ω_{ρ_c}) and the k value across the orifice meter (ω_k). Ultimately, the model calculates the amount each parameter impact the total uncertainty of the final concentration calculation. If the parameters representing the primary measurements are summed (ΔP_a , T_a , P_a , RH_a , P_{sata} , Q_{LFE} , D_0 , ΔP_c , T_c , P_c , RH_c , P_{satc}), then the “Percentage of Total Uncertainty” (as the column is titled in the following uncertainty calculation tables) results in 100% of the total uncertainty.

The following scenario evaluations are included in Tables 4.2 and 4.3 (with the calculations included in Figures 4.3 – 4.6 that follow):

1. TAMU Gravimetric Sampling – $Q \approx 0.000278 \text{ m}^3\text{s}^{-1}$ (0.6 cfm)
2. TAMU Gravimetric Sampling – $Q \approx 0.0184 \text{ m}^3\text{s}^{-1}$ (39 cfm)
3. TAMU Gravimetric Sampling – $Q \approx 0.0236 \text{ m}^3\text{s}^{-1}$ (50 cfm)
4. TAMU Gravimetric Sampling – $Q \approx 0.0283 \text{ m}^3\text{s}^{-1}$ (60 cfm)

The last three scenarios use the exact same high volume sampling setup with the instrumentation as previously listed in Table 4.1. The first scenario utilizes a similar setup; however, a low volume pump is used to move the air in lieu of the air high volume fan. Additionally, the filters from the low volume setup (scenario #1) are weighed on a more sensitive balance. A picture of the high volume sampling setup can be seen in Figure 4.7, and a visual of the low volume sampling setup is in Figure 4.8.

C = W/V	69.31 $\mu\text{g}/\text{m}^3$				
σ_c	8.2124E-06 g/m^3	8.21 $\mu\text{g}/\text{m}^3$	OR	11.88%	
					% of TOTAL Uncertainty
σ_w	1.41421E-07 g	$\delta C/\delta W$	0.333205773		0.0033%
σ_v	0.355610452 m^3	$\delta C/\delta V$	-2.3093E-05		99.9967%
W = W_f - W_i					
	0.000208 g				
σ_w	1.41421E-07 g				
					% of Partial Uncertainty % of Total Uncertainty
σ_{w_f}	1.00E-07 g	$\delta W/\delta W_f$	1	50.0000%	0.0016%
σ_{w_i}	1.00E-07 g	$\delta W/\delta W_i$	-1	50.0000%	0.0016%
V = QΔt					
	105.9645585 ft^3	3.001148 m^3			
σ_v	12.5582646 ft^3	0.35561 m^3			
					% of Partial Uncertainty % of Total Uncertainty
σ_Q	0.2 min	$\delta V/\delta Q$	0.588803103	0.0088%	0.0088%
$\sigma_{\Delta t}$	0.089765 cfm	$\delta V/\delta \Delta t$	180	99.9912%	99.9979%
Q = 5.976 * k * D_o² * sqrt($\Delta P_c/\rho_c$) (uncertainty in D _o is already accounted for in the calibration of k)					
	0.568803 cfm				(assume F _A = 1)
σ_Q	0.069765 cfm				
					% of Partial Uncertainty % of Total Uncertainty
σ_{D_o}	0 (accounted for in k)	$\delta Q/\delta D_o$	6.28057	0.0000%	0.0000%
$\sigma_{\Delta P_c}$	0.211758353 in of H ₂ O	$\delta Q/\delta \Delta P_c$	0.27405	68.1930%	69.1847%
σ_k	0.047614479	$\delta Q/\delta k$	0.8108	30.6217%	30.6180%
σ_{ρ_c}	0.000735715 lbs/ft^3	$\delta Q/\delta \rho_c$	-4.06157	0.1853%	0.1852%
k = Q_{measured} / (5.976 * D_o² * sqrt($\Delta P_c/\rho_c$))					
	0.726200327				
σ_k	0.047614479				
					% of Partial Uncertainty % of Total Uncertainty
$\sigma_{Q_{measured}}$	0.00795 cfm	$\delta k/\delta Q_{measured}$	1.4524	5.8807%	1.8006%
σ_{D_o}	0.001 in	$\delta k/\delta D_o$	-7.7461	2.6466%	0.8103%
$\sigma_{\Delta P_c}$	0.1 in of H ₂ O	$\delta k/\delta \Delta P_c$	-0.4539	90.8646%	27.8209%
σ_{ρ_c}	0.000761678 lbs/ft^3	$\delta k/\delta \rho_c$	4.87458	0.6081%	0.1862%
$\rho_c = ((P_c - (RH_c * P_{sat})) / (0.37 (460 + T_c))) + ((RH_c * P_{sat}) / (0.596 (460 + T_c)))$					
	0.074488482 lbs/ft^3				
σ_{ρ_c}	0.000761678 lbs/ft^3				
					% of Partial Uncertainty % of Total Uncertainty
σ_{RH_c}	0.025	$\delta \rho_c/\delta RH_c$	-0.0007	0.0531%	0.0001%
$\sigma_{P_{sat}}$	0.0001 psia	$\delta \rho_c/\delta P_{sat}$	-0.00097	0.0000%	0.0000%
σ_{P_c}	0.14678 psia	$\delta \rho_c/\delta P_c$	0.0051	98.5422%	0.1797%
σ_{T_c}	1 ° F	$\delta \rho_c/\delta T_c$	-0.00014	3.4047%	0.0063%
$\rho_a = ((P_a - (RH_a * P_{sat})) / (0.37 (460 + T_a))) + ((RH_a * P_{sat}) / (0.596 (460 + T_a)))$					
	0.072129422 lbs/ft^3				
σ_{ρ_a}	0.000735715 lbs/ft^3				% of Total Uncertainty
					% of Partial Uncertainty % of Total Uncertainty
σ_{RH_a}	0.0174	$\delta \rho_a/\delta RH_a$	-0.0011	0.0703%	0.0001%
$\sigma_{P_{sat}}$	0.0001 psia	$\delta \rho_a/\delta P_{sat}$	-0.0011	0.0000%	0.0000%
σ_{P_a}	0.14678 psia	$\delta \rho_a/\delta P_a$	0.00496	97.8587%	0.1813%
σ_{T_a}	0.8 ° F	$\delta \rho_a/\delta T_a$	-0.0001	2.0711%	0.0038%

Figure 4.3. TAMU – Q $\approx 0.000278 \text{ m}^3\text{s}^{-1}$ (0.6 cfm) – Uncertainty Analysis.

$C = WV$	69.23 $\mu\text{g}/\text{m}^3$					
ω_c	8.41E-06 g/m^3	8.41 $\mu\text{g}/\text{m}^3$	OR	12.18%		
					% of TOTAL Uncertainty	
ω_W	0.00028284 g		$\delta C/\delta W$	0.00503058	2.8623%	
ω_V	23.8037135 m^3		$\delta C/\delta V$	-3.482E-07	97.1377%	
$W = W_f - W_i$	0.01378 g					
ω_W	0.000282843 g					
					% of Partial Uncertain	% of Total Uncertainty
ω_{wf}	2.00E-04 g	$\delta W/\delta W_f$	1	50.0000%		1.4312%
ω_{wi}	2.00E-04 g	$\delta W/\delta W_i$	-1	50.0000%		1.4312%
$V = Q\Theta$	7020.005311 ft^3	198.784 m^3				
ω_V	840.8202073 ft^3	23.8037 m^3				
					% of Partial Uncertain	% of Total Uncertainty
ω_Θ	0.2 min	$\delta V/\delta \Theta$	39.0000295	0.0086%		0.0084%
ω_Q	4.689911 cfm	$\delta V/\delta Q$	180	99.9914%		97.1293%
$Q = 5.976 * k * D_o^2 * \text{sqrt}(\Delta P_a/\rho_a)$	(uncertainty in D_o is already accounted for in the calibration of k)					
	39 cfm	(assume $F_A = 1$)				
ω_Q	4.68991 cfm					
					% of Partial Uncertain	% of Total Uncertainty
ω_{D_o}	0 (accounted for in k)	$\delta Q/\delta D_o$	52	0.0000%		0.0000%
$\omega_{\Delta P_a}$	0.20780982 in of H_2O	$\delta Q/\delta \Delta P_a$	20.6872	84.7457%		82.3129%
ω_k	0.03729956	$\delta Q/\delta k$	48.6075	15.0729%		14.6402%
ω_{ρ_a}	0.00073572 lbs/ft^3	$\delta Q/\delta \rho_a$	-270.35	0.1814%		0.1762%
$k = Q/\Theta / (5.976 * D_o^2 * \text{sqrt}(\Delta P_a/\rho_a))$						
	0.80234559					
ω_k	0.03729956					
					% of Partial Uncertain	% of Total Uncertainty
$\omega_{Q/\Theta}$	0.344 cfm	$\delta k/\delta Q/\Theta$	0.01605	2.1902%		0.3207%
ω_{D_o}	0.025 in	$\delta k/\delta D_o$	-1.0698	51.4130%		7.5270%
$\omega_{\Delta P_a}$	0.1 in of H_2O	$\delta k/\delta \Delta P_a$	-0.2507	45.1872%		6.6155%
ω_{ρ_a}	0.00076168 lbs/ft^3	$\delta k/\delta \rho_a$	5.3857	1.2095%		0.1771%
$\rho_a = ((P_a - (RH_a * P_{sat})) / (0.37 (460 + T_a))) + ((RH_a * P_{sat}) / (0.596 (460 + T_a)))$						
	0.07448848 lbs/ft^3					
ω_{ρ_a}	0.00073572 lbs/ft^3					
					% of Partial Uncertain	% of Total Uncertainty
ω_{RH_a}	0.025	$\delta \rho_a/\delta RH_a$	-0.0007	0.0531%		0.0001%
$\omega_{P_{sat}}$	0.0001 psia	$\delta \rho_a/\delta P_{sat}$	-0.001	0.0000%		0.0000%
ω_{P_a}	0.14676 psia	$\delta \rho_a/\delta P_a$	0.0051	98.5422%		0.1710%
ω_{T_a}	1 ° F	$\delta \rho_a/\delta T_a$	-0.0001	3.4047%		0.0060%
$\rho_a = ((P_a - (RH_a * P_{sat})) / (0.37 (460 + T_a))) + ((RH_a * P_{sat}) / (0.596 (460 + T_a)))$						
	0.07212942 lbs/ft^3					
ω_{ρ_a}	0.00073572 lbs/ft^3					
					% of Partial Uncertain	% of Total Uncertainty
ω_{RH_a}	0.0174	$\delta \rho_a/\delta RH_a$	-0.0011	0.0703%		0.0001%
$\omega_{P_{sat}}$	0.0001 psia	$\delta \rho_a/\delta P_{sat}$	-0.0011	0.0000%		0.0000%
ω_{P_a}	0.14676 psia	$\delta \rho_a/\delta P_a$	0.00496	97.8587%		0.1724%
ω_{T_a}	0.8 ° F	$\delta \rho_a/\delta T_a$	-0.0001	2.0711%		0.0036%

Figure 4.4. TAMU – $Q \approx 0.0184 \text{ m}^3\text{s}^{-1}$ (39 cfm) – Uncertainty Analysis.

$C = W/V$	69.06 $\mu\text{g}/\text{m}^3$				
ω_c	6.0862E-08 g/m^3	6.09 $\mu\text{g}/\text{m}^3$		8.81%	
					% of TOTAL Uncertainty
ω_w	0.00028284 g		$\delta C/\delta W$	0.00392385	3.3253%
ω_v	22.0831855 m^3		$\delta C/\delta V$	-2.7098E-07	96.6747%
$W = W_f - W_i$	0.0178 g				
ω_w	0.000282843 g				
					% of Partial Uncertainty % of Total Uncertainty
ω_{wf}	2.00E-04 g		$\delta W/\delta W_f$	1	50.0000% 1.8626%
ω_{wi}	2.00E-04 g		$\delta W/\delta W_i$	-1	50.0000% 1.8626%
$V = Q\Delta t$	8999.998854 ft^3	254.8515 m^3			
ω_v	779.8598285 ft^3	22.08317 m^3			
					% of Partial Uncertainty % of Total Uncertainty
$\omega_\Delta t$	0.2 min		$\delta V/\delta \Delta t$	49.9999825	0.0164% 0.0159%
ω_Q	4.332197268 cfm		$\delta V/\delta Q$	180	99.9836% 96.8588%
$Q = 5.976 * k * D_o^2 * \text{sqrt}(\Delta P_a/\rho_a)$					(Uncertainty in D_o is already accounted for in the calibration of k)
	49.99998 cfm				(assume $F_a = 1$)
ω_Q	4.332197 cfm				
					% of Partial Uncertainty % of Total Uncertainty
ω_{D_o}	0 (accounted for in k)		$\delta Q/\delta D_o$	66.8866	0.0000% 0.0000%
$\omega_{\Delta P_a}$	0.22601105 in of H_2O		$\delta Q/\delta \Delta P_a$	16.136	70.8658% 68.4980%
ω_k	0.03729856		$\delta Q/\delta k$	62.3173	28.7878% 27.8259%
ω_{ρ_a}	0.00073572 lbs/ft^3		$\delta Q/\delta \rho_a$	-346.599	0.3465% 0.3349%
$k = Q/\Delta t / (5.976 * D_o^2 * \text{sqrt}(\Delta P_a/\rho_a))$					
	0.80234559				
ω_k	0.03729856				
					% of Partial Uncertainty % of Total Uncertainty
$\omega_{Q/\Delta t}$	0.344 cfm		$\delta k/\delta Q/\Delta t$	0.01805	2.1902% 0.6085%
ω_{D_o}	0.025 in		$\delta k/\delta D_o$	-1.06979	51.4130% 14.3081%
$\omega_{\Delta P_a}$	0.1 in of H_2O		$\delta k/\delta \Delta P_a$	-0.25073	45.1872% 12.5737%
ω_{ρ_a}	0.00076168 lbs/ft^3		$\delta k/\delta \rho_a$	5.3857	1.2095% 0.3386%
$\rho_a = ((P_a - (RH_a * P_{sat})) / (0.37 (460 + T_a))) + ((RH_a * P_{sat}) / (0.596 (460 + T_a)))$					
	0.07448848 lbs/ft^3				
ω_{ρ_a}	0.00076168 lbs/ft^3				
					% of Partial Uncertainty % of Total Uncertainty
ω_{RH_a}	0.025		$\delta \rho_a/\delta RH_a$	-0.0007	0.0531% 0.0002%
$\omega_{P_{sat}}$	0.0001 psia		$\delta \rho_a/\delta P_{sat}$	-0.00097	0.0000% 0.0000%
ω_{P_a}	0.14676 psia		$\delta \rho_a/\delta P_a$	0.0051	96.5422% 0.3249%
ω_{T_a}	1 ° F		$\delta \rho_a/\delta T_a$	-0.00014	3.4047% 0.0115%
$\rho_a = ((P_a - (RH_a * P_{sat})) / (0.37 (460 + T_a))) + ((RH_a * P_{sat}) / (0.596 (460 + T_a)))$					
	0.07212942 lbs/ft^3				
ω_{ρ_a}	0.00073572 lbs/ft^3				
					% of Total Uncertainty
					% of Partial Uncertainty % of Total Uncertainty
ω_{RH_a}	0.0174		$\delta \rho_a/\delta RH_a$	-0.00112	0.0703% 0.0002%
$\omega_{P_{sat}}$	0.0001 psia		$\delta \rho_a/\delta P_{sat}$	-0.00109	0.0000% 0.0000%
ω_{P_a}	0.14676 psia		$\delta \rho_a/\delta P_a$	0.00496	97.8587% 0.3277%
ω_{T_a}	0.8 ° F		$\delta \rho_a/\delta T_a$	-0.00013	2.0711% 0.0089%

Figure 4.5. TAMU – $Q \approx 0.0236 \text{ m}^3 \text{ s}^{-1}$ (50 cfm) – Uncertainty Analysis.

C = W/V	69.06 $\mu\text{g}/\text{m}^3$				
ω_c	5.0838E-06 g/m^3	8.08 $\mu\text{g}/\text{m}^3$	OR	7.58%	
					% of TOTAL Uncertainty
ω_w	0.000282843 g		$\delta C/\delta W$	0.003269877	3.3069%
ω_v	22.13631212 m^3		$\delta C/\delta V$	-2.2682E-07	96.6901%
W = W_f - W_i					
	0.02112 g				
ω_w	0.000282843 g				
					% of Partial Uncertainty % of Total Uncertainty
ω_{wf}	2.00E-04 g		$\delta W/\delta W_f$	1	50.0000% 1.8549%
ω_{wi}	2.00E-04 g		$\delta W/\delta W_i$	-1	50.0000% 1.8549%
V = QΔt					
	10799.99901 ft^3	306.8219 m^3			
ω_v	781.7364849 ft^3	22.13631 m^3			
					% of Partial Uncertainty % of Total Uncertainty
$\omega_{\Delta t}$	0.2 min		$\delta V/\delta \Delta t$	59.99999448	0.0236% 0.0228%
ω_Q	4.3424688 cfm		$\delta V/\delta Q$	180	99.9764% 96.8673%
Q = 5.976 * k * D₀^{2.5} * sqrt($\Delta P_a/\rho_a$) (uncertainty in D ₀ is already accounted for in the calibration of k) 59.99999 cfm (assume F _k = 1)					
ω_Q	4.342469 cfm				
					% of Partial Uncertainty % of Total Uncertainty
ω_{D_0}	0 (accounted for in k)		$\delta Q/\delta D_0$	79.99999	0.0000% 0.0000%
$\omega_{\Delta P_a}$	0.246462198 in of H ₂ O		$\delta Q/\delta \Delta P_a$	13.44869	58.2449% 20.5038%
ω_k	0.037299561		$\delta Q/\delta k$	74.79074	41.2585% 39.8835%
ω_{ρ_a}	0.000735715 lbs/ft^3		$\delta Q/\delta \rho_a$	-415.919	0.4966% 0.4800%
k = C/Qfe / (5.976 * D₀^{2.5} * sqrt($\Delta P_c/\rho_c$))					
	0.802345667				
ω_k	0.037299561				
					% of Partial Uncertainty % of Total Uncertainty
ω_{Qfe}	0.344 cfm		$\delta k/\delta Qfe$	0.016047	2.1902% 0.8735%
ω_{D_0}	0.025 in		$\delta k/\delta D_0$	-1.08979	51.4130% 20.5053%
$\omega_{\Delta P_c}$	0.1 in of H ₂ O		$\delta k/\delta \Delta P_c$	-0.25073	45.1872% 18.0222%
ω_{ρ_c}	0.000761678 lbs/ft^3		$\delta k/\delta \rho_c$	5.385702	1.2096% 0.4824%
$\rho_c = ((P_c - (RH_c * P_{sat})) / (0.37 (460 + T_c))) + ((RH_c * P_{sat}) / (0.596 (460 + T_c)))$					
	0.074488482 lbs/ft^3				
ω_{ρ_c}	0.000761678 lbs/ft^3				
					% of Partial Uncertainty % of Total Uncertainty
ω_{RHc}	0.025		$\delta \rho_c/\delta RHc$	-0.0007	0.0531% 0.0003%
$\omega_{P_{satc}}$	0.0001 psia		$\delta \rho_c/\delta P_{satc}$	-0.00097	0.0000% 0.0000%
ω_{P_c}	0.14676 psia		$\delta \rho_c/\delta P_c$	0.005099	96.5422% 0.4667%
ω_{Tc}	1 ° F		$\delta \rho_c/\delta Tc$	-0.00014	3.4047% 0.0164%
$\rho_a = ((P_a - (RH_a * P_{sat})) / (0.37 (460 + T_a))) + ((RH_a * P_{sat}) / (0.596 (460 + T_a)))$					
	0.072129422 lbs/ft^3				
ω_{ρ_a}	0.000735715 lbs/ft^3	% of Total Uncertainty			
					% of Partial Uncertainty % of Total Uncertainty
ω_{RHa}	0.0174		$\delta \rho_a/\delta RHa$	-0.00112	0.0703% 0.0003%
$\omega_{P_{sata}}$	0.0001 psia		$\delta \rho_a/\delta P_{sata}$	-0.00109	0.0000% 0.0000%
ω_{P_a}	0.14676 psia		$\delta \rho_a/\delta P_a$	0.004959	97.8567% 0.4697%
ω_{Ta}	0.8 ° F		$\delta \rho_a/\delta Ta$	-0.00013	2.0711% 0.0099%

Figure 4.6. TAMU – Q \approx 0.0283 m^3s^{-1} (60 cfm) – Uncertainty Analysis.



Figure 4.7. High Volume Sampling Setup.



Figure 4.8. Low Volume Sampling Setup.

Table 4.2 summarizes the overall concentration uncertainty for each of the evaluated four scenarios, and Table 4.3 breaks down the uncertainty into the contribution of each measurement to the total uncertainty. Table 4.3 is in the form of a spreadsheet model. The areas with normal black text represent the initial values that the user inputs into the spreadsheet. The other text areas in blue are values that the user cannot modify because these cells contain values calculated by the spreadsheet program.

Table 4.2. Total Uncertainty for Gravimetric Sampling.

Sampler Conditions	Concentration ($\mu\text{g}/\text{m}^3$)	Uncertainty ($\mu\text{g}/\text{m}^3$)	Uncertainty (%)
TAMU – 1 m^3/hr	69.31	8.21	11.85
TAMU – 39 cfm	69.22	8.41	12.15
TAMU – 50 cfm	69.06	6.09	8.81
TAMU – 60 cfm	69.06	5.08	7.36

In evaluating Table 4.3 of all four scenarios, it is important to note that the leading contributor to the uncertainty in the final concentration calculation is the pressure drop across the orifice meter. If we are to seek a higher degree of certainty in our final concentration calculation, then the optimal decision would be to decrease the uncertainty in the measurement of the pressure drop across the orifice meter.

Table 4.3. Gravimetric Sensitivity Analysis for Uncertainty Propagation.

	Param.	Units	TAMU High Volume (50 cfm)			TAMU Low Volume (1 m ³ /hr)			TAMU High Volume (39 cfm)			TAMU High Volume (60 cfm)		
			Nominal Value	Uncertainty	% of Total Uncertainty	Nominal Value	Uncertainty	% of Total Uncertainty	Nominal Value	Uncertainty	% of Total Uncertainty	Nominal Value	Uncertainty	% of Total Uncertainty
Mass	W _f	G	9.1	2.00E-04	1.66%	10.30	1.00E-07	0.002%	9.786	2.00E-04	1.431%	9.832	2.00E-04	1.66%
	W _i	G	9.7	2.00E-04	1.66%	10.3	1.00E-07	0.002%	9.7	2.00E-04	1.431%	9.7	2.00E-04	1.66%
Volume	θ(Time)	Min	180	0.20000	0.02%	180	0.20000	0.009%	180	0.200	0.008%	180	0.20000	0.02%
	Q	Cfm	50.0	4.33	96.7%	0.59	0.07	99.99%	39.0	4.67	97.13%	60.00	4.34	96.7%
Q	ΔP _a	in of H ₂ O	1.55	0.23	68.5%	1.07	0.21	69.2%	0.94	0.208	82.31%	2.231	0.25	56.3%
	ρ _a	Lbs/ft ³	0.07	7.36E-04	0.34%	0.07	7.36E-04	0.19%	0.072	7.36E-04	0.176%	0.072	7.36E-04	0.48%
	k		0.80	0.037	27.83%	0.73	0.048	30.6%	0.80	0.037	14.64%	0.802	0.037	39.9%
ρ _a	T _a	° F	85	0.8	0.007%	85	0.8	0.004%	85	0.8	0.004%	85	0.8	0.01%
	P _a	Psia	14.7	0.147	0.33%	14.7	0.147	0.18%	14.7	0.147	0.17%	14.68	0.147	0.47%
	RH _a		0.58	0.017	0.0002%	0.58	0.017	0.0001%	0.58	0.017	0.0001%	0.58	0.017	0.0003%
	P _{sata}	Psia	0.60	0.0001	0.000%	0.60	0.0001	0.000%	0.60	0.0001	0.00%	0.596	0.0001	0.00%
K	Q _{LFE} / Q _{massflow}	Cfm	50	0.344	0.61%	0.5	0.008	1.80%	50	0.34	0.32%	50	0.344	0.88%
	ΔP _c	in of H ₂ O	1.6	0.1	12.6%	0.8	0.1	27.8%	1.6	0.1	6.62%	1.6	0.1	18.0%
	D _o	Inches	1.5	0.025	14.3%	0.19	0.001	0.81%	1.5	0.025	7.53%	1.5	0.025	20.5%
	ρ _c	Lbs/ft ³	0.074	7.62E-03	0.34%	0.07	7.62E-03	0.19%	0.074	7.62E-03	0.17%	0.074	7.62E-03	0.48%
ρ _c	T _c	° F	70	1	0.01%	70	1	0.006%	70	1	0.006%	70	1	0.02%
	P _c	Psia	14.7	0.147	0.33%	14.7	0.147	0.18%	14.7	0.147	0.171%	14.68	0.147	0.47%
	RH _c		0.5	0.025	0.0002%	0.5	0.025	0.0001%	0.5	0.025	0.0001%	0.5	0.025	0.0003%
	P _{satc}	Psia	0.36	0.0001	0.00%	0.36	0.0001	0.00%	0.36	0.0001	0.00%	0.363	0.0001	0.00%

Ammonia – Uncertainty Discussion

For field concentration measurements, ammonia (NH_3) is measured using a passive sampler technique based off of the UC Davis setup. This technique utilizes a citric acid-coated cellulose filter to trap the ammonia gas because of the basic nature of the gas (Rabaud et al., 2001). A schematic of the NH_3 passive sample is shown in Figure 4.9.

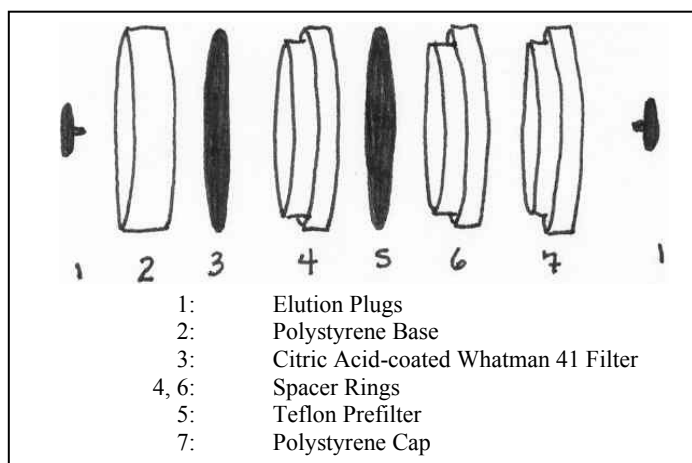


Figure 4.9. UC Davis Passive Ammonia Sampler. (adapted from Rabaud et al., 2001)

This setup is basically a 4-piece sampling cassette made of 37 mm styrene acrylonitrile filter holders, which is a filter cap and base with elution plugs on each, 2 spacer rings, a 2 micron pore size Teflon filter, and a 0.12 M citric acid coated Whatman 41 filter (Rabaud et al., 2001). The 0.12 M citric acid solution is created by a mix of 1.921 g citric acid monohydrate added to 10 mL of ethanol and 50 mL of diethyl ether. The filters are coated, assembled, and disassembled in a glove box containing ammonia-free air as to not contaminate the filter. This citric acid coating has caused concern about the

validity of using the citric acid. The volatility of the citric acid could have compromised the data collection during the UC Davis sampler testing (Rabaud et al., 2001; Perrino and Gheradi, 1999).

A study in Italy in 1999 indicated a potential volatilization of the citric acid coating during half of the test runs resulting in an ammonia collection efficiency that was much less than that of oxalic or phosphorous acid. Literature also noted that in testing this type of passive sampling device, the lower collection efficiency was significant for the runs with longer sampling time periods (Perrino and Gheradi, 1999). The same researchers continued to evaluate this phenomena and discovered that in many cases the ammonia mass balance was not satisfied, and the insufficient strength of the bond between the citric acid coating and the ammonia layer results in a release of some ammonia into the air flow (8% after a 2 hour period and 40% after a 12 hour period), decreasing the efficiency of the passive sampling device (Perrino and Gheradi, 1999). Thus, through extensive laboratory experimentation these researchers concluded that the citric acid was not suitable for ammonia determination. Additionally, there was concern about the misrepresentation of the ammonia and ammonium particles because there was the potential for reactions between the gas entering the filter pack and the filter material and particles already entrained in the filter (Perrino and Gheradi, 1999).

Thus, the amount of uncertainty in measuring the concentration of ammonia and the correct mass of ammonia on the citric acid coated filter made it difficult, if not

impossible, to quantitatively state the uncertainty surrounding this concentration measurement method. Thus, this subsection will discuss a qualitative analysis of the ammonia sampling protocol in lieu of a quantitative analysis.

The sampling method in this research utilized the UC Davis approach, and it corrected for artifact ammonia-N by keeping three blank filters that never left the lab and three blank filters that were taken to the field but never opened. The mass of ammonia collected on the blank field filters was subtracted from the amount accumulated on the filter in the filter pack during a run at the sampling location.

Assuming that the mass of ammonia on the filter was accurately measured, the effective volumetric flow rate of air through the passive sampler was calculated by knowing the results of a co-located active reference sampler. This co-located reference sampler is a boric acid bubbler utilizing the mass of ammonia and a known volume of air sampled. The volumetric flow rate was calculated by equation 4.12 (Rabaud et al., 2001).

$$\dot{V} = \frac{m_{filter}/t}{m_{bubbler}/V} \quad (4.12)$$

where \dot{V} is the volumetric flow rate of air (in L/hr), m_{filter} is the mass of ammonia on the passive filter (in $\mu\text{g NH}_4\text{-N}$), $m_{bubbler}$ is the mass of the ammonia collected by the bubbler (in $\mu\text{g NH}_4\text{-N}$), and V is the volume of air sampled by the bubbler device (in L).

Currently, in order to determine the uncertainty in the calculation of the effective air volumetric flow rate, researchers calculate the linear correlation between the passive filter mass and the $\text{NH}_4\text{-N}$ air concentration established by the co-located active 0.1 Normal sulfuric acid bubbler. The standard error of the slope of this correlation curve serves as the researchers' calculation of uncertainty.

There is uncertainty inherent in each of the parameters of equation 4.12 resulting in the total uncertainty in \dot{V} . Uncertainty exists in the time measurement, which is dependant upon the measuring device used to determine the actual sampling time period.

Additional uncertainty exists in the measurement of the mass of ammonia collected by the bubbler and the volume of air sampled by the bubbler. The uncertainty in these measurements hinges upon the instrumentation used to collect this data.

CHAPTER V

WIND VELOCITY UNCERTAINTY

As previously mentioned in the literature review section, accurate meteorological data is essential for valid dispersion modeling estimates. These data include wind speed, wind direction, solar radiation, and ambient air temperature measurements at various time intervals at the site where concentration data has been collected or will be predicted. Continuously changing wind conditions result in the inherent variation in the wind profile measurements used to calculate hourly vector averages for use in dispersion modeling.

Researchers in the Center for Agricultural Air Quality Engineering and Science have noticed the occurrence of extreme particulate matter peak in the evening hours around 2200. This perplexing increase in concentration has led to a variety of hypotheses in order to better understand the occurrence of this phenomenon. One hypothesis is that an overall reduction of wind speed occurs during those late evening hours along with the possibility of the existence of a low atmospheric inversion layer. Thus, there has been a keen interest in collecting data on the wind speed and direction profile co-located with total suspended particulate matter (TSP) samplers on a tower located downwind from an emitting source in order to understand the wind velocity profile at the sampling location.



Figure 5.1. Tower with Co-located Anemometers and Receptors.

The wind profiling test data was gathered at Feedyard C, which was the same location where the particulate matter and ammonia concentration discussed in this research was collected. Starting with the July 2003 sampling trip, a tower was assembled downwind of the feedyard. This tower consisted of co-located anemometers and low volume total suspended particulate matter samplers as seen in Figure 5.1 above. These anemometers located at heights of approximately 2 m, 4.4 m, 6.5 m, and 9.4 m.

Currently, only two feedyard sampling trips have been made that utilized the tower, anemometer, and low volume TSP assembly. Therefore, there has not been enough

evening information collected to quantitatively make a firm statement on the behavior of the atmosphere. Future uses of the tower need to also include temperature and relative humidity sensors co-located with the anemometers and TSP receptors in order to analyze the vertical temperature gradient during the sampling periods. The current data provides some assessment of the relative wind speed and wind direction of the respective samplers as seen in Figure 5.2.

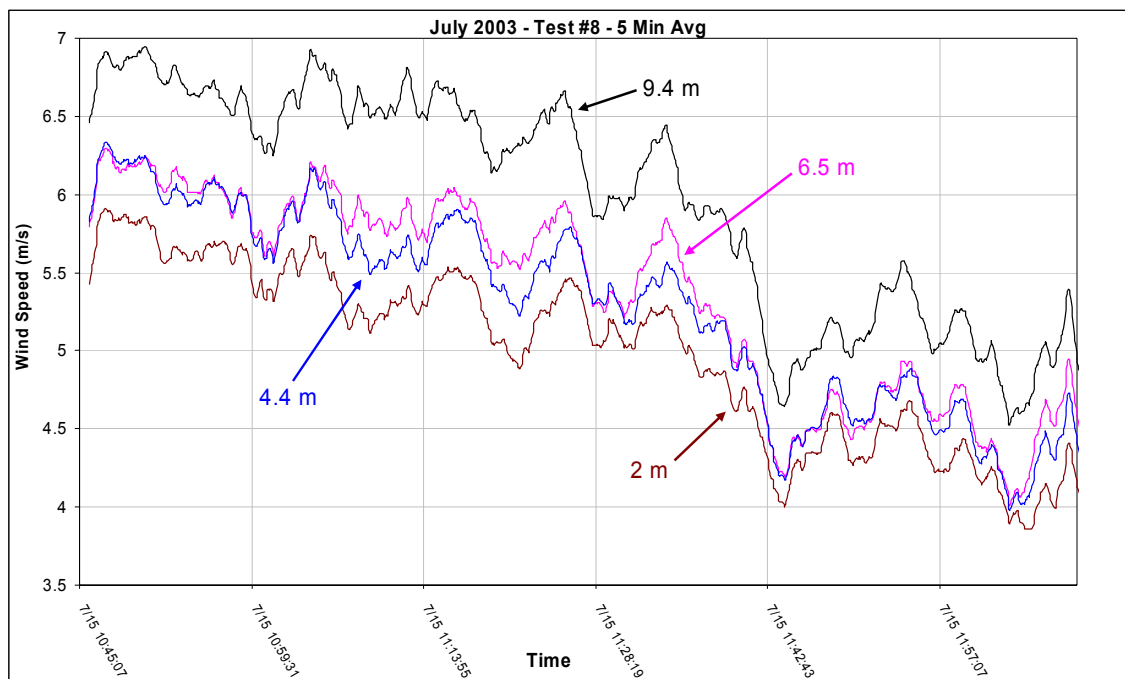


Figure 5.2. Measured Wind Speed as a Function of Time at Various Heights.

These data were taken from an evening test in which a rather large concentration peak was observed. It is interesting to note the crossover on the speed data between the

anemometer located at a height of 4.4 meters and the anemometer located at a height of 6.5 meters.

At this time, wind direction data is a little harder to get a quantitative understanding of.

Each anemometer must be placed in a specific orientation towards true North.

Currently, this process is done visually. Error exists in this placement process and the assurance that the anemometers match up in terms of the directional component.

Therefore, researchers are currently revising this assembly process to determine a more appropriate method to ensure the orientation of the four anemometers to true North.

CHAPTER VI

DISPERSION MODELING

Dispersion models provide a means to mathematically simulate the transport of gases and particles through the atmosphere. Estimates of pollutant concentrations downwind of a source can be established using the pollutant emission rate from the source and the meteorological conditions using a defined mathematical model. Additionally, dispersion modeling provides a scientific method for the regulatory agency to measure air quality compliance of a future source (one that has not been constructed), and it can be utilized to quantify the impact of the change in an abatement strategy of an existing source (Bultjes, 2003). Both models in this chapter assume a horizontally uniform emission source.

This chapter considers the use of concentration data for particulate matter (PM) and ammonia (NH_3) to back-calculate the emission rate of each of these species from a feedlot surface. To perform this back-calculation, a Gaussian Plume dispersion model, ISC-ST3 (Industrial Source Complex – Short Term Version 3), with the Breeze user (Trinity Consultants, 12801 N. Central Exp., Suite 1200, Dallas, TX, 75243), was evaluated and compared to a backward-Lagrangian stochastic based model, WindTrax, (Thunder Beach Scientific, 4B-1127 Cartaret Street, Halifax, Nova Scotia, Canada, BH3 3P2). Equivalent test data was input into each dispersion model for comparison of back-calculated emission rates.

Receptor Layouts

Figure 6.1 describes the basic layout of Feedyard C and the location of the passive ammonia samplers. Seven passive samplers (receptors), which are depicted by red on Figure 6.1, were placed along the downwind fence line of the feedyard. Additionally, a tower was placed at a location halfway down the width of the feedyard, and receptors were placed at three different heights along this tower: 1.5 m, 3 m, and 6 m.

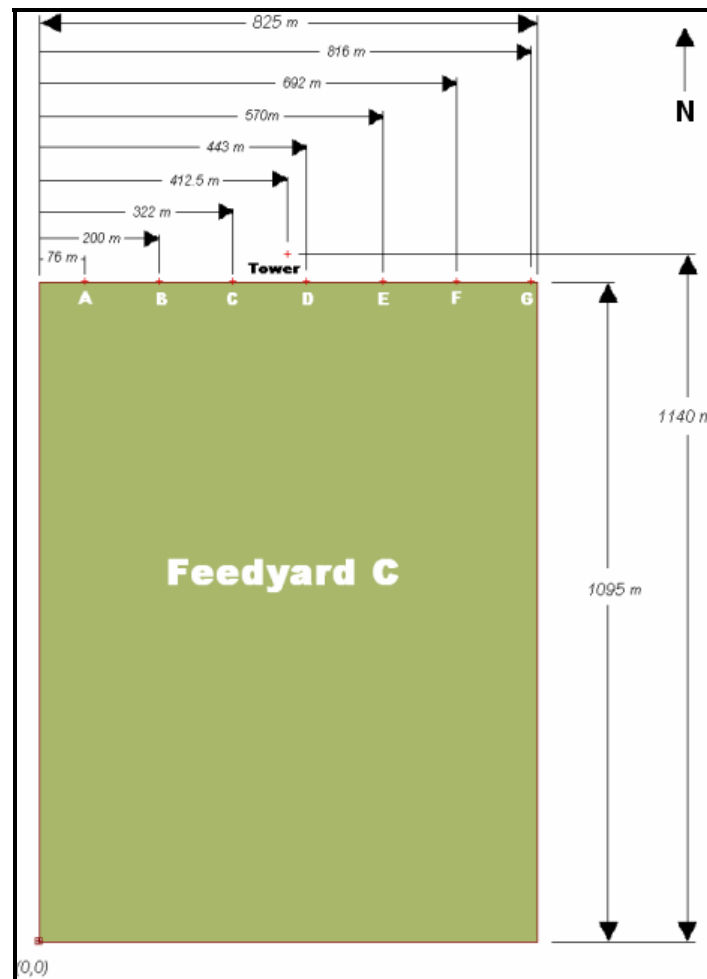


Figure 6.1. Ammonia Passive Sampler Feedyard Layout.

Model Inputs Defined

Back-calculated ammonia emission rates from concentration and meteorological field condition data were used to compare the two models. Identical meteorological and concentration data for each test period were used in both models to determine the average emission rate for each respective test period. The meteorological data used in this comparison can be found in Appendix D.

The stability of the atmosphere was the only input that was not directly measured by a sensor and was determined based on other data. Atmospheric stability was described using the Pasquill-Gifford parameters where A corresponded to very unstable conditions, B corresponded to moderately unstable conditions, C corresponded to slightly unstable conditions, D corresponded to neutral conditions, E corresponded to slightly stable conditions, and F corresponded to stable conditions (Cooper and Alley, 2002). These stability classes were determined using the Solar Radiation Delta-T (SRDT) Method for Estimating the Pasquill-Gifford Stability Class from the *Meteorological Monitoring Guidance for Regulatory Modeling Applications* published by the EPA and used in regulatory compliance monitoring, which can be seen in Table 6.1 (USEPA, 2000). The SRDT method requires the surface layer wind speed, the daytime solar radiation measurements, and the nighttime vertical temperature gradients measured at the sampling location as data inputs. The basic rationale of Turner's method, which provides an initial way to determine the Pasquill-Gifford stability classes from National

Weather Service data, supplies the foundation for the SRDT method (Turner, 1964). However, the SRDT method accounts for the time periods with cloud cover and ceiling (USEPA, 2000a). With the weather data, given in Appendix D, daytime stability classes were determined easily based from the solar radiation value and the wind speed. However, during the data collection period, nighttime vertical temperature gradients were not available. Since the ammonia concentration data was collected in August, 2002, it was assumed that the vertical temperature gradient was less than zero (the temperature of the local air decreases as the height increases). Data, which can be found in Appendix D, indicated that in the evening hours, the soil temperature was greater than the air temperature above the soil, so this assumption was valid at the surface, and it was assumed that this trend continued as the height is increased.

Table 6.1. SRDT Method for Estimating Stability Class. (adapted from USEPA, 2000a)

Daytime				
Wind Speed (m/s)	Solar Radiation (Watts/m ²)			
	≥ 925	925 – 675	675 – 175	< 175
< 2	A	A	B	D
2 – 3	A	B	C	D
3 – 5	B	B	C	D
5 – 6	C	C	D	D
≥ 6	C	D	D	D
Nighttime				
Wind Speed (m/s)	Vertical Temperature Gradient			
	< 0		≥ 0	
< 2.0	E		F	
2.0 – 2.5	D		E	
≥ 2.5	D		D	

With all of the input data defined, the average back-calculated emission rate for each test was determined using the two different dispersion models: ISC-ST3 (Gaussian based) and WindTrax (backward-Lagrangian based).

Gaussian Plume Dispersion Model

The Gaussian plume based dispersion model Industrial Source Complex – Short Term version 3 (ISC-ST3) is recommended by the EPA for industrial sources, rural or urban areas, flat or rolling terrain, transport distances less than 50 kilometers, one-hour to annual averaging times, and continuous toxic air emissions (Trinity Consultants, 2000). Thus, it was appropriate to model an agricultural operation such as Feedyard C using this model.

For the Gaussian Plume based dispersion model, ISC-ST3 was used with the Breeze user interface. The method used in this analysis to back-calculated emission rate from the area source is the method used by researchers from the Center for Agricultural Air Quality Engineering and Science at Texas A&M University.

The ISC-ST3 model was graphically built with the feedyard layout and receptor layout as shown in Figure 6.1. The ISC-ST3 layout can be seen in Figure 6.2. By going into the data screen on ISC, an emission rate for the area source was set at 6×10^{-6} g/m²/s, and the start and stop test times were specified. Next, a meteorological file was built using

the MetView add-in and inputting the hourly wind speed, wind direction, and stability class information as measured at the feedyard. This file was then linked as the meteorological data for the model. Note that the ISC model assumes a constant wind vector field across the entire area source for the hourly time period. Further information on running the ISC-ST3 application (Breeze Interface) can be obtained from the Center for Agricultural Air Quality Engineering and Science or Trinity Consultants (CAAQS, 2004; Trinity Consultants, 2000).

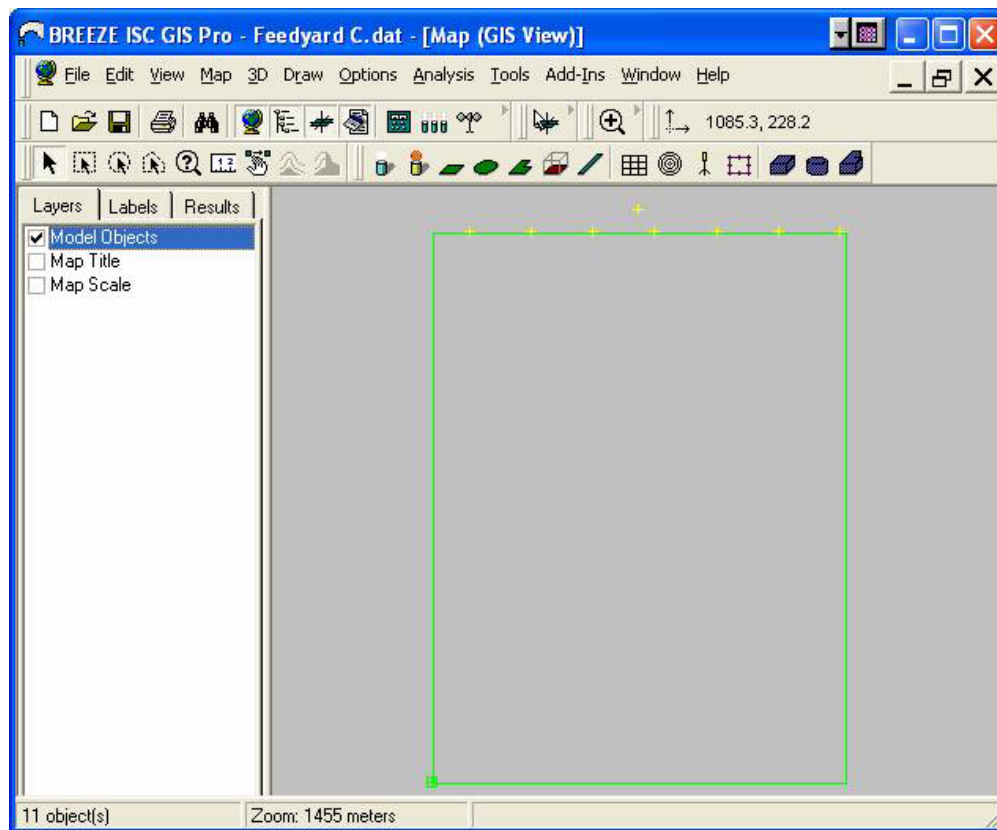


Figure 6.2. ISC Layout Screen Shot.

With the input data established, the ISC model was run. The results of each test period of the ISC model are shown in Appendix E. The governing equation for the ISC model is the Gaussian equation as noted in Chapter III, equation 3.1. This equation shows the direct relationship that exists between the concentration (C) and the emission rate (Q). As C is increased by a factor of x, Q is also increased by a factor of x. Thus, by defining the initial emission rate guess into ISC-ST3 ($6 \cdot 10^6$ g/m²/s) as Q_1 and the output concentration at a receptor as C_1 , the actual net measured concentration, C_2 , can be used to find the emission rate, Q_2 , needed to generate this concentration at receptor i based off of the relationship in equation 6.1.

$$\left(\frac{C_1}{Q_1}\right) = \left(\frac{C_2}{Q_2}\right) \quad (6.1)$$

which can be rewritten as

$$Q_2 = \left(\frac{C_2}{C_1}\right) * Q_1 \quad (6.2)$$

Because the passive samplers were located on the same fence line of the feedyard, no single more downwind sampler exists. Therefore, an average was taken from these 10 receptor emission rate calculations to determine the average emission rate for the test period. Using the same conceptual equation as in 6.1 and the ISC-ST3 model, this emission rate was used to predict the pollutant concentration at each receptor location had the average emission rate been used with the same input data (with the predicted concentration as C_2 and the average emission rate as Q_2 as seen below in equation 6.3).

$$C_2 = \left(\frac{Q_2}{Q_1} \right) * C_1 \quad (6.3)$$

This process was performed for each set of test data. Table 6.2 shows the average back-calculated emission rates for each of the test periods.

Table 6.2 Average Calculated Emission Rates Using ISC-ST3.

Test #	ISC ER g/(m ² -s)	Test Length (hrs)	Stability Classes in this Test
111	8.66E-06	2	D, C
112	1.03E-05	3	C, B, C
113	6.68E-06	3	All D
114	4.64E-06	12	All D
121	3.60E-06	7	D,D,D,D,D,D,C
122	7.62E-06	5	All D
123	5.31E-06	12	All D
131	6.03E-06	3	All D
132	1.03E-05	3	All D
133	1.05E-05	3	All D
134	7.17E-06	3	All D
135	4.47E-06	12	All D
141	4.42E-06	3	D, D, C
142	3.90E-06	3	C, C, B
143	7.06E-06	3	All B
144	8.14E-06	3	C, C, D
145	2.98E-06	12	All D
151	6.56E-06	3	All D
152	7.53E-06	3	C, C, B
153	1.14E-05	3	B, C, C
154	8.15E-06	3	All D
155	2.48E-06	12	D, D, D, D, E, E, E, E, E, D, D, D

Backward Lagrangian Stochastic (bLs) Model

The backward Lagrangian model is a local dispersion model (it should be used for short term modeling, not long term modeling). Since regulatory monitoring to comply with regulations such as the NAAQS is performed near the source, this model may be applied. Additionally, the relatively flat surface of the rural environment provides a perfect emission surface of the Lagrangian trajectory model.

For this part of the analysis, Windtrax (Version 1.0, Release 1.4.2, Thunder Beach Scientific, Alberta, Canada) was utilized as the backward-Lagrangian stochastic model. The user's guide notes that this model is restricted to ground level sources only (elevated sources are not possible with this algorithm), and the source to receptor distances must be less than about 1 km (Thunder Beach Scientific, 2003). The source to receptor distances in the feedyard example were about 1.1 km apart, which was at the upper boundary of the valid source to receptor distance. Additionally, it states that WindTrax 1.0 is only valid where the source is bare ground (or short vegetation), and the wind blows undisturbed (Thunder Beach Scientific, 2003).

Before proceeding with the evaluation of the bLs model, it is important to restate the underlying assumptions as described in the literature review (Liu and Seinfeld, 1975). First, the coordinate system is defined as a moving coordinate system that moves horizontally with velocities equal to the wind speed thus eliminating advection, which is

the standard assumption of trajectory models. Second, horizontal diffusion is neglected by assuming that the horizontal concentration gradients contribute negligibly to the overall mass balance of the system. Third, the vertical wind component has been ignored, thus assuming that air parcel movement is two-dimensional. Finally, the wind shear is neglected because the Lagrangian model assumes that the column height of the air parcel remains intact throughout the trajectory. The backward-Lagrangian model is a modified version of the original Lagrangian model in order to account for the touchdown of particles at various locations on the source surface. Thus, the assumptions of the bLS model are horizontally homogenous flow and a spatially uniform emission rate of the modeled species (Flesch et al., 1995).

Pre-modeling Tests

Before the model is run, various tests were used to determine how the bLS model functions because the actual source code for this particular model is not in the public domain unlike the ISC Gaussian model. The modeling procedure will be detailed in the following section.

First, the reversibility of the model was tested. Using the receptor layout at the feedyard as shown in Figure 6.1, a random emission rate ($6 \mu\text{g}/\text{m}^2/\text{s}$) was used to generate concentration data at each receptor for a given set of meteorological data. Then, the emission rate was set as unknown and calculated from the same given set of

meteorological and previously generated concentration data. The calculated emission rate ($6.07 \mu\text{g}/\text{m}^2/\text{s}$) was within 1% of the original emission rate. This error was most likely attributed to a rounding error. The calculated concentrations for each receptor was rounded when re-input into the model. This alone could cause the 1% difference. Thus, the reversibility of the model was affirmed.

Next, the relationship between the emission rate and the concentration at the receptor was verified. A simplified plot was used with a single area source and single concentration receptor with an unknown concentration. The emission rate was set at $10 \mu\text{g}/\text{m}^2/\text{s}$, and the receptor concentration was calculated to be $67.9 \mu\text{g}/\text{m}^3$. Then, the emission rate was multiplied by a factor of 2 to $20 \mu\text{g}/\text{m}^2/\text{s}$, and the receptor concentration was calculated to be $136 \mu\text{g}/\text{m}^3$. Thus, the concentration at the receptor was also increased by a factor of 2 when the emission rate was increased by the same factor. The emission rate was then multiplied by a factor of 3, 4, and 5, and the receptor concentration increased by a factor of 3, 4, and 5, respectively. Therefore, it can be said that a directly proportional relationship exists between the species emission rate and the concentration of that species at a downwind receptor.

In order to use the ammonia concentration data collected over a time period longer than that of the meteorological data and to ensure that the models are being compared in the same way, the bLS model was used to back-calculate the emission rate in the same way as the ISC-ST3 model. A random emission rate is used to generate concentration values

at each receptor for each hour of meteorological data. Then, an emission rate necessary to calculate this receptor concentration was calculated by utilizing the proportional relationship that exists between the emission rate and the concentration at the receptor. For comparison purposes, an average emission rate was computed from the ten calculated emission rates. The process of determining these values in the bLS model is discussed in the next subsection.

Determination of the Area Emission Rate

The process for back-calculating an emission rate in the bLS model is different than that of the ISC (Gaussian) model. In order to back-calculate an emission rate for an area source in the bLS model, the user must input the following parameters:

1. Coordinates of the area source
2. Wind speed at the main anemometer
3. Wind direction at the main anemometer
4. Height of the main anemometer
5. Atmospheric stability (in terms of Pasquill-Gifford Stability Class, Monin-Obukhov length, general stability condition description, present weather conditions, or the gradient Richardson number)
6. Pollutant background concentration at a receptor
7. Height of the receptor
8. Coordinate location of each receptor

9. Soil surface data

This subsection goes step by step through the bLS method used in this comparative analysis.

Figure 6.3, as seen on the following page, displays the toolbar used when building a model in WindTrax. When a new file is opened, a project tower will be placed on the grid. That tower was left alone for the time being. First, the origin and grid spacing were defined by choosing the grid spacing tool (#2 on the toolbar in Figure 6.3). To change the grid spacing, double click on the background grid. The default grid spacing is 2.0 m, but this value can be changed to any value necessary. After the grid was sized and the grid tool was still engaged, the coordinate origin was defined by clicking on the current origin (the gray bulls eye symbol on the grid) and dragging it to the desired location. This point represented the origin (0, 0) on the coordinate grid, and receptor locations were referenced to this point.

Next, the area source was defined using the draw area source tool (#5 in Figure 6.3). The type of area that was desired was chosen (the options were: polygon, free shape, square, rectangle, circle, and ellipse). For modeling Feedyard C, a rectangle was an appropriate representation of the area source with the dimensions of 825 m X 1095 m.

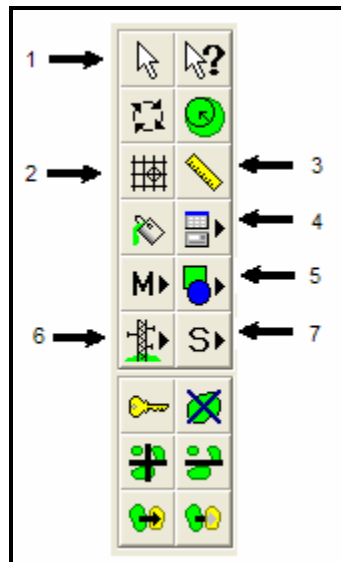


Figure 6.3. WindTrax Toolbar.

Next, the project tower given was located, and the components were defined by inputting the data as in the screen in Figure 6.4. The project tower contained all of the main anemometer inputs, including the wind speed, wind direction, location, height, stability class, and pollutant background concentration. Each model run utilized hourly wind speed, wind direction, and stability class data from the input file. So, these values were not necessary to input into the project tower at this time. Under the “Properties” tab of the Project Tower input screen, the location of the tower was input (relative to the origin) at (260, -60).

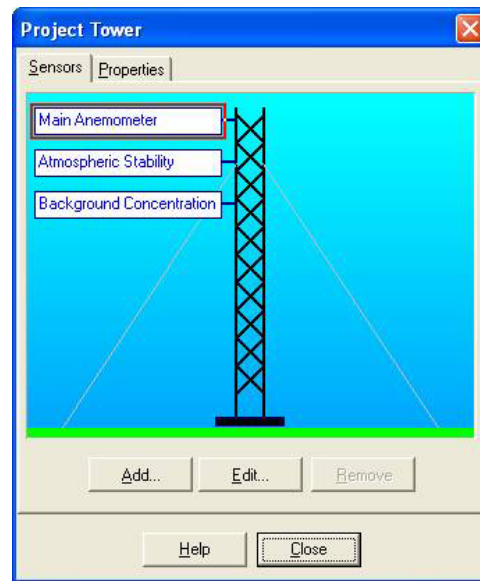
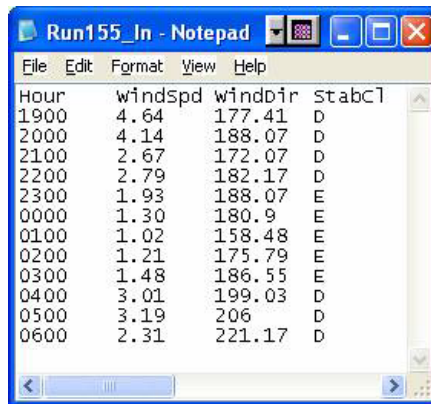


Figure 6.4. Project Tower Screen Shot.

By clicking on each of the tower properties, input data that will not change throughout the sampling time was entered. The main anemometer was set at 3 m for the test, and the background concentration was set to $0 \mu\text{g}/\text{m}^3$ because the concentration values used in the comparison were assumed to be net concentration values.

Since the wind speed, wind direction, and stability class vary over each sampling time period, these values were not input into this location. Instead, a text file was created with this data dependant on the time interval of data collected. Figure 6.5 is a screen shot of an example input data file from the last run of the data used in the comparative analysis. Column headings were used, but the row with column headings were skipped when the model runs. The Flesch bLS model assumes that concentration data exists for the same time interval as the wind speed and direction data, and this concentration data

was added as an additional column in the input file. Note that the data should be listed in columns, and the data should also be of equivalent time periods. However, for these tests, concentration data were not available for the same time period as the meteorological data, thus this information was not included in the input data file.



Hour	windspd	winddir	stabc1
1900	4.64	177.41	D
2000	4.14	188.07	D
2100	2.67	172.07	D
2200	2.79	182.17	D
2300	1.93	188.07	E
0000	1.30	180.9	E
0100	1.02	158.48	E
0200	1.21	175.79	E
0300	1.48	186.55	E
0400	3.01	199.03	D
0500	3.19	206	D
0600	2.31	221.17	D

Figure 6.5. Input Data Screen Shot.

This meteorological data input file was attached to the project tower by using the file button and choosing the input data file on the project toolbar (#4 in Figure 6.3). A small input file data button was added to the screen and moved close to the location where the data are linked. After selecting the appropriate input file name, the “Connections” tab was chosen. Here the input data were linked with the model. Initially, the “File columns” box remained blank except for numbers 1 through n (based on having n columns). After a column number and a piece of available data were selected, the “<” button was selected. This added that data name to the column number in the left box

(refer to Figure 6.6 based off of the input file shown in Figure 6.5). Note that the necessary data are chosen to correspond with the appropriate file columns.

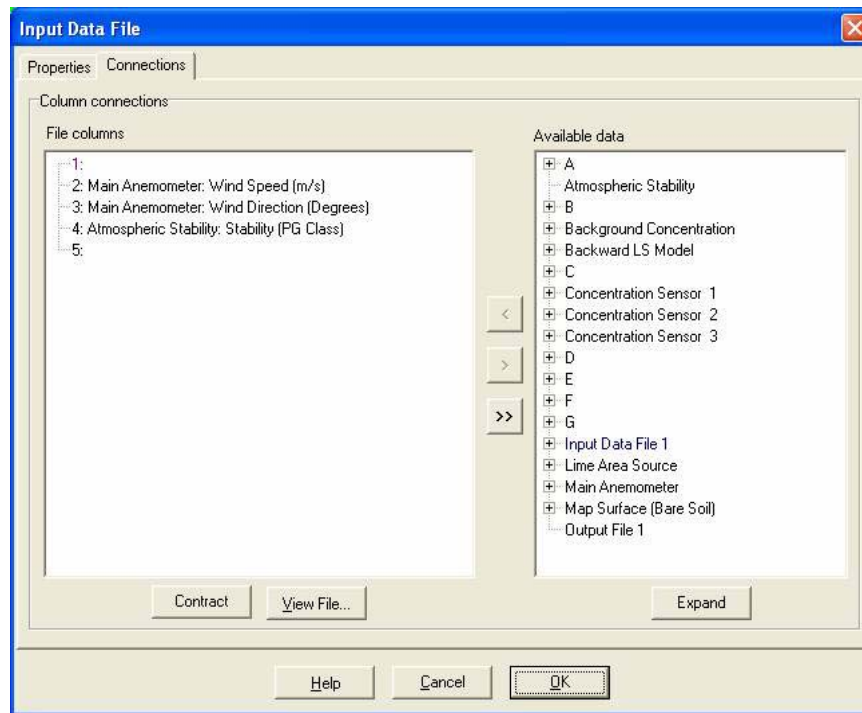


Figure 6.6. Input Data File Screen Shot.

After choosing OK on the Input Data File Screen, a green connecting line was then placed between the input data file icon and the project tower on the overall project grid as seen in the bottom center of Figure 6.7.

Next, receptors were placed at defined locations in the model (buttons #6 and #7 in Figure 6.3). Button #7 was used to put a single concentration receptor in the model. Button #6 was used to put a tower at a specific location so that multiple concentration

receptors and/or anemometers can be placed at different heights along the vertical stretch of the tower. For the model in this comparison, concentration receptors were placed at a 3.0 m height along the fence line at 76 m, 200 m, 322 m, 443 m, 570 m, 692 m, and 816 m. Additionally, a tower was placed at (412.5 m, 1140 m) with concentration receptors placed at 1.5 m, 3 m, and 6 m. All 10 concentration receptors in the model were set in the unknown mode of the sensor output by clicking on the unknown option under the “Measurement” tab of the concentration sensor window. At this point, the previously drawn area source was given an emission rate. For the comparison in this research an emission rate of $6 \mu\text{g}/\text{m}^2/\text{s}$ is used to determine relative concentrations at each receptor.

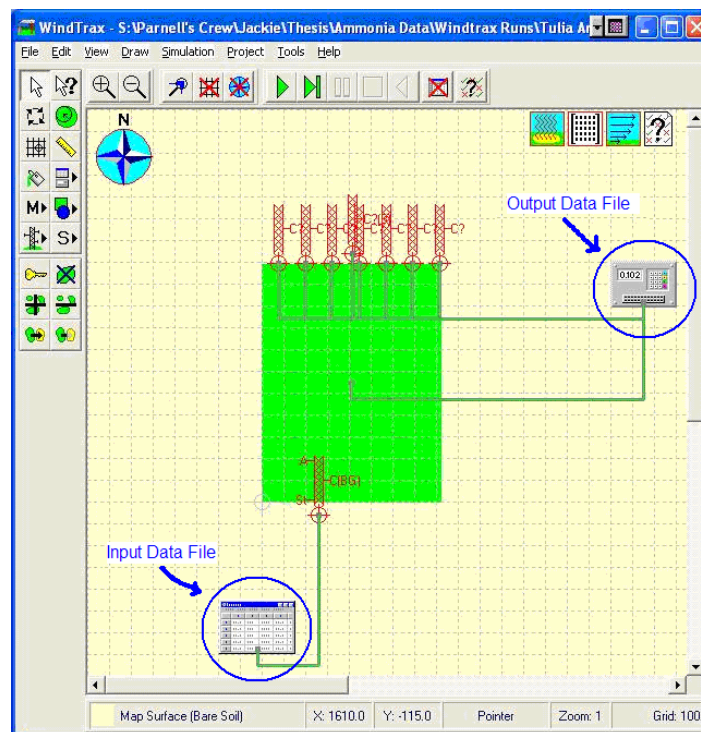


Figure 6.7. Screen Shot of the BLS Prior to Running the Model.

Finally, an output data file was needed to store the specified output of the model. The same file button as shown in Figure 6.3 and labeled with the number 4 was chosen as before. The output data option was chosen, and a small output data file icon was placed on the model's grid. Double-clicking on this icon opened the Output File box where the name of the output file was specified. Unlike the Input Data File menu, an output file did not have to previously exist. The model will create the new file. Under the "Connections" tab, the data desired in the output file was selected. After closing this box, the output data file icon was connected by a green line to each of the model components that will be written to the file as seen in Figure 6.7. Because the feedyard is bare soil, the soil surface data was left unchanged (the default for this parameter is bare soil).

With all of the inputs to the model specified, the model was run using the green arrow at the top of the screen. While the model ran, the individual backward particle trajectories were seen as a series of red dots on the model as seen in two different tests in Figure 6.8.

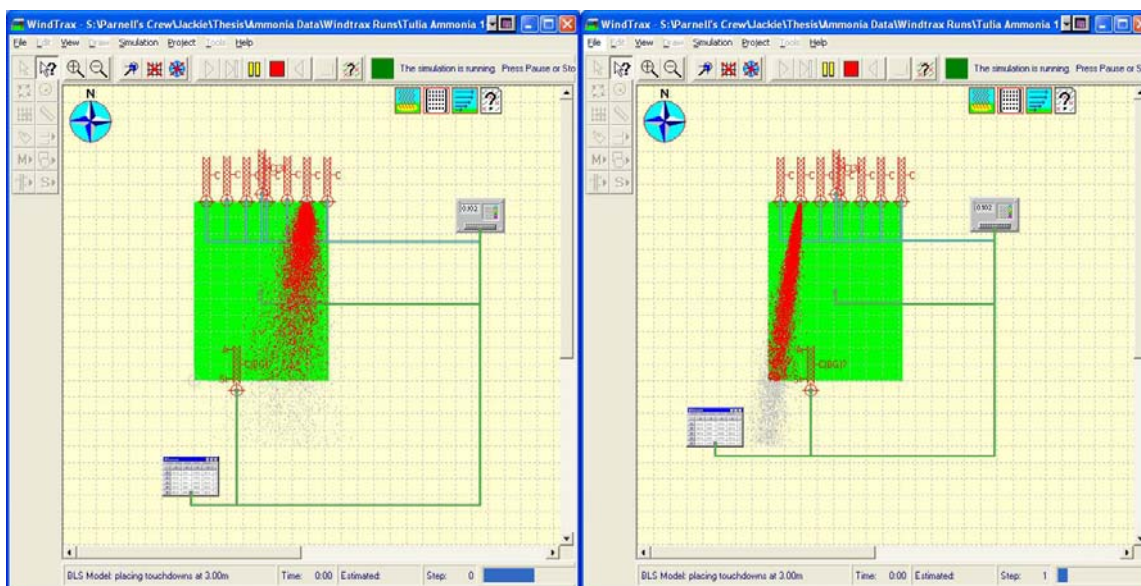


Figure 6.8. Examples of the BLS Model During 2 Different Runs.

After the model completed its run, the created output file was accessed to see the concentration data generated by the bLS model for a given emission rate. This information was then used to calculate the average emission rate for a test period. These calculation spreadsheets are included in Appendix F.

When the model ran with the current feedyard conditions, a warning was generated because the source to receptor distance (noted as the tracking distance in the model output) exceeded the 1 km specified maximum distance. The length of the feedyard was 9.5% over this maximum distance (1.095 km). The user's guide notes that the analysis of this model is restricted to source to receptor distances of less than about 1 km (Thunder Beach Scientific, 2003). Within a reasonably small error, the source to

receptor distance in the model was at the upper boundary of the source to receptor distance considered to be valid to run the model.

In order to ensure that the same outputs were being compared, the WindTrax model was run the same manner as ISC-ST3 in order to back-calculate an emission rate from the feedyard area source. This method was followed because the passive ammonia concentration data used was over a larger time frame than the relatively small Δt between concentration measurements assumed by the bLS model. So, a method similar to that used in determining the average emission rate for a time period with the ISC model was employed. Each test ran with the previously described layout, parameters, and a standard emission rate of $6 \mu\text{g}/\text{m}^2/\text{s}$. The bLS model was used to calculate pollutant concentrations at each of the input receptors with the given meteorological data and standard emission rate. For comparison purposes, the emission rate necessary to achieve a given concentration at a receptor was calculated in the exact same manner as the ISC model method previously described using equation 6.1.

Equation 6.1 shows the direct relationship that exists between the concentration (C) and the emission rate (Q), and the pre-modeling tests verify the validity of using this directly proportional relationship of C and Q. As C increased by a factor of x, Q also increased by a factor of x. Thus, by defining the initial emission rate guess into the bLS model, Windtrax, ($6 \cdot 10^6 \text{ g}/\text{m}^2/\text{s}$) as Q_1 and the output concentration at a receptor as C_1 , the actual net measured concentration, C_2 , was used to find the emission rate, Q_2 , needed to

generate this concentration as in equation 6.2. As previously done in the ISC model calculations, an average of the 10 receptor emission rate calculations was used to determine the average emission rate for the test period. This was done because no single more downwind sampler existed since the passive samplers were located on the same fence line of the feedyard. Using equation 6.3, the emission rate was used to generate the bLS predicted concentration at the receptor location had the average emission rate been used with the same input data (with the predicted concentration as C_2 and the average emission rate as Q_2).

This emission rate back-calculation process was performed for each set of test data. Table 6.3 shows the average emission rate results of the bLS analysis for each of the test periods. With the average emission rates for each test calculated, the bLS model results were in a form that could be easily compared to the Gaussian model results.

Table 6.3 Average Calculated Emission Rates Using WindTrax.

Test #	bLS ER	Test Length	Stability Classes
	g/m ² /s	(hrs)	
111	9.05E-05	2	D, C
112	1.03E-04	3	C, B, C
113	6.99E-05	3	All D
114	4.84E-05	12	All D
121	3.64E-05	7	D,D,D,D,D,D,C
122	9.09E-05	5	All D
123	5.57E-05	12	All D
131	6.31E-05	3	All D
132	1.08E-04	3	All D
133	1.08E-04	3	All D
134	7.55E-05	3	All D
135	4.67E-05	12	All D
141	4.67E-05	3	D, D, C
142	3.53E-05	3	C, C, B
143	5.68E-05	3	All B
144	8.22E-05	3	C, C, D
145	3.14E-05	12	All D
151	6.51E-05	3	All D
152	7.24E-05	3	C, C, B
153	1.13E-04	3	B, C, C
154	8.56E-05	3	All D
155	1.86E-05	12	D, D, D, D, E, E, E, E, E, D, D, D

Model Output Discussion

After running the Gaussian based ISC-ST3 model and the backward Lagrangian Stochastic based WindTrax models, the outputs can be compared. The average emission rate for each test as computed by each model were computed in a way to ensure that the model inputs are the same. Table 6.4 summarizes the comparison of the emission rates from the two models evaluated in this research: the EPA regulatory approved ISC-ST3 Gaussian based dispersion model and the backward-Lagrangian Stochastic based WindTrax model. The first column of Table 6.4 indicates the test number of the data. The second column shows the emission rate generated by the ISC model (Gaussian based). The third column displays the emission rate generated by the WindTrax model (bLS based). The fourth column calculates the difference between the bLS model and the ISC model. The next column computes the order of magnitude difference between the emission rates generated in each model (it is the bLS back-calculated emission rate divided by the ISC back-calculated emission rate).

When the model generated back-calculated emission rates are compared, it is interesting to see the emission rates only differ by a factor of 10. Additionally, a comparison of the individual test data pieces in Appendices E and F reveals that the calculated emission concentrations from each model are extremely close. The implications of these observations are discussed in Chapter VII.

Literature evaluated in Chapter III notes that assuming a continuously emitting source and homogenous turbulence, the Gaussian plume equation becomes the solution to the Lagrangian equation (Lamb and Seinfeld, 1973). A complete derivation of this solution can be found in the paper written by Lamb and Seinfeld (1973). However, in

Table 6.4. Overall Comparison of Summary Model Outputs.

Test #	ISC ER	bLS ER	Diff	Factor (bLS/ ISC)	Day/ Night	Δt	Stability Classes
	$\mu\text{g}/\text{m}^2/\text{s}$	$\mu\text{g}/\text{m}^2/\text{s}$	$\mu\text{g}/\text{m}^2/\text{s}$			(hrs)	
111	8.66	90.5	81.9	10.46	Day	2	D, C
112	1.03	103	93.1	10.06	Day	3	C, B, C
113	6.68	69.9	63.3	10.47	Day	3	All D
114	4.64	48.4	43.7	10.43	Night	12	All D
121	3.60	36.4	32.8	10.11	Day	7	D,D,D,D,D,D,C
122	7.62	90.9	83.2	11.93	Day	5	All D
123	5.31	55.7	50.3	10.49	Night	12	All D
131	6.03	63.1	57.1	10.46	Day	3	All D
132	10.3	108	97.5	10.43	Day	3	All D
133	10.5	108	97.4	10.25	Day	3	All D
134	7.17	75.5	68.3	10.53	Day	3	All D
135	4.47	46.7	42.3	10.45	Night	12	All D
141	4.42	46.7	42.3	10.57	Day	3	D, D, C
142	3.90	35.3	31.4	9.06	Day	3	C, C, B
143	7.06	56.8	49.7	8.04	Day	3	All B
144	8.14	82.2	74.0	10.09	Day	3	C, C, D
145	2.98	31.4	28.4	10.53	Night	12	All D
151	6.56	651	58.5	9.93	Day	3	All D
152	7.53	72.4	64.8	9.61	Day	3	C, C, B
153	11.4	113	102	9.96	Day	3	B, C, C
154	8.15	85.6	77.5	10.51	Day	3	All D
155	2.48	18.6	16.2	7.50	Night	12	D, D, D, D, E, E, E, E, E, D, D, D
Overall Average	6.72	68.3	61.6	10.17		5.3	
Day Average	7.53	76.6	69.1	10.18		3.3	
Night Average	3.98	38.5	34.5	9.68		12.0	

nonstationary and inhomogenous turbulence, the Gaussian equation estimates the Lagrangian model within a reasonable order of magnitude in practical circumstances (Lamb and Seinfeld, 1973). Thus, it is not all too surprising how close these emission rate back-calculations are. What is troubling, though, is the factor of 10 (an order of magnitude) difference between the two model calculations. This phenomena occurs in all of the trials, no matter the atmospheric stability.

Additionally, it is interesting to note that the factor slightly decreases for test number 143, in which the stability class is B (moderately unstable) for each hour during the measurement time. In a moderately unstable atmosphere, the rate of cooling of an air parcel moving upward is less than that of the surrounding air, so it is rapidly accelerated upward due to buoyant forces (Cooper and Alley, 2002). Also, as the air parcel moves downward, buoyant forces cause the particle to accelerate downward due to the parcel warming at a slower rate than its surrounding environment (Cooper and Alley, 2002). Thus, this moderately unstable stability class is characterized by much more vertical mixing. This increased instability likely leads to an increase in the uncertainty in both model outputs and a decrease in the factor of difference between the models. This is because the Gaussian model does not model unstable atmosphere accurately (Trinity Consultants, 2000), and it serves as a solution to the Lagrangian model (Lamb and Seinfeld, 1973).

CHAPTER VII

CONCLUSIONS AND FUTURE RESEARCH

This research focused on the emission rate determination procedure used in the permitting and regulation of facilities under the Clean Air Act. Using gathered pollutant concentration data, a defined mathematical model (dispersion modeling) was used to back-calculate the emission rate of a pollutant from a given source. Using this generated source pollutant emission rate and the meteorological conditions, future estimates of pollutant concentrations downwind of a source were predicted. These modeled downwind concentrations are the basis for which these facilities are regulated.

This research specifically evaluated particulate matter and ammonia concentration data as well as two modeling methods, a backward Lagrangian stochastic model and a Gaussian plume dispersion model. The analysis estimated the uncertainty surrounding each sampling procedure in order to gain a better understanding of the uncertainty in the final emission rate calculation (a basis for federal regulation). Additionally, the differences between emission rates generated using two different dispersion models, a Gaussian based model and a backward-Lagrangian stochastic model, were assessed.

An evaluation of the emission rates generated by both the Industrial Source Complex (Gaussian) model and the WindTrax (backward-Lagrangian stochastic) model revealed that the calculated emission concentrations (Q_2 as used in equations 6.2 and 6.3) from

each model using the average emission rate generated by the model are extremely close. Though, as previously mentioned and seen in Table 6.4, the average emission rates calculated by the models varied by a factor of 10. This is extremely troubling.

Current and future sources are regulated by the emission rate data from previous time periods. Emission factors are published for regulation of various sources, and these emission factors are derived based upon back-calculated model emission rates and site management practices. Thus, a factor of 10 ratio in the emission rates could prove troubling in terms of regulation if the model that the emission rate is back-calculated from is not used as the model to predict a future downwind pollutant concentration.

For example, it is necessary to look at interchanging the two back-calculated emission rates. If the emission rate generated by the ISC (Gaussian) model is used in the WindTrax (bLS) model and assuming the validity of the two models, then the predicted downwind concentrations will be almost a factor of 10 *less* than what the actual concentration is downwind of the source. An under-representation of the downwind pollutant concentration could lead to jeopardizing the public health and welfare, which is entirely opposite the mission of the Clean Air Act. Or the opposite situation could occur. If the emission rate generated by the WindTrax (bLS) model is used in the ISC (Gaussian) model and assuming the validity of the two models, the model would overpredict the downwind pollutant concentration, resulting in the over regulation of an emitting source. This affirms the thought that emission rates back-calculated from one

model cannot be used as the input into another model and result in valid downwind concentration predictions. Regulatory agencies are looking into moving to Calpuff as the dispersion modeling standard. Currently, there are a large number of published emission rates and emission factors used for regulatory compliance monitoring based off of the ISC model. Will these values be valid in other regulatory models? Future research needs to address this question.

Neither of these scenarios is desirable, but they illustrate the importance of properly reported data and the effect that improperly reported scientific data can have on the environment surround us. Nonetheless, realistic engineering and sound science is vital not only in the creation of public policy but also in the enforcement of this policy.

Additional future research will be to further determine the wind velocity profile as well as determining the vertical temperature gradient during the modeling time period. This information will help to further quantify the uncertainty of the meteorological model inputs, which will aid in understanding the propagated uncertainty in the modeling outputs.

Numerous groups impact the regulation of air pollution including regulated industries, regulating agencies (the EPA as well as SAPRAs), scientists, engineers, the public, and special interest groups. However, regulatory decision making must rely upon sound science and engineering as the core of appropriate policy making (objective analysis in lieu of

subjective opinion). Various single interest groups attempt to make public statements based upon poor science and engineering in order to manipulate public opinion and impact the air pollution regulatory decisions negatively. The regulatory agencies have to continue to keep its goal in sight: to protect the public health and welfare in the most economically feasible way. The only way to accomplish this is to lean upon the expertise of the scientific community, who understand the impact of appropriate scientific publication, to provide the most sound science available. Additionally, regulatory agencies must rely upon the knowledge of the engineers, who apply the sound science practices while considering feasibility, when engaging in regulatory policy actions. And these engineers must continue to be knowledgeable of and involved in regulatory policy decision making, implementation, and evaluation.

REFERENCES

- 40 CFR Part 50. 1999. *National Primary and Secondary Ambient Air Quality Standards*. Washington, DC: USEPA.
- 40 CFR Part 51. 1999. *Legally enforceable procedures*. Washington, DC: USEPA.
- 40 CFR Part 53. 1999. *Ambient Air Monitoring Reference and Equivalent Methods*. Washington, DC: USEPA.
- 40 CFR Part 60. 2002. *Standards of Performance for New Stationary Sources*. Washington, DC: USEPA.
- 40 CFR Part 61. 1999. *National Emission Standards for Hazardous Air Pollutants*. Washington, DC: USEPA.
- 40 CFR Part 63. 1999. *National Emission Standards for Hazardous Air Pollutants for Source Categories*. Washington, DC: USEPA.
- 40 CFR Part 70. 1999. *State Operating Permit Program*. Washington, DC: USEPA.
- 40 CFR Part 71. 1996. *Federal Operating Permit Program*. Washington, DC: USEPA.
- Alaska Department of Environmental Conservation v. EPA*. 2004. Supreme Court of the United States, January 2004; 124 S. Ct. 983; 157 L. Ed. 2d 967; 2004 U.S. LEXIS 820; 72 U.S.L.W. 4133; 57 ERC (BNA) 1801; 17 Fla. L. Weekly Fed. S 105.
- American Trucking Associations (ATA) v. EPA*. 2002. United States Court of Appeals for the D.C. Circuit, March 26, 2002; 283 F.3d 355; 2002 U.S. App. LEXIS 4985.
- American National Standards Institute/American Society of Mechanical Engineers (ANSI/ASME). 1998. *Test Uncertainty, Performance Test Code 19.1 – 1998*. New York: ASME.
- Aneja, V. P., D. R. Nelson, P. A. Roelle, and J. T. Walker. 2003. Agricultural Ammonia Emissions and Ammonium Concentrations Associated with Aerosols and Precipitation in the Southeast United States. *Journal of Geophysical Research*, 108(D4): 4152.

- Aneja, V. P., P. A. Roelle, G. C. Murray, J. Southerland, J. W. Erisman, D. F. Willem, A.H. Asman, and N. Patni. 2001. Atmospheric Nitrogen Compounds II: Emissions, Transport, Transformation, Deposition and Assessment. *Atmospheric Environment*, 35: 1903-1911.
- Appl, M. 1999. *Ammonia: Principles and Industrial Practice*. Weinheim, Germany: Wiley-VCH.
- Arogo, J., P.W. Westerman, A.J. Heber, W.P. Robarge, and J.J. Classen. 2001. Ammonia in Animal Production – A Review. *2001 ASAE Annual International Meeting*. Paper No. 014089. St. Joseph, MI.: ASAE.
- Arya, S. P. 2001. *Introduction to Micrometeorology*. San Diego, CA: Academic Press.
- Battye, R., W. Battye, C. Overcash, and S. Fudge. 1994. *Development and Selection of Ammonia Emission Factors*. EPA/600/R-94/190. Research Triangle Park, NC: U.S. EPA, Office of Research and Development
- Builtjes, P. 2003. The Problem – Air Pollution. Chapter 1 of *Air Quality Modeling – Theories, Methodologies, Computational Techniques, and Available Databases and Software. Volume I – Fundamentals*. P Zannetti, Ed. Pittsburgh, PA: Air & Waste Management Association.
- Center for Agricultural Air Quality Engineering and Science (CAAQES). 2004. Dispersion Modeling with ISCST3 in BREEZE. Instructional Handout. College Station, TX: Texas A&M CAAQES.
- Chevron, USA, Inc. v. Natural Resources Defense Council*. 1984. United States Supreme Court, 467 U.S. 837, 104 S.Ct. 2778, 81 L.Ed.2d 694.
- Coleman, Hugh W., and W. G. Steele. 1999. *Experimentation and Uncertainty Analysis for Engineers*. (2nd ed.) New York: John Wiley & Sons.
- Cooper, C. D. and F.C. Alley. 2002. *Air Pollution Control: A Design Approach*. (3rd ed.) Prospect Heights, IL.: Waveland Press, Inc.
- Flesch, T.K., J.D. Wilson, L.A. Harper, B.P. Crenna, and R.R. Sharpe. 2004a. Deducing Ground-to-Air Emissions from Observed Trace Gas Concentrations: A Field Trial. *Journal of Applied Meteorology*, 43: 487-502.
- Flesch, T.K., J.D. Wilson, L.A. Harper, R.R. Sharpe, and B.P. Crenna. 2004b. Tracer Emissions Inferred from a Backward Lagrangian Stochastic Dispersion Model: A Validation Study. In *Proceedings of the 25th Conference on Agricultural & Forest Meteorology*, Paper No. 9.8. Seattle, WA.

- Flesch, T. K., J. D. Wilson, and E. Yee. 1995. Backward-Time Lagrangian Stochastic Dispersion Models and Their Application to Estimate Gaseous Emissions. *Journal of Applied Meteorology*, 34: 1320-1332.
- Fritz, B.K. 2002. Dispersion modeling of Particulate Emission from Low Level Point Sources. Unpublished PhD diss. College Station: Texas A&M University, Department of Biological and Agricultural Engineering.
- Goodrich, L.B., C.B. Parnell, Jr., S. Mukhtar, R.E. Lacey, and B.W. Shaw. 2003. A Science-Based PM10 Emission Factor for Freestall Dairies. 2003 Annual International Meeting of the American Society of Agricultural Engineers. Paper No. 034115. St. Joseph, MI.: ASAE.
- Gupta, A., R. Kumar, K. M. Kumari and S. S. Srivastava. 2003. Measurement of NO₂, HNO₃, NH₃ and SO₂ and related particulate matter at a rural site in Rampur, India. *Atmospheric Environment*, 34(34): 4837-4846.
- Hinds, W. C. 1999. *Aerosol Technology*. New York: John Wiley & Sons.
- Holman, J.P. 2001. *Experimental Methods for Engineers*. (7th ed.). Boston, MA: McGraw Hill.
- International Standards Organization (ISO). 1995. *Guide to the Expression of Uncertainty in Measurement*. Geneva, Switzerland: ISO.
- Kline, S.J. 1985. The Purposes of Uncertainty Analysis. *Journal of Fluids Engineering*. 107: 153-161.
- Kline, S.J., and F.A. McClintock. 1953. Describing Uncertainties in Single-Sample Experiments. *Mechanical Engineering*. 75: 3-8.
- Lacey, R. E., J. S. Redwine, C. B. Parnell, Jr. 2002. Emission Factors for Broiler Production Operations: a Stochastic Modeling Approach. 2002 Annual International Meeting of the American Society of Agricultural Engineers. ASAE Paper No. 024212. St. Joseph, MI.: ASAE.
- Lamb, R. G. and J. H. Seinfeld. 1973. Mathematical Modeling of Urban Air Pollution – General Theory. *Environmental Science & Technology*. 7: 253-261.
- Langford, A.O., F.C. Fehsenfeld, J. Zachariassen, and D.S. Schimel. 1992. Gaseous Ammonia Fluxes and Background Concentrations in Terrestrial Ecosystems of the United States. *Global Biogeochem. Cycles*, 4: 459-483.

- Liu, M. K., and J. H. Seinfeld. 1975. On the Validity of Grid and Trajectory Models of Urban Air Pollution. *Atmospheric Environmen*, 9: 555-574.
- Makar, P.A., M.D. Moran, M.T. Scholtz, and A. Taylor. 2003. Speciation of Volatile Organic Compound Emissions for Regional Air Quality Modeling of Particulate Matter and Ozone. *Journal of Geophysical Research*, 108(D2), 4041.
- Ministry of Agriculture, Fisheries and Food (MAFF). 1998. *Code of Good Agricultural Practice for the Protection of Air*. London, United Kingdom: Welsh Office Agriculture Department.
- National Institute of Standards and Technology (NIST). 1994. *Guidelines for Evaluating and Expressing the Uncertainty of NIST Measurement Results*. NIST Technical Note 1297. United States Department of Commerce. Washington, DC: US GPO.
- Olesen, J.E. and S.G. Sommer. 1993. Modeling Effects of Wind Speed and Surface Cover on Ammonia Volatilization from Stored Pig Slurry. *Atmospheric Environment*, 27:2567-2574.
- Parnell, Jr., C. B. 2000. *Engineering Implications of Air Quality Regulations for Agriculture*. Continuous Professional Development Course #7. Texas A&M University & ASAE SE-305.
- Parnell, Jr., C. B. and S. E. Parnell-Molloy. 2002. Air Pollution Regulatory Process (APRP) and Agricultural Operations. *2002 Annual International Meeting of the American Society of Agricultural Engineers*. ASAE Paper No. 024218. St. Joseph, MI.: ASAE.
- Perrino, C. and M. Gherardi. 1999. Optimization of the Coating Layer for the Measurement of Ammonia by Diffusion Denuders. *Atmospheric Environment*, 33: 4579-4587.
- Puxbaum, H., G. Haumer, K. Moser, and R. Ellinger. 1993. Seasonal Variation of HNO₃, HCl, SO₂, NH₃, and Particulate Matter at a Rural Site in Northeastern Austria. *Atmospheric Environment*, 27A(15): 2445-2447.
- Rabaud, N. E., T. A. James, L. L. Ashbaugh, and R. G. Flocchini. 2001. A Passive Sampler for the Determination of Airborne Ammonia Concentrations near Large-Scale Animal Facilities. *Environmental Science & Technology*, 35: 1190-1196.
- Schoenbaum, T. J., R. H. Rosenberg, and H. D. Doremus, ed. 2002. *Environmental Policy Law: Problems, Cases, and Readings* (4th ed.). New York: Foundation Press.

- Seinfeld, J. H. and S. N. Pandis. 1998. *Atmospheric Chemistry and Physics: From Air Pollution to Climate Change*. New York: John Wiley & Sons, Inc.
- Sorenson, J.W., and C. B Parnell, Jr. 1991. *Agricultural Processing Technology*. College Station: Texas A&M University.
- Sullivan, T. F., ed. 2001. *Environmental Law Handbook* (16th ed.). Rockville, MD: Government Institutes.
- Texas Natural Resource Conservation Commission (TNRCC). 2001. *Guidance for Conducting Ecological Risk Assessments at Remediation Sites in Texas*. Toxicology and Risk Assessment Section. Austin, TX: TNRCC.
- Thunder Beach Scientific. 2003. *Welcome to WindTrax*. Edmonton, Alberta, Canada: Thunder Beach Scientific.
- Trinity Consultants. 2000. *Fundamentals of Dispersion Modeling*. Dallas, TX: Trinity Consultants.
- Turner, D. B. 1964. A Diffusion Model for an Urban Area. *Journal of Applied Meteorology*, 3: 83-91.
- US EPA. 2002. *Review of Emission Factors and Methodologies to Estimate Ammonia Emissions from Animal Waste Handling*. Research Triangle Park, NC: U.S. EPA, Office of Research and Development.
- US EPA, 2000a. *Meteorological Monitoring Guidance for Regulatory Modeling Applications*. EPA-454/R-99-005. Research Triangle Park, NC: US GPO.
- US EPA. 2000b. *Supplements to the Compilation of Air Pollutant Emission Factors, AP-42* (5th ed.), *Volume I: Stationary Point and Area Sources*. Research Triangle Park, NC: US GPO.
- US EPA. 1995. *Compilation of Air Pollutant Emission Factors, AP-42*. (5th ed.) *Volume I: Stationary Point and Area Sources*. Research Triangle Park, NC: US GPO.
- Wang, L. 2000. A New Engineering Approach to Cyclone Design for Cotton Gins. MS Thesis. College Station, Texas: Texas A&M University, Department of Biological and Agricultural Engineering.

- Wanjura, J. D., C. B. Parnell, Jr., R. E. Lacey, B. W. Shaw, and M. D. Buser. 2003. Dispersion Modeling of Agricultural Low Level Point Sources. *2003 ASAE Annual International Meeting*. ASAE Paper No. 034117. St. Joseph, MI.: ASAE.
- Warneck, P. 2000. *Chemistry of the Natural Atmosphere*. (2nd ed.) San Diego, CA: Academic Press, Inc.
- Yamamoto, N., N. Kabeya, M. Onodera, S. Takahahi, Y. Komori, E. Nakazuka, and T. Shirai. 1988. Seasonal Variation of Atmospheric Ammonia and Particulate Ammonium Concentrations in the Urban Atmosphere of Yokohama over a 5-Year Period. *Atmospheric Environment*, 22(11): 2621-2623.
- Yegnan, A., D.G. Williamson, A.J. Graettinger. 2002. Uncertainty Analysis in Air Dispersion Modeling. *Environmental Modeling & Software*. 17: 639-649.

Supplemental Sources Consulted

- Arya, S. P. 1999. *Air Pollution Meteorology and Dispersion*. New York: Oxford University Press, Inc.
- Bertram, H., T. Flesch, S. McGinn, T. Coates, P. Dzikowski, P. Llewellyn, and L. Cheng. 2003. *Measurement of Ammonia Emissions from Intensive Livestock Facilities by Open Path Tunable Diode Laser*. Alberta, Canada: Alberta Research Council.
- Devore, J. L. 1995. *Probability and Statistics for Engineering and the Sciences*. (4th ed.). Pacific Grove, CA: Brooks/Cole.
- National Academy of Sciences. 2004. Preventing Air Pollution Requires Broader Approach, Panel Finds. Press Release. Available at: <http://usinfo.state.gov/gi/Archive/2004/Feb/02-204575.html>. Accessed: 08 April 2004.
- Stavins, R. N. 2004. Introduction to the Political Economy of Environmental Regulation. Regulatory Policy Program Working Paper RPP-2004-03. Cambridge, MA: Center for Business and Government, John F. Kennedy School of Government, Harvard University.
- US EPA. 1990. *Clean Air Act Amendments*. Available at http://www.epa.gov/oar/oaqps/peg_caa/pegcaain.html. Accessed 25 May 2004.
- Wark, K., C. F. Warner, and W. T. Davis. 1998. *Air Pollution: Its Origin and Control*. (3rd ed.). Menlo Park, CA: Addison-Wesley.

APPENDIX A

APPENDIX A

**FURTHER DISCUSSION ON THE IMPORTANCE OF
ENGINEERING IN REGULATORY DECISION MAKING**

Engineering plays an essential role in the regulatory process. The engineer designs the least costly air pollution abatement system(s) to achieve and maintain compliance with these rules and regulations. Therefore, it is critical that engineers remain actively involved in the formulation of air pollution policy. The courts do not and cannot be expected to have the scientific or engineering knowledge to adequately assess the validity of the science from a technical standpoint.

This is where the difference between a law and a regulation come into play, and why engineering expertise is essential in the formulation of both. The Clean Air Act is a law, and must be followed no matter what (laws must be followed no matter how inappropriate they may be in individual circumstances). For example, in the Clean Air Act Amendments of 1990, Congress wrote in a provision that required states to reduce Volatile Organic Compound (VOC) emissions in all ozone non-attainment areas of all industries by 3% per year. This seems like a rational and worthy idea on the surface: VOCs and NO_x each combine with the hydroxyl radical to eventually form ozone through a set of chemical reactions, so a reduction in VOCs will reduce ozone formation. However, that is not the entire picture and will not solve the initial intent of Congress to bring ozone non-attainment areas into attainment.

First, the VOC and NO_x molecules compete with each other for the hydroxyl radical. This competition causes the ozone production to be dependant on not only the VOC concentration but also the NO_x concentration, displayed graphically by scientists in an ozone isopleth diagram (Seinfeld and Pandis, 1998). This relationship diagram shows that a reduction in VOCs can actually lead to *no change at all* in the ozone concentration, when the NO_x concentration remains the same, and if the NO_x concentration increases or decreases while the VOC concentration decreases, then the amount of ozone produce can actually *increase* (depending on where you are in the isopleth diagram). In most of the troposphere, which is the atmospheric layer closest to the Earth's surface, the availability of NO_x governs the production of ozone (except in area with unusually strong sources of NO_x), not simply the VOC concentration (Seinfeld and Pandis, 1998).

To exacerbate this problem, look at the environmental conditions naturally surrounding Houston, Texas, for example. Not only is there the challenge of the VOC/NO_x ratio, but also there is the factor that it would cost the industries in the city around \$1 billion dollars to meet this 3% industry decrease. And it wouldn't even have an impact on the ozone concentrations (Parnell and Parnell-Molloy, 2002)! Why? Biogenics, which are plants, bushes, grass, and trees, contribute to over 50% of the reactive VOCs in the Houston area. Thus, reducing VOC concentration from industrial facilities by 3% will hardly have an impact on the amount of ozone formation in a non-attainment area such

as Houston, Texas. However, the Texas SAPRA must follow this provision in the Clean Air Act Amendments because this is written into law by Congress, and you have to follow the law.

On the contrary, the classification of an area as *non-attainment* is part of a regulation. To declare an area as non-attainment, the pollutant concentration measurements must exceed the NAAQS three or more times in that area during the regulated time period. Sometimes these exceedances are due to natural causes and cause an area to become misclassified. For example, the EPA wanted to designate Lubbock, Texas, as a non-attainment area for Particulate Matter (PM). However, a large number of the NAAQS exceedances occurred during sand storms, a natural phenomena, in the area (Parnell, 2000). The Texas SAPRA went back and forth with the EPA because the EPA staff was not located in the panhandle of Texas and did not understand the concept of a sand storm and continued to insist classifying this area as non-attainment (Parnell, 2000). However, after the EPA staff was in a meeting with the Texas SAPRA in the Lubbock area, the vehicle they were driving was forced to pull over due to a lack of visibility from a sand storm. Needless to say, Lubbock was not classified as non-attainment for PM (Parnell, 2000).

Air Pollution Litigation

In a discussion of regulatory policy, it is necessary to explore some important pieces of air pollution litigation, both past and present.

Chevron, USA, Inc. v. Natural Resources Defense Council

United States Supreme Court, 1984

First, *Chevron, USA, Inc. v. Natural Resources Defense Council*, is one of the most cited in future air pollution regulation cases. This case deals with a question of a federal agency's (in specific, the EPA's) interpretation of a vague Congressional statute (*Chevron*, 1984). It affirms the power of an administrative agency to oversee a congressionally created program and to fill in any gaps left by Congress. The Clean Air Act Amendments of 1977 served as a key piece of legislation and incorporated many changes and additions to the Clean Air Act. These amendments held the same federal basic philosophy: federal management (oversight) with state implementation.

At this time, the EPA decided to allowed *bubble* definitions of pollution sources in Clean Air Act non-attainment areas. The bubble policy permits polluters to treat entire plants as if they exist under a large bubble. This is important because it would allow a polluting company to change processes and equipment within the bubbled plant as long as the total amount of pollution coming out of the bubble does not increase. The Court of Appeals ruled that the pollution reducing purpose of the non-attainment area

provisions made the EPA's *bubble* policy inappropriate for use in those areas. The Supreme Court upheld the Court of Appeals decision that the term *source* was ambiguous and the *bubble* policy is appropriate when the goal is to *maintain* the air quality in a specific area. However, the goal of a non-attainment area is to improve area quality. Therefore, the use of a *bubble* policy in a non-attainment area was inappropriate (Chevron, 1984).

In formulating this *Chevron* decision, the US Supreme Court defines 2 questions to evaluate when reviewing an agency's creation of the statute which it administers (Chevron, 1984):

Has Congress directly addressed the precise question of the issue?

(aka "Chevron Step 1")

If the statute is ambiguous with respect to the specific issue (the answer to question 1 is no), is the agency's answer based on a permissible construction of the statute?

(aka "Chevron Step 2")

This case is just one of the many air pollution cases that depends on the science and the application of the science in the regulatory policy (the law) as well as EPA's implementation of this science and engineering in their decision making process. Engineering input in the policy making as well as the policy implementation is essential.

American Trucking Associations v. EPA

United States Court of Appeals for the D.C. Circuit, March 2002

In 1997, the EPA issued more stringent NAAQS for PM and ozone. Thus, these NAAQS and related implementation decisions by the EPA became the focus of much litigation. This case is actually the consolidation of much litigation between the American Trucking Associations (ATA) and the EPA (*ATA*, 2002). This decision was on remand from the US Supreme Court. Basically, the ATA challenged the EPA on these NAAQS. Initially, the ATA raised a number of concerns across a broad range of issues, including the constitutionality of the Clean Air Act and the legality of these standards. The Court of Appeals (as well as the Supreme Court) held that economic standards were to play no part in the formulation of ambient air standards. The Court contended that the EPA announced the potential changes to the NAAQS, opened them up for public comment (and received more than 50,000 comments), and considered these comments as well as the latest scientific information when settling the final NAAQS (*ATA*, 2002). The petitioners claimed that the EPA failed to establish a “safe” level for PM; however, the Court notes that the EPA did identify “safe” PM levels through thorough review of epidemiological studies. Also, the Court remarks that EPA’s lack of ability to guarantee the accuracy or increase the precision of these PM NAAQS does not challenge the validity of these standards; moreover, it simply indicates the scientific uncertainty surrounding the health effects of the pollutant at low concentrations.

Yet again, practical engineering input is essential in the development of air pollution regulatory standards (the NAAQS). Engineering input not only helps to identify the potential environmental impacts of the potential policy, but also recognizes the impacts of this policy on industry.

Alaska Department of Environmental Conservation v. EPA

United States Supreme Court, January 2004

Next, one of the most recent pieces of litigation concerning air pollution and the EPA's role is a lawsuit settled by the United States Supreme Court in January, 2004, *Alaska Department of Environmental Conservation v. EPA*, by an extremely divided court (with a final vote of 5 justices assenting, 4 justices dissenting). Basically, this case affirmed the EPA as the ultimate regulatory authority over every SAPRA as implied by the Clean Air Act (*Alaska, 2004*). In this ruling, the US Supreme Court reaffirmed Clean Air Act § 113(a)(5), which allows the EPA to intervene when it does not feel that a SAPRA has abided by a requirement in the Clean Air Act.

The SAPRA, the Alaska Department of Environmental Conservation (ADEC), reissued a company a PSD (Prevention of Significant Deterioration program – part of the Clean Air Act) permit when the facility expanded. The original PSD permit listed a certain technology as the Best Available Control Technology (BACT), which is defined as the technology that achieves the reduction in pollutant concentration at the least cost.

However, in the renewal process, the company requested to use a different technology other than the BACT and could not quantifiably justify the usage of this different control technology in lieu of the BACT. The EPA claimed that the SAPRA accepted this PSD permit change in error, and the company must utilize the specified BACT because it has failed to quantifiably prove that the BACT places an undue burden on the industry, which is larger than that of the low – NO_x technology (*Alaska*, 2004).

Nonetheless, realistic engineering is vital not only in the policy creation but also in the permitting process. Had the company identified the low – NO_x technology in the PSD permit as the BACT, there would be no basis for this case. Not only did this case reaffirm the position of the EPA as the ultimate regulatory authority, but also it affirmed the importance of sound engineering in the process of permit writing, whether the permitted party is specifying a BACT or a pollutant allowable emission rate. The information contained in the approved permit will be the foundation of future regulation of the permitted facility.

APPENDIX B

APPENDIX B

FURTHER DISCUSSION ON AMMONIA –

PROPERTIES, SOURCES, AND POTENTIAL IMPACT

Molecular Properties

The ammonia molecule has a considerable dipole moment and bond angle similar to that of a water molecule due to the polarization of the hydrogen-nitrogen bonds and the asymmetrical molecular arrangement as seen in Figure B.1.

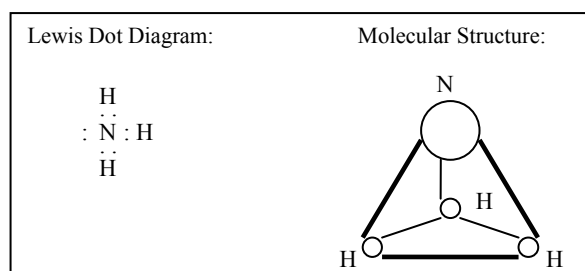


Figure B.1. Ammonia Diagrams.

Thus, due to its atomic molecular structure, ammonia tends to behave similarly in many reactions to water (Appl, 1999).

Physical Properties

As previously noted, the ammonia molecule reacts with other species similarly to the water molecule reaction. Thus, ammonia is extremely water soluble and is a good solvent. As a gas phase molecule, ammonia is the most prevalent alkaline gas in the atmosphere and reacts with the hydroxyl radical, sulfuric acid, ammonium hydrogen sulfate, nitric acid, and hydrochloric acid to form various ammonium aerosols.

When Effective Screening Level (ESL) thresholds are exceeded, potential consequences result from these over-threshold concentrations of oxidized and reduced forms of organic and inorganic nitrogen. First, ammonia serves as a precursor to the formation of small particles and exposure to large concentrations of these fine aerosols (PM_{2.5}) can lead to respiratory diseases. Second, unreacted ammonia can be absorbed by water molecules and redposited in the form of acid rain (wet deposition), disturbing the balance of biological systems in the environment (Aneja et al., 2001). This disturbance results in nitrate contamination of drinking water as well as eutrophication of species in the water, which is visible in the form of algae (Arogo et al., 2001). Next, NH₃ reactions result in an increase in concentration levels of N₂O, which is the primary source of NO_x in the stratosphere and a key component to ozone depletion in the stratosphere (Seinfeld and Pandis, 1998). Finally, this nitrogen saturates forest soils and results in soil acidification through the processes of nitrification and leaching (Arogo et al., 2001).

In general, literature notes that the ammonia concentration levels increase almost linearly as the ambient air temperature increases (Yamamoto, 1998; Warneck, 2000; US EPA, 2002). Thus, ammonia exhibits a strong diurnal variation with a maximum in the midday when the sun is at its peak in the sky and a minimum during the early morning right before the sun rises. Additionally, NH_3 exhibits a seasonal variation with summer concentration values greater than the winter concentration values (Warneck, 2000). These NH_3 molecules combine with other molecules in the atmosphere to form ammonium aerosols, as described by equations B.4 – B.8 in the next section.

Additionally, literature observes that when compared to NH_4^+ , the ratio of $\text{NH}_3/\text{NH}_4^+$ is usually less than one (Warneck, 2000). Thus, the NH_3 concentration is typically less than the concentration of NH_4^+ . Further research has shown that the concentration of the sulfate aerosol has a large impact on the amount of NH_3 that remains in the gas phase (Langford, et al., 1992). Thus, this demonstrates the strong binding force of the sulfuric acid molecule (H_2SO_4) in equation B.4.

Finally, the gas-to-particle conversion rate of NH_3 to NH_4^+ governs the NH_3 contribution to atmospheric nitrogen deposition. In the atmosphere, NH_3 has a relatively short lifetime ($\tau = 1\text{--}5$ days or less). NH_3 typically has a low source height and a relatively high dry deposition velocity; therefore, NH_3 tends to deposit close to its source. NH_4^+ has a longer atmospheric lifetime than NH_3 ($\tau = 1\text{--}15$ days) and is likely to deposit much farther downwind of sources than NH_3 (Arogo et al., 2001).

Sources

The biogenic decomposition of organic materials and fertilizer production and utilization produce atmospheric ammonia. Literature notes that ammonia emissions from animal operations contribute substantially to these NH₃ emissions (Battye et al., 1994; Aneja et al., 2003; Argo, et al., 2001). Table B.1 lists the various contributors and relative experimental estimates of NH₃ emissions in the U.S. It is important to note that research suggests that significant NH₃ emissions may exist from undisturbed soils as well as biomass burning and domestic animal excretions, which are not accounted for in Table B.1 (Battye, et al., 1994).

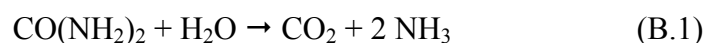
Table B.1. Relative Contribution of Ammonia Sources. (adapted from Battye, et al, 1994)

Source Category	Percentage of Ammonia Emissions in US
Cattle and Calves	43.4 %
Poultry	26.7 %
Hogs and Pigs	10.1 %
Fertilizer Application	9.5 %
Refrigeration	5.1 %
Publicly Owned Treatment Works	2.0 %
Combustion	1.3 %
Humans	1.2 %
Sheep and Lambs	0.7%
Industry AP-42	~ 0.0%

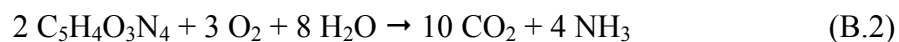
According to Table B.1, approximately 80% of Ammonia emissions result from nitrogen emissions from certain farm animals, such as cattle, calves, poultry, hogs, and pigs. These animals ingest a large amount of nitrogen containing substances in their feed. This intake subsequently produces ammonia through the bacterial activity involving their excreted organic nitrogen substrates (Arogo et al., 2001). Ammonia emissions are sensitive to fluctuations in factors such as the diet of the animals, atmospheric temperature and humidity, waste-handling practices, wind speed, and other source and surface characteristics. Due to the many uncertainties surrounding these factors, obtaining accurate ammonia emissions estimates becomes quite challenging (Aneja et al., 2003).

Bacterial activity involving the excreted organic nitrogen substrates from the various sources produces ammonia. Of this activity, the degradation of uric acid, urea, and undigested proteins are the primary sources of NH_3 production in livestock facilities (Arogo et al., 2001). The primary ammonia source comes from the hydrolysis of Urea ($\text{CO}(\text{NH}_2)_2$) in the reaction described by equation B.1. The secondary source of ammonia is the decomposition of Uric Acid ($\text{C}_5\text{H}_4\text{O}_3\text{N}_4$) in the reaction described by equation B.2. Additionally, undigested protein will also produce NH_3 through the mineralization process.

- Hydrolysis of Urea



- Aerobic Uric Acid Decomposition



Volatilization of Ammonia

Ammonia volatilization not only includes the production of ammonia but also incorporates the diffusive and convective transport within the NH_3 source and NH_3 transport through the surface boundary (Arogo et al., 2001). The NH_3 volatilization process has been explored by many researchers and can be summarized by Figure B.2 as presented in Arogo et al., 2001, where H is defined as Henry's Law constant, T is the temperature, v is the wind speed, K_d is the dissociation constant, pH is the pH of the source, and UA is the Urease activity.

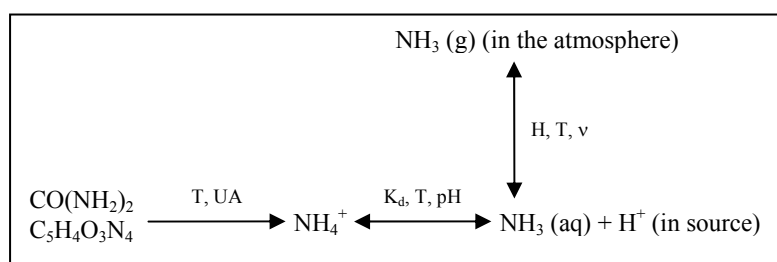


Figure B.2. Ammonia Volatilization Equilibria. (adapted from Arogo et al., 2001)

As seen in Figure B.2, different variables influence the ammonia volatilization equilibria. NH_3 volatilization increases curvilinearly with temperature, wind speed, and solution pH and linearly with the total ammoniacal nitrogen concentration (Olesen and

Sommer, 1993). Specifically, with a substance with a pH below 7, NH_3 is in the NH_4^+ form and not liable to volatilization (Arogo et al., 2001). Additionally, there exists a positive correlation of temperature and the dissociation constant, K_d , of the reaction, which is defined by equation B.3.

$$K_d = \frac{[\text{NH}_3][\text{H}^+]}{[\text{NH}_4^+]} \quad (\text{B.3})$$

where $[\text{NH}_3]$, $[\text{H}^+]$, and $[\text{NH}_4^+]$ define the molar concentrations of each of the respective species.

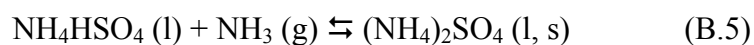
Ammonium Aerosol Formation Reactions

Five reactions characterize the usual formation of ammonium aerosols, a key component of secondary PM_{fine} ($\text{PM}_{2.5}$):

- Ammonium Hydrogen Sulfate



- Ammonium Sulfate



- Ammonium Nitrate



- Ammonium Chloride

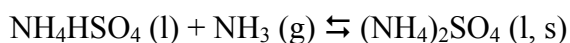
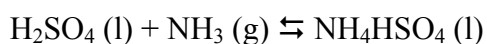


- Ammonium and Hydroxyl Radical (Dissociation)



This section will focus mainly on the first three reactions (reactions B.4 – B.6).

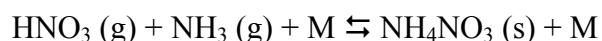
Ammonium Hydrogen Sulfate/Ammonium Sulfate Formation Reactions



For the Ammonium Sulfate formation, consider a simple system containing purely Sulfuric Acid (H_2SO_4), NH_3 , and water. Seinfeld and Pandis graphically depict the aerosol composition for a system as a function of total concentration using the molar ratio of NH_3 and H_2SO_4 . First, according to Seinfeld and Pandis, when the ratio is less than 0.5, which is a case of very acidic atmospheres, H_2SO_4 solutions dominate the aerosol particle type (1998). When the ratio is between 0.5 and 1.25, NH_4HSO_4

dominates the system's aerosol component. As the ratio goes from 1.25 to 1.5, the salt letovicite $[(\text{NH}_4)_3\text{H}(\text{SO}_4)_2] (\text{s})$ is the most prevailing aerosol phase of the system. As the ammonia concentration level increases even more from 1.5 to 2, the aerosol contains only $(\text{NH}_4)_2\text{SO}_4 (\text{s})$. At or above a molar ratio of NH_3 and H_2SO_4 of 2, some of the ammonia continues to exist in the gaseous phase (Seinfeld and Pandis, 1998).

Ammonium Nitrate Formation Reaction



In areas with high ammonia concentrations and high nitric acid concentrations as well as low sulfate concentrations, ammonium nitrate forms (Seinfeld and Pandis, 1998).

Additionally, conditions of high relative humidity and low temperature favor the formation of particulate ammonium nitrate (Gupta, 2003; Puxbaum, 1993; Seinfeld and Pandis, 1998). The dissociation constant for this reaction, $K_p(T)$, is described by equation B.9.

$$K_p(t) = p_{\text{nh}_3} * p_{\text{hno}_3} \quad (\text{B.9})$$

The estimate of this equation by integrating the van't Hoff equation (and assuming 1 atm of total pressure and K_p is in units of ppb^2) is:

$$\ln K_p = 84.6 - \frac{24220}{T} - 6.1 * \ln\left(\frac{T}{298}\right) \quad (\text{B.10})$$

Looking at the graph of the $K_p(T)$ of this reaction as shown in Seinfeld and Pandis, the constant can be seen as quite sensitive to temperature changes. Thus, higher temperatures relate to higher values of K_p , and henceforth higher equilibrium values of the gas-phase concentrations of NH_3 and HNO_3 . Furthermore, these higher temperatures shift the system equilibrium from the aerosol phase. Thus decreasing the concentration of the ammonium nitrate aerosol, NH_4NO_3 as the temperature increases.

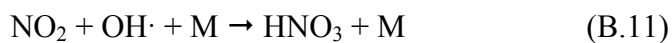
Competition Between Sulfate and Nitrate Reactions

The previous subsections analyze the sulfate reactions (equations B.4 and B.5) independently from the nitrate reaction (equation B.6). However, in reality, this independence is an invalid assumption. Sulfates and nitrates compete for the available ammonia complicating the simple systems in the previous subsections. Seinfeld and Pandis, 1998, present two systems of interest: ammonia-rich and ammonia-poor. In the ammonia-poor system, the total ammonia molar concentration [TA] is less than twice the total sulfate molar concentration [TS]. In the ammonia-rich system, [TA] is greater than twice [TS].

First, in the ammonia-poor system, the entire available sulfate is not neutralized due to an insufficient concentration of NH_3 , creating an acidic aerosol phase. Thus, a low vapor pressure of NH_3 exists resulting in a low product of the partial pressures of NH_3 and HNO_3 , reducing the nitrate levels to close to or at zero. At these low [TA] concentration levels, sulfuric acid and bisulfate dominate the aerosol composition (Seinfeld and Pandis, 1998). Next, in the ammonia-rich system, where the water concentration is at a minimum, the excess ammonia extensively neutralizes the aerosol phase components of the system. Excess ammonia that does not react with sulfate reacts with nitrate to form ammonium nitrate, NH_4NO_3 . As the [TA] increases, NH_4NO_3 , becomes a much larger portion of the aerosol composition because the decrease in the [TS] frees up ammonia to react with the available nitric acid (Seinfeld and Pandis, 1998).

Example of the Impact of These Aerosols

Los Angeles is a great example of the chemistry and impact of these aerosols (specifically the ammonium nitrate aerosol) on the surrounding area. The air current typically runs from the ocean to Los Angeles to the agricultural operations (mainly dairies) in the Chino area to the east side of the area near Riverside and Moreno Valley. NO_x emissions from the Los Angeles area (shown in yellow in Figure B.3) combine with the hydroxyl radical to create nitric acid, as described by equation B.11.



The wind carries the nitric acid (HNO_3) formed by the reaction in equation B.11 over the agricultural operations in the Chino, CA, area (shown in green in Figure B.3). At this point, HNO_3 combines with the volatilized ammonia from the agricultural operations to generate NH_4NO_3 , as previously described by the reaction in equation B.6 and shown in red in Figure B.3. As shown in Figure B.3, this aerosol travels east towards the Riverside and Moreno Valley areas, causing reduced visibility in the area, annoying odors, and environmental damage in this downwind area.



Figure B.3. Graphical Representation of the NO_x/NH_3 Problem near Los Angeles.

Agricultural operations contribute significantly to the overall anthropogenic ammonia emissions. These NH_3 emissions serve as crucial elements of atmospheric models

because ammonia is one of the most prevalent alkaline gaseous found in the planetary boundary layer (PBL), and ammonia concentrations affect the overall acidity of precipitation, cloud water, and atmospheric aerosols (Aneja et al., 2001).

These ammonia atmospheric aerosols have the attention of the EPA and other regulatory agencies because, when Effective Screening Level (ESL) thresholds are exceeded, potential consequences result from these over-threshold concentrations of oxidized and reduced forms of organic and inorganic nitrogen. These aerosols comprise a large part of secondary PM_{2.5}, and research has shown that a large percentage of PM_{2.5} penetrates human respiratory system and deposits in the lungs and alveolar region, subsequently jeopardizing the public health (Hinds, 1999; Aneja et al., 2001). Additionally, these atmospheric aerosols have can cause major environmental damage when redeposited on land and water and have a significant influence on global warming and ozone depletion (MAFF, 1998; Aneja et al., 2001; Arogo et al., 2001; Seinfeld and Pandis, 1998).

An important component to understanding the impact of ammonia atmospheric aerosols is understanding the volatilization of ammonia and the chemical reactions of ammonia and other species in the atmosphere. Typically, ammonia reacts with acidic species to form ammonium sulfate ((NH₄)₂SO₄), ammonium nitrate (NH₄NO₃), ammonium chloride (NH₄Cl), ammonium and the hydroxyl radical (NH₄⁺ and OH⁻), and this paper explores in detail specifics concerning the primary reactions of ammonia and sulfate and nitrate molecules.

Subsequently, ammonia emissions from agricultural operations have drawn attention from individuals in the agricultural industry as well as the general public outside of the agricultural industry.

APPENDIX C

APPENDIX C

Sensitivity Coefficient Determination

$$C = \frac{W}{V} \quad (\text{refer to equation 4.6})$$

$$\frac{\delta C}{\delta W} = \frac{1}{V}$$

$$\frac{\delta C}{\delta V} = -\frac{W}{V^2}$$

$$W = 0.16 * (W_f - W_i) \quad (\text{refer to equation 4.7})$$

$$\frac{\delta W}{\delta W_f} = 0.16$$

$$\frac{\delta W}{\delta W_i} = -0.16$$

$$V = Q * \Theta \quad (\text{refer to equation 4.8})$$

$$\frac{\delta V}{\delta Q} = \Theta$$

$$\frac{\delta V}{\delta \Theta} = Q$$

$$Q = 5.976 * k * (D_0)^2 * \sqrt{\frac{\Delta P_a}{\rho_a}} \quad (\text{refer to equation 4.9})$$

$$\frac{\delta Q}{\delta k} = 5.976 * (D_0)^2 * \sqrt{\frac{\Delta P_0}{\rho_a}}$$

$$\frac{\delta Q}{\delta D_0} = 11.952 * k * (D_0) * \sqrt{\frac{\Delta P_0}{\rho_a}}$$

$$\frac{\delta Q}{\delta \Delta P_0} = 2.988 * k * (D_0)^2 * \sqrt{\frac{1}{\Delta P_0 * \rho_a}}$$

$$\frac{\delta Q}{\delta \rho_a} = -2.988 * k * (D_0)^2 * \sqrt{\frac{\Delta P_0}{(\rho_a)^3}}$$

$$\rho_a = \left[\frac{P_a - RH * P_s}{0.37 * (460 + T)} \right] + \left[\frac{RH * P_s}{0.596 * (460 + T)} \right] \quad (\text{refer to equation 4.10})$$

$$\frac{\delta \rho_a}{\delta RH_a} = \frac{P_{sa}}{460 + T_a} * \left[\frac{1}{0.596} - \frac{1}{0.37} \right]$$

$$\frac{\delta \rho_a}{\delta P_{sa}} = \frac{RH_a}{460 + T_a} * \left[\frac{1}{0.596} - \frac{1}{0.37} \right]$$

$$\frac{\delta \rho_a}{\delta P_a} = \frac{1}{0.37 * (460 + T_a)}$$

$$\frac{\delta \rho_a}{\delta T_a} = \frac{1}{(460 + T_a)^2} * \left[\frac{-P_a}{0.37} + RH_a * P_{sa} * \left[\frac{1}{0.37} - \frac{1}{0.596} \right] \right]$$

$$k = \frac{Q_{LFE}}{5.976 * (D_0)^2 * \sqrt{\frac{\Delta P_c}{\rho_c}}} \quad (\text{refer to equation 4.11})$$

$$\frac{\delta k}{\delta Q_{LFE}} = \frac{1}{5.976 * (D_0)^2 * \sqrt{\frac{\Delta P_c}{\rho_c}}}$$

$$\frac{\delta k}{\delta D_0} = \frac{-2 * Q_{LFE}}{5.976 * (D_0)^3 * \sqrt{\frac{\Delta P_c}{\rho_c}}}$$

$$\frac{\delta k}{\delta \Delta P_c} = \frac{-\frac{1}{2} * Q_{LFE}}{5.976 * (D_0)^2 * \sqrt{\frac{\Delta P_c^3}{\rho_c}}}$$

$$\frac{\delta k}{\delta \Delta P_c} = \frac{\frac{1}{2} * Q_{LFE}}{5.976 * (D_0)^2 * \sqrt{\Delta P_c * \rho_c}}$$

APPENDIX D

Date	Time		AirTemp (°C)	Radiat (Watts/m ²)	Wspeed (m/s)	Direction (°)
	Start	End	Avg	Avg	Avg	Avg
8/19/2002	0:00	0:59	26.37	0	6.49	175.1
	1:00	1:59	25.3	0	5.32	180.1
	2:00	2:59	24.67	0	4.79	183.72
	3:00	3:59	23.9	0	3.67	186.62
	4:00	4:59	22.88	0	3.03	185.45
	5:00	5:59	22.33	0	3.56	182.45
	6:00	6:59	22.14	0.2	4.07	181.34
	7:00	7:59	22.73	26.3	4.65	183.93
	8:00	8:59	24.17	122.63	5.3	185.83
	9:00	9:59	25.5	259	6.18	191.28
	10:00	10:59	27.64	386	7.89	197.69
	11:00	11:59	28.6	380.47	6.75	205.52
	12:00	12:59	30.51	669.63	5.84	206.59
	13:00	13:59	32.21	785.47	5.08	198.45
	14:00	14:59	33.35	789.8	4.95	202.62
	15:00	15:59	34.2	613.1	4.71	175.14
	16:00	16:59	34	433.73	5.52	177.48
	17:00	17:59	29.9	202.63	7.36	150.17
	18:00	18:59	25.46	162	8.11	114.28
	19:00	19:59	25.09	41.03	5.35	122.28
	20:00	20:59	23.91	4.2	6.86	115.76
	21:00	21:59	22.82	0	4.87	123.97
	22:00	22:59	22	0	3.42	162.03
	23:00	23:59	24.06	0	4.98	163.59
8/20/2002	0:00	0:59	24.07	0	6.27	204.97
	1:00	1:59	22.1	0.8	6.02	217.83
	2:00	2:59	21.6	0.8	4.44	218.52
	3:00	3:59	21.3	0	2.89	215.86
	4:00	4:59	21.19	0	2.81	209.86
	5:00	5:59	21.31	0	3.45	203
	6:00	6:59	21.19	0	3.5	206.31
	7:00	7:59	21.21	4.8	4.3	202.97
	8:00	8:59	20.74	13.2	4.49	196.66
	9:00	9:59	20.16	12	3.99	155.9
	10:00	10:59	19.84	10.6	3.53	155.52
	11:00	11:59	20.44	69.47	3.06	136.76
	12:00	12:59	21.84	120.53	3.7	131.21
	13:00	13:59	23.76	364.67	4.86	148.59
	14:00	14:59	25.96	348.93	5.48	182.9
	15:00	15:59	27.87	533.27	6.62	188.28
	16:00	16:59	27.31	447.87	6.75	159
	17:00	17:59	25.83	437.53	5.68	112.52
	18:00	18:59	25.05	327.7	7.21	111.59
	19:00	19:59	23.82	125.63	7.29	130.97
	20:00	20:59	23.11	9.27	6.28	146.34
	21:00	21:59	22.23	0	5.33	154.21
	22:00	22:59	21.85	0	6.77	169.55
	23:00	23:59	21.9	0	8.41	177.66

Date	Time		AirTemp (°C)	Radiat (Watts/m ²)	Wspeed (m/s)	Direction (°)
	Start	End	Avg	Avg	Avg	Avg
8/21/2002	0:00	0:59	22.07	0.8	7.33	185.96
	1:00	1:59	22.39	0	7.4	198.48
	2:00	2:59	21.75	0	5.46	222.52
	3:00	3:59	21.39	0	4.22	215.69
	4:00	4:59	21.57	0	3.47	200.14
	5:00	5:59	20.67	0	1.81	161.17
	6:00	6:59	19.49	0	1.92	146.34
	7:00	7:59	19.33	20.37	2.24	160.69
	8:00	8:59	22.1	165.3	5.6	184.24
	9:00	9:59	23.29	183.97	6.6	189.1
	10:00	10:59	25.97	460	7.97	194.38
	11:00	11:59	26.17	337.4	7.23	194.93
	12:00	12:59	26.82	455	7.12	203.9
	13:00	13:59	27.64	577.1	6.77	201.69
	14:00	14:59	29.04	750.6	6.48	198.38
	15:00	15:59	29.94	660.8	5.85	194.03
	16:00	16:59	31.08	589.03	6.07	185.76
	17:00	17:59	31.74	439.2	6.56	180.17
	18:00	18:59	31.25	242.33	6.38	185.28
	19:00	19:59	29.51	52.03	4.92	178.93
	20:00	20:59	28.05	11.57	4.2	175.79
	21:00	21:59	26.64	0	5.16	168.83
	22:00	22:59	25.58	0	6.21	176.48
	23:00	23:59	24.13	0	5.65	186.38
8/22/2002	0:00	0:59	23.05	0	5.14	194.55
	1:00	1:59	22.38	0	5.22	200.93
	2:00	2:59	21.63	0	5.28	204.41
	3:00	3:59	21.09	0	4.41	210.48
	4:00	4:59	20.61	0	4.15	217.31
	5:00	5:59	20.04	0	3.34	239.34
	6:00	6:59	19.21	0	2.41	226.45
	7:00	7:59	19.46	43.4	2.39	200.83
	8:00	8:59	22.43	173.87	3.85	218.97
	9:00	9:59	23.87	291.8	3.72	271.83
	10:00	10:59	24.92	484.47	2.01	272.59
	11:00	11:59	26.86	611.93	2.79	240.69
	12:00	12:59	28.08	743.93	2.61	193.24
	13:00	13:59	29.44	780.8	2.42	185.34
	14:00	14:59	30.22	764.5	3.39	196.72
	15:00	15:59	30.98	696.67	3.97	180.41
	16:00	16:59	31.96	594.67	4.02	170
	17:00	17:59	32.5	401.83	4.32	162.28
	18:00	18:59	31.34	114.07	4.88	147.76
	19:00	19:59	30.71	66.03	4.22	151.59
	20:00	20:59	28.23	6.73	2.56	146.55
	21:00	21:59	26.27	0	3.34	150.31
	22:00	22:59	25.3	0	3.79	154.69
	23:00	23:59	24.01	0	3.4	159.21

Date	Time		AirTemp (°C)	Radiat (Watts/m ²)	Wspeed (m/s)	Direction (°)
	Start	End	Avg	Avg	Avg	Avg
8/23/2002	0:00	0:59	22.65	0	2.63	158.55
	1:00	1:59	21.83	0	2.09	166.76
	2:00	2:59	21.91	0.8	2.14	169.21
	3:00	3:59	20.75	0	1.66	197.21
	4:00	4:59	19.88	0	1.55	208.69
	5:00	5:59	19.63	0	2.34	219.72
	6:00	6:59	20.21	0	2.32	211.34
	7:00	7:59	21.51	26.37	3.21	213.62
	8:00	8:59	23.36	150	3.73	211.76
	9:00	9:59	25.62	319.4	5.02	211.69
	10:00	10:59	27.26	487.1	3.92	228.83
	11:00	11:59	28.97	629.23	3.18	202.9
	12:00	12:59	30.04	729.1	3.47	181.03
	13:00	13:59	32.42	777.13	4.87	170.14
	14:00	14:59	33.79	769.3	5.61	172.48
	15:00	15:59	34.45	709.77	5.6	174.72
	16:00	16:59	34.3	474.4	5.83	174.62
	17:00	17:59	33.12	151.9	5.5	177.66
	18:00	18:59	33.66	178.8	6.1	173.48
	19:00	19:59	31.73	33.33	4.64	177.41
	20:00	20:59	30.31	4.2	4.14	188.07
	21:00	21:59	28.01	0	2.67	172.07
	22:00	22:59	26.11	0	2.79	182.17
23:00	23:59	24.06	0	1.93	188.07	
8/24/2002	0:00	0:59	21.96	0	1.3	180.9
	1:00	1:59	20.6	0.8	1.02	158.48
	2:00	2:59	20.03	0	1.21	175.79
	3:00	3:59	19.38	0	1.48	186.55
	4:00	4:59	20.35	0	3.01	199.03
	5:00	5:59	20.75	0	3.19	206
	6:00	6:59	19.61	0	2.31	221.17
	7:00	7:59	20.37	26.6	3.23	226.21
	8:00	8:59	23.8	185.07	5.59	208.24
	9:00	9:59	25.32	212.4	6.59	210.31
	10:00	10:59	27.73	492.9	6.85	213.07
	11:00	11:59	29.88	564.7	6.55	199.48
	12:00	12:59	30.84	642.87	6.89	186.69
	13:00	13:59	33.11	752.1	7.05	197.66
	14:00	14:59	34.63	769.4	6.55	191.9
	15:00	15:59	35.07	622	5.58	185.93
	16:00	16:59	33.69	207.6	5.03	182.59
	17:00	17:59	35.3	379.37	4.9	179.62
	18:00	18:59	34.25	201.53	5.85	185.93
	19:00	19:59	33.42	99.77	5.2	179.76
	20:00	20:59	29.83	6.57	2.82	155
	21:00	21:59	26.17	0	2.01	147.34
	22:00	22:59	24.5	0	2.09	154.72
23:00	23:59	24.57	0	2.43	170.79	

APPENDIX E

Ammonia Summary Sheet

Test #	Model Avg. Period (HRS)	Sampler	C2 Net Measured Concentration μg/m ³	C1 ISCST3 Avg. Conc. μg/m ³	Q1 ISCST3 Flux g/s-m ²	ISCST3 Avg. Conc. μg/m ³	Diff	Q2 ISCST3 Flux g/s-m ²	ER to Match Measured Concentration g/s-m ²
112	3	A	633.7	313.03	6.00E-06	536.5	-97.2	1.03E-05	1.21E-05
		B	672.9	390.1	6.00E-06	668.6	-4.3	1.03E-05	1.03E-05
		C	701.6	422.5	6.00E-06	724.1	22.5	1.03E-05	9.96E-06
		D	562.9	440	6.00E-06	754.1	191.2	1.03E-05	7.68E-06
		E	743.5	440.9	6.00E-06	755.6	12.1	1.03E-05	1.01E-05
		F	755	433	6.00E-06	742.1	-12.9	1.03E-05	1.05E-05
		G	521.5	347.7	6.00E-06	595.9	74.4	1.03E-05	9.00E-06
		T 1.5	905	391.6	6.00E-06	671.1	-233.9	1.03E-05	1.39E-05
		T 3	667	378.3	6.00E-06	648.3	-18.7	1.03E-05	1.06E-05
		T6	491	339.8	6.00E-06	582.4	91.4	1.03E-05	8.67E-06
							24.6	average	1.03E-05
								std dev	1.75E-06
113	3	A	440	505.7	6.00E-06	563.0	123.0	6.68E-06	5.22E-06
		B	402	496.1	6.00E-06	552.3	150.3	6.68E-06	4.86E-06
		C	354	473.9	6.00E-06	527.6	173.6	6.68E-06	4.48E-06
		D	451	437.5	6.00E-06	487.1	36.1	6.68E-06	6.19E-06
		E	356	394.8	6.00E-06	439.5	83.5	6.68E-06	5.41E-06
		F	405	324.2	6.00E-06	360.9	-44.1	6.68E-06	7.50E-06
		G	195	107.5	6.00E-06	119.7	-75.3	6.68E-06	1.09E-05
		T 1.5	609	429.3	6.00E-06	477.9	-131.1	6.68E-06	8.51E-06
		T 3	499	393.6	6.00E-06	438.2	-60.8	6.68E-06	7.61E-06
		T6	329	321.4	6.00E-06	357.8	28.8	6.68E-06	6.14E-06
							284.1	average	6.68E-06
								std dev	1.97E-06

Test #	Model Avg. Period (HRS)	Sampler	C2 Net Measured Concentration $\mu\text{g}/\text{m}^3$	C1 ISCST3 Avg. Conc. $\mu\text{g}/\text{m}^3$	Q1 ISCST3 Flux $\text{g}/\text{s}\cdot\text{m}^2$	ISCST3 Avg. Conc. $\mu\text{g}/\text{m}^3$	Diff	Q2 ISCST3 Flux $\text{g}/\text{s}\cdot\text{m}^2$	ER to Match Measured Concentration $\text{g}/\text{s}\cdot\text{m}^2$
114	12	A	542.7	455.1	6.00E-06	351.7	-191.0	4.64E-06	7.16E-06
		B	444.9	605.7	6.00E-06	468.1	23.2	4.64E-06	4.41E-06
		C	589.6	682.3	6.00E-06	527.2	-62.4	4.64E-06	5.18E-06
		D	328.1	735.7	6.00E-06	568.5	240.4	4.64E-06	2.68E-06
		E	543	740.3	6.00E-06	572.1	29.1	4.64E-06	4.40E-06
		F	561.2	698.3	6.00E-06	539.6	-21.6	4.64E-06	4.82E-06
		G	346.2	572.7	6.00E-06	442.5	96.3	4.64E-06	3.63E-06
		T 1.5	588	706.4	6.00E-06	545.9	-42.1	4.64E-06	4.99E-06
		T 3	506	644.0	6.00E-06	497.7	-8.3	4.64E-06	4.71E-06
		T6	384	525.6	6.00E-06	406.1	22.1	4.64E-06	4.38E-06
							85.7	average	4.64E-06
								std dev	1.15E-06
121	7	A	407	705.7	6.00E-06	423.5	16.5	3.60E-06	3.46E-06
		B	384	755.6	6.00E-06	453.4	69.4	3.60E-06	3.05E-06
		C	336	760.7	6.00E-06	456.5	120.5	3.60E-06	2.65E-06
		D	360	729.1	6.00E-06	437.5	77.5	3.60E-06	2.96E-06
		E	377	640.2	6.00E-06	384.2	7.2	3.60E-06	3.53E-06
		F	343	512.9	6.00E-06	307.8	-35.2	3.60E-06	4.01E-06
		G	164	234.3	6.00E-06	140.6	-23.4	3.60E-06	4.20E-06
		T 1.5	533	719.7	6.00E-06	431.9	-101.1	3.60E-06	4.44E-06
		T 3	442	668.9	6.00E-06	401.4	-40.6	3.60E-06	3.96E-06
		T6	341	548.4	6.00E-06	329.1	-11.9	3.60E-06	3.73E-06
							79.0	average	3.60E-06
								std dev	5.80E-07

Test #	Model Avg. Period (HRS)	Sampler	C2 Net Measured Concentration $\mu\text{g}/\text{m}^3$	C1 ISCST3 Avg. Conc. $\mu\text{g}/\text{m}^3$	Q1 ISCST3 Flux $\text{g}/\text{s}\cdot\text{m}^2$	ISCST3 Avg. Conc. $\mu\text{g}/\text{m}^3$	Diff	Q2 ISCST3 Flux $\text{g}/\text{s}\cdot\text{m}^2$	ER to Match Measured Concentration $\text{g}/\text{s}\cdot\text{m}^2$
122	5	A	619	495.7	6.00E-06	629.3	10.3	7.62E-06	7.49E-06
		B	586	517.8	6.00E-06	657.3	71.3	7.62E-06	6.79E-06
		C	552	497.0	6.00E-06	630.9	78.9	7.62E-06	6.66E-06
		D	613	645.4	6.00E-06	819.3	206.3	7.62E-06	5.70E-06
		E	524	425.3	6.00E-06	539.9	15.9	7.62E-06	7.39E-06
		F	535	648.3	6.00E-06	823.0	288.0	7.62E-06	4.95E-06
		G	281	216.5	6.00E-06	274.8	-6.2	7.62E-06	7.79E-06
		T 1.5	890	673.5	6.00E-06	855.0	-35.0	7.62E-06	7.93E-06
		T 3	683	408.7	6.00E-06	518.9	-164.1	7.62E-06	1.00E-05
		T6	646	339.0	6.00E-06	430.3	-215.7	7.62E-06	1.14E-05
							249.7	average	7.62E-06
								std dev	1.91E-06
123	12	A	616	667.4	6.00E-06	590.3	-25.7	5.31E-06	5.54E-06
		B	562	735.9	6.00E-06	650.9	88.9	5.31E-06	4.58E-06
		C	566	758.2	6.00E-06	670.6	104.6	5.31E-06	4.48E-06
		D	539	744.2	6.00E-06	658.3	119.3	5.31E-06	4.35E-06
		E	543	694.3	6.00E-06	614.1	71.1	5.31E-06	4.69E-06
		F	572	589.2	6.00E-06	521.2	-50.8	5.31E-06	5.83E-06
		G	320	321.1	6.00E-06	284.0	-36.0	5.31E-06	5.98E-06
		T 1.5	796	758.8	6.00E-06	671.2	-124.8	5.31E-06	6.29E-06
		T 3	686	696.1	6.00E-06	615.7	-70.3	5.31E-06	5.91E-06
		T6	509	563.3	6.00E-06	498.2	-10.8	5.31E-06	5.42E-06
							65.5	average	5.31E-06
								std dev	7.18E-07

Test #	Model Avg. Period (HRS)	Sampler	C2 Net Measured Concentration $\mu\text{g}/\text{m}^3$	C1 ISCST3 Avg. Conc. $\mu\text{g}/\text{m}^3$	Q1 ISCST3 Flux $\text{g}/\text{s}\cdot\text{m}^2$	ISCST3 Avg. Conc. $\mu\text{g}/\text{m}^3$	Diff	Q2 ISCST3 Flux $\text{g}/\text{s}\cdot\text{m}^2$	ER to Match Measured Concentration $\text{g}/\text{s}\cdot\text{m}^2$
131	3	A	1020	852.6	6.00E-06	857.4	-162.6	6.03E-06	7.18E-06
		B	818	919.2	6.00E-06	924.3	106.3	6.03E-06	5.34E-06
		C	802	917.7	6.00E-06	922.8	120.8	6.03E-06	5.24E-06
		D	718	913.7	6.00E-06	918.8	200.8	6.03E-06	4.72E-06
		E	716	832.4	6.00E-06	837.0	121.0	6.03E-06	5.16E-06
		F	859	708.7	6.00E-06	712.7	-146.3	6.03E-06	7.27E-06
		G	475	374.7	6.00E-06	376.8	-98.2	6.03E-06	7.61E-06
		T 1.5	1049	947.7	6.00E-06	953.0	-96.0	6.03E-06	6.64E-06
		T 3	860	865.8	6.00E-06	870.6	10.6	6.03E-06	5.96E-06
		T6	619	711.8	6.00E-06	715.8	96.8	6.03E-06	5.22E-06
							153.1	average	6.03E-06
								std dev	1.05E-06
132	3	A	430.7	218.1	6.00E-06	376.0	-54.7	1.03E-05	1.18E-05
		B	454	375.8	6.00E-06	647.9	193.9	1.03E-05	7.25E-06
		C	898	444.8	6.00E-06	767.0	-131.0	1.03E-05	1.21E-05
		D	685	470.3	6.00E-06	810.8	125.8	1.03E-05	8.74E-06
		E	540	478.3	6.00E-06	824.6	284.6	1.03E-05	6.77E-06
		F	1061	479.3	6.00E-06	826.4	-234.6	1.03E-05	1.33E-05
		G	872	479.3	6.00E-06	826.5	-45.5	1.03E-05	1.09E-05
		T 1.5	940	486.7	6.00E-06	839.2	-100.8	1.03E-05	1.16E-05
		T 3	790	444.8	6.00E-06	767.0	-23.0	1.03E-05	1.07E-05
		T6	628	366.3	6.00E-06	631.6	3.6	1.03E-05	1.03E-05
							18.3	average	1.03E-05
								std dev	2.13E-06

Test #	Model Avg. Period (HRS)	Sampler	C2 Net Measured Concentration	C1 ISCST3 Avg. Conc.	Q1 ISCST3 Flux	ISCST3 Avg. Conc.	Q2 ISCST3 Flux	ER to Match Measured Concentration

Test #	Model Avg. Period (HRS)	Sampler	C2 Net Measured Concentration $\mu\text{g}/\text{m}^3$	C1 ISCST3 Avg. Conc. $\mu\text{g}/\text{m}^3$	Q1 ISCST3 Flux $\text{g}/\text{s}\cdot\text{m}^2$	ISCST3 Avg. Conc. $\mu\text{g}/\text{m}^3$	Diff	Q2 ISCST3 Flux $\text{g}/\text{s}\cdot\text{m}^2$	ER to Match Measured Concentration $\text{g}/\text{s}\cdot\text{m}^2$
135	12	A	408	423.6	6.00E-06	315.8	-92.2	4.47E-06	5.78E-06
		B	410	586.1	6.00E-06	437.0	27.0	4.47E-06	4.20E-06
		C	478	673.5	6.00E-06	502.2	24.2	4.47E-06	4.26E-06
		D	456	727.4	6.00E-06	542.4	86.4	4.47E-06	3.76E-06
		E	436	759.7	6.00E-06	566.5	130.5	4.47E-06	3.44E-06
		F	724	775.8	6.00E-06	578.5	-145.5	4.47E-06	5.60E-06
		G	432	666.7	6.00E-06	497.1	65.1	4.47E-06	3.89E-06
		T 1.5	612	713.8	6.00E-06	532.3	-79.7	4.47E-06	5.14E-06
		T 3	518	649.5	6.00E-06	484.3	-33.7	4.47E-06	4.79E-06
		T6	344	531.6	6.00E-06	396.4	52.4	4.47E-06	3.88E-06
							34.5	average	4.47E-06
								std dev	8.10E-07
141	3	A	416	288.1	6.00E-06	212.0	-204.0	4.42E-06	6.43E-06
		B	367	556.5	6.00E-06	409.6	42.6	4.42E-06	2.97E-06
		C	756	705.8	6.00E-06	519.4	-236.6	4.42E-06	3.60E-06
		D	396	799.7	6.00E-06	588.5	192.5	4.42E-06	2.97E-06
		E	509	847.6	6.00E-06	623.8	114.8	4.42E-06	3.60E-06
		F	660	879.1	6.00E-06	646.9	-13.1	4.42E-06	4.50E-06
		G	985	903.8	6.00E-06	665.1	-319.9	4.42E-06	6.54E-06
		T 1.5	592	735.3	6.00E-06	541.1	-50.9	4.42E-06	4.83E-06
		T 3	513	673.2	6.00E-06	495.5	-17.5	4.42E-06	4.57E-06
		T6	378	548.6	6.00E-06	403.7	25.7	4.42E-06	4.13E-06
							-466.3	average	4.42E-06
								std dev	1.26E-06

Test #	Model Avg. Period (HRS)	Sampler	C2 Net Measured Concentration $\mu\text{g}/\text{m}^3$	C1 ISCST3 Avg. Conc. $\mu\text{g}/\text{m}^3$	Q1 ISCST3 Flux $\text{g}/\text{s}\cdot\text{m}^2$	ISCST3 Avg. Conc. $\mu\text{g}/\text{m}^3$	Diff	Q2 ISCST3 Flux $\text{g}/\text{s}\cdot\text{m}^2$	ER to Match Measured Concentration $\text{g}/\text{s}\cdot\text{m}^2$
142	3	A	206	259.5	6.00E-06	168.5	-37.5	3.90E-06	4.76E-06
		B	467	413.9	6.00E-06	268.7	-198.3	3.90E-06	6.77E-06
		C	447	483.1	6.00E-06	313.7	-133.3	3.90E-06	5.55E-06
		D	165	539.0	6.00E-06	350.0	185.0	3.90E-06	1.84E-06
		E	140	568.1	6.00E-06	368.8	228.8	3.90E-06	1.48E-06
		F	202	584.0	6.00E-06	379.2	177.2	3.90E-06	2.08E-06
		G	120	582.2	6.00E-06	378.0	258.0	3.90E-06	1.24E-06
		T 1.5	363	319.8	6.00E-06	207.6	-155.4	3.90E-06	6.81E-06
		T 3							
		T6	219	289.5	6.00E-06	188.0	-31.0	3.90E-06	4.54E-06
293.5								average	3.90E-06
								std dev	2.27E-06
143	3	A	412	509.5	6.00E-06	599.9	187.9	7.06E-06	4.85E-06
		B	381	546.5	6.00E-06	643.4	262.4	7.06E-06	4.18E-06
		C	287	550.5	6.00E-06	648.1	361.1	7.06E-06	3.13E-06
		D	768	551.1	6.00E-06	648.7	-119.3	7.06E-06	8.36E-06
		E	126	541.0	6.00E-06	636.9	510.9	7.06E-06	1.40E-06
		F	706	520.9	6.00E-06	613.2	-92.8	7.06E-06	8.13E-06
		G	676	349.1	6.00E-06	410.9	-265.1	7.06E-06	1.16E-05
		T 1.5	821	468.5	6.00E-06	551.5	-269.5	7.06E-06	1.05E-05
		T 3	727	458.6	6.00E-06	539.9	-187.1	7.06E-06	9.51E-06
		T6	628	421.7	6.00E-06	496.5	-131.5	7.06E-06	8.93E-06
257.0								average	7.06E-06
								std dev	3.43E-06

Test #	Model Avg. Period (HRS)	Sampler	C2 Net Measured Concentration $\mu\text{g}/\text{m}^3$	C1 ISCST3 Avg. Conc. $\mu\text{g}/\text{m}^3$	Q1 ISCST3 Flux $\text{g}/\text{s}\cdot\text{m}^2$	ISCST3 Avg. Conc. $\mu\text{g}/\text{m}^3$	Diff	Q2 ISCST3 Flux $\text{g}/\text{s}\cdot\text{m}^2$	ER to Match Measured Concentration $\text{g}/\text{s}\cdot\text{m}^2$
144	3	A	622	631.6	6.00E-06	857.0	235.0	8.14E-06	5.91E-06
		B	695	627.8	6.00E-06	851.9	156.9	8.14E-06	6.64E-06
		C	863	616.2	6.00E-06	836.1	-26.9	8.14E-06	8.40E-06
		D	536	569.1	6.00E-06	772.2	236.2	8.14E-06	5.65E-06
		E	519	525.6	6.00E-06	713.2	194.2	8.14E-06	5.92E-06
		F	468	406.6	6.00E-06	551.7	83.7	8.14E-06	6.91E-06
		G	177	58.4	6.00E-06	79.3	-97.7	8.14E-06	1.82E-05
		T 1.5	835	554.4	6.00E-06	752.3	-82.7	8.14E-06	9.04E-06
		T 3	684	525.9	6.00E-06	713.6	29.6	8.14E-06	7.80E-06
		T6	521	449.3	6.00E-06	609.6	88.6	8.14E-06	6.96E-06
							816.9	average	8.14E-06
								std dev	3.70E-06
145	12	A	587	1066.3	6.00E-06	529.5	-57.5	2.98E-06	3.30E-06
		B	622	1241.4	6.00E-06	616.4	-5.6	2.98E-06	3.01E-06
		C	705	1327.3	6.00E-06	659.1	-45.9	2.98E-06	3.19E-06
		D	625	1337.4	6.00E-06	664.1	39.1	2.98E-06	2.80E-06
		E	544	1292.2	6.00E-06	641.7	97.7	2.98E-06	2.53E-06
		F	553	1135.1	6.00E-06	563.6	10.6	2.98E-06	2.92E-06
		G	199	671.0	6.00E-06	333.2	134.2	2.98E-06	1.78E-06
		T 1.5	821	1362.3	6.00E-06	676.4	-144.6	2.98E-06	3.62E-06
		T 3	718	1245.8	6.00E-06	618.6	-99.4	2.98E-06	3.46E-06
		T6	538	1011.7	6.00E-06	502.4	-35.6	2.98E-06	3.19E-06
							-107.0	average	2.98E-06
								std dev	5.28E-07

Test #	Model Avg. Period (HRS)	Sampler	C2 Net Measured Concentration $\mu\text{g}/\text{m}^3$	C1 ISCST3 Avg. Conc. $\mu\text{g}/\text{m}^3$	Q1 ISCST3 Flux $\text{g}/\text{s}\cdot\text{m}^2$	ISCST3 Avg. Conc. $\mu\text{g}/\text{m}^3$	Diff	Q2 ISCST3 Flux $\text{g}/\text{s}\cdot\text{m}^2$	ER to Match Measured Concentration $\text{g}/\text{s}\cdot\text{m}^2$
151	3	A	947	255.4	6.00E-06	279.0	-668.0	6.56E-06	2.22E-05
		B	380	550.0	6.00E-06	600.9	220.9	6.56E-06	4.15E-06
		C	750	682.0	6.00E-06	745.2	-4.8	6.56E-06	6.60E-06
		D	447	813.2	6.00E-06	888.5	441.5	6.56E-06	3.30E-06
		E	1055	906.2	6.00E-06	990.1	-64.9	6.56E-06	6.99E-06
		F	688	963.6	6.00E-06	1052.8	364.8	6.56E-06	4.28E-06
		G	984	985.3	6.00E-06	1076.6	92.6	6.56E-06	5.99E-06
		T 1.5	569	774.1	6.00E-06	845.8	276.8	6.56E-06	4.41E-06
		T 3	447	693.6	6.00E-06	757.8	310.8	6.56E-06	3.87E-06
		T6	351	564.8	6.00E-06	617.2	266.2	6.56E-06	3.73E-06
							1235.9	average	6.56E-06
								std dev	5.66E-06
152	3	A	842	323.3	6.00E-06	405.5	-436.5	7.53E-06	1.56E-05
		B	398	469.3	6.00E-06	588.7	190.7	7.53E-06	5.09E-06
		C	581	525.2	6.00E-06	658.8	77.8	7.53E-06	6.64E-06
		D	423	566.1	6.00E-06	710.1	287.1	7.53E-06	4.48E-06
		E	374	589.0	6.00E-06	738.8	364.8	7.53E-06	3.81E-06
		F	864	600.2	6.00E-06	752.8	-111.2	7.53E-06	8.64E-06
		G	921	566.6	6.00E-06	710.7	-210.3	7.53E-06	9.75E-06
		T 1.5	656	477.6	6.00E-06	599.0	-57.0	7.53E-06	8.24E-06
		T 3	531	462.2	6.00E-06	579.7	48.7	7.53E-06	6.89E-06
		T6	423	416.9	6.00E-06	522.9	99.9	7.53E-06	6.09E-06
							254.0	average	7.53E-06
								std dev	3.41E-06

Test #	Model Avg. Period (HRS)	Sampler	C2 Net Measured Concentration $\mu\text{g}/\text{m}^3$	C1 ISCST3 Avg. Conc. $\mu\text{g}/\text{m}^3$	Q1 ISCST3 Flux $\text{g}/\text{s}\cdot\text{m}^2$	ISCST3 Avg. Conc. $\mu\text{g}/\text{m}^3$	Diff	Q2 ISCST3 Flux $\text{g}/\text{s}\cdot\text{m}^2$	ER to Match Measured Concentration $\text{g}/\text{s}\cdot\text{m}^2$
153	3	A	813	395.4	6.00E-06	749.5	-63.5	1.14E-05	1.23E-05
		B	655	396.4	6.00E-06	751.3	96.3	1.14E-05	9.92E-06
		C	630	397.1	6.00E-06	752.8	122.8	1.14E-05	9.52E-06
		D	656	401.1	6.00E-06	760.2	104.2	1.14E-05	9.81E-06
		E	630	390.9	6.00E-06	740.9	110.9	1.14E-05	9.67E-06
		F	702	361.9	6.00E-06	685.9	-16.1	1.14E-05	1.16E-05
		G	288	144.4	6.00E-06	273.7	-14.3	1.14E-05	1.20E-05
		T 1.5	923	362.5	6.00E-06	687.2	-235.8	1.14E-05	1.53E-05
		T 3	774	350.6	6.00E-06	664.6	-109.4	1.14E-05	1.32E-05
		T6	542	314.3	6.00E-06	595.8	53.8	1.14E-05	1.03E-05
							48.8	average	1.14E-05
								std dev	1.89E-06
154	3	A	498	610.1	6.00E-06	828.2	330.2	8.15E-06	4.90E-06
		B	623	612.0	6.00E-06	830.7	207.7	8.15E-06	6.11E-06
		C	769	611.9	6.00E-06	830.7	61.7	8.15E-06	7.54E-06
		D	493	604.2	6.00E-06	820.3	327.3	8.15E-06	4.90E-06
		E	414	612.3	6.00E-06	831.2	417.2	8.15E-06	4.06E-06
		F	546	583.5	6.00E-06	792.1	246.1	8.15E-06	5.61E-06
		G	1130	217.0	6.00E-06	294.5	-835.5	8.15E-06	3.12E-05
		T 1.5	690	636.9	6.00E-06	864.6	174.6	8.15E-06	6.50E-06
		T 3	556	576.3	6.00E-06	782.3	226.3	8.15E-06	5.79E-06
		T6	389	486.2	6.00E-06	660.0	271.0	8.15E-06	4.80E-06
							1426.7	average	8.15E-06
								std dev	8.18E-06

Test #	Model Avg. Period (HRS)	Sampler	C2 Net Measured Concentration $\mu\text{g}/\text{m}^3$	C1 ISCST3 Avg. Conc. $\mu\text{g}/\text{m}^3$	Q1 ISCST3 Flux $\text{g}/\text{s}\cdot\text{m}^2$	ISCST3 Avg. Conc. $\mu\text{g}/\text{m}^3$	Diff	Q2 ISCST3 Flux $\text{g}/\text{s}\cdot\text{m}^2$	ER to Match Measured Concentration $\text{g}/\text{s}\cdot\text{m}^2$
155	12	A	576	1454.8	6.00E-06	602.2	26.2	2.48E-06	2.38E-06
		B	660	1651.5	6.00E-06	683.6	23.6	2.48E-06	2.40E-06
		C	689	1717.9	6.00E-06	711.1	22.1	2.48E-06	2.41E-06
		D	578	1735.2	6.00E-06	718.3	140.3	2.48E-06	2.00E-06
		E	565	1703.0	6.00E-06	704.9	139.9	2.48E-06	1.99E-06
		F	751	1627.4	6.00E-06	673.7	-77.3	2.48E-06	2.77E-06
		G	597	1144.8	6.00E-06	473.9	-123.1	2.48E-06	3.13E-06
		T 1.5	825	1797.2	6.00E-06	744.0	-81.0	2.48E-06	2.75E-06
		T 3	726	1630.8	6.00E-06	675.1	-50.9	2.48E-06	2.67E-06
		T6	543	1389.5	6.00E-06	575.2	32.2	2.48E-06	2.34E-06
							51.9	average	2.48E-06
								std dev	3.54E-07

APPENDIX F

Ammonia Summary Sheet

Test #	Model Avg. Period (HRS)	Sampler	C2	C1	Q1	bLs Avg. Conc. $\mu\text{g}/\text{m}^3$	Diff	Q2	ER to Match Measured Concentration $\text{g}/\text{s}\cdot\text{m}^2$
			Net Measured Concentration $\mu\text{g}/\text{m}^3$	bLs Avg. Test Conc. $\mu\text{g}/\text{m}^3$	bLs ER $\text{g}/\text{s}\cdot\text{m}^2$			bLs ER $\text{g}/\text{s}\cdot\text{m}^2$	
112	3	A	633.7	32.39	6.00E-06	558.2	-75.5	1.03E-04	1.17E-04
		B	672.9	39.84	6.00E-06	686.8	13.9	1.03E-04	1.01E-04
		C	701.6	42.59	6.00E-06	734.0	32.4	1.03E-04	9.88E-05
		D	562.9	43.89	6.00E-06	756.5	193.6	1.03E-04	7.70E-05
		E	743.5	44.26	6.00E-06	762.9	19.4	1.03E-04	1.01E-04
		F	755	43.74	6.00E-06	753.9	-1.1	1.03E-04	1.04E-04
		G	521.5	35.94	6.00E-06	619.5	98.0	1.03E-04	8.71E-05
		T 1.5	905	40.46	6.00E-06	697.3	-207.7	1.03E-04	1.34E-04
		T 3	667	36.15	6.00E-06	623.0	-44.0	1.03E-04	1.11E-04
		T6	491	28.51	6.00E-06	491.5	0.5	1.03E-04	1.03E-04
							29.7	average	1.03E-04
								std dev	1.56E-05
113	3	A	440	48.49	6.00E-06	565.2	125.2	6.99E-05	5.44E-05
		B	402	47.39	6.00E-06	552.4	150.4	6.99E-05	5.09E-05
		C	354	45.37	6.00E-06	528.9	174.9	6.99E-05	4.68E-05
		D	451	42.71	6.00E-06	497.8	46.8	6.99E-05	6.34E-05
		E	356	38.78	6.00E-06	452.0	96.0	6.99E-05	5.51E-05
		F	405	32.85	6.00E-06	382.9	-22.1	6.99E-05	7.40E-05
		G	195	10.72	6.00E-06	125.0	-70.0	6.99E-05	1.09E-04
		T 1.5	609	39.86	6.00E-06	464.6	-144.4	6.99E-05	9.17E-05
		T 3	499	35.78	6.00E-06	417.0	-82.0	6.99E-05	8.37E-05
		T6	329	28.07	6.00E-06	327.2	-1.8	6.99E-05	7.03E-05
							272.9	average	6.99E-05
								std dev	2.00E-05

Test #	Model Avg. Period (HRS)	Sampler	C2 Net Measured Concentration $\mu\text{g}/\text{m}^3$	C1 bLs Avg. Test Conc. $\mu\text{g}/\text{m}^3$	Q1 bLs ER $\text{g}/\text{s}\cdot\text{m}^2$	bLs Avg. Conc. $\mu\text{g}/\text{m}^3$	Q2 bLs ER $\text{g}/\text{s}\cdot\text{m}^2$	ER to Match Measured Concentration $\text{g}/\text{s}\cdot\text{m}^2$	
114	12	A	542.7	45.97	6.00E-06	370.6	-172.1	4.84E-05	7.08E-05
		B	444.9	60.29	6.00E-06	486.0	41.1	4.84E-05	4.43E-05
		C	589.6	67.26	6.00E-06	542.2	-47.4	4.84E-05	5.26E-05
		D	328.1	71.40	6.00E-06	575.6	247.5	4.84E-05	2.76E-05
		E	543	71.73	6.00E-06	578.2	35.2	4.84E-05	4.54E-05
		F	561.2	67.52	6.00E-06	544.3	-16.9	4.84E-05	4.99E-05
		G	346.2	54.20	6.00E-06	436.9	90.7	4.84E-05	3.83E-05
		T 1.5	588	66.10	6.00E-06	532.8	-55.2	4.84E-05	5.34E-05
		T 3	506	59.16	6.00E-06	476.9	-29.1	4.84E-05	5.13E-05
		T6	384	46.00	6.00E-06	370.8	-13.2	4.84E-05	5.01E-05
							80.6	average	4.84E-05
								std dev	1.12E-05
121	7	A	407	71.38	6.00E-06	433.3	26.3	3.64E-05	3.42E-05
		B	384	76.22	6.00E-06	462.6	78.6	3.64E-05	3.02E-05
		C	336	76.88	6.00E-06	466.7	130.7	3.64E-05	2.62E-05
		D	360	73.25	6.00E-06	444.6	84.6	3.64E-05	2.95E-05
		E	377	65.57	6.00E-06	398.0	21.0	3.64E-05	3.45E-05
		F	343	53.20	6.00E-06	322.9	-20.1	3.64E-05	3.87E-05
		G	164	23.38	6.00E-06	141.9	-22.1	3.64E-05	4.21E-05
		T 1.5	533	70.53	6.00E-06	428.1	-104.9	3.64E-05	4.53E-05
		T 3	442	63.16	6.00E-06	383.4	-58.6	3.64E-05	4.20E-05
		T6	341	49.36	6.00E-06	299.6	-41.4	3.64E-05	4.14E-05
							94.2	average	3.64E-05
								std dev	6.43E-06

Test #	Model Avg. Period (HRS)	Sampler	C2 Net Measured Concentration $\mu\text{g}/\text{m}^3$	C1 bLs Avg. Test Conc. $\mu\text{g}/\text{m}^3$	Q1 bLs ER $\text{g}/\text{s}\cdot\text{m}^2$	bLs Avg. Conc. $\mu\text{g}/\text{m}^3$	Q2 bLs ER $\text{g}/\text{s}\cdot\text{m}^2$	ER to Match Measured Concentration $\text{g}/\text{s}\cdot\text{m}^2$	
122	5	A	619	48.36	6.00E-06	732.3	113.3	9.09E-05	7.68E-05
		B	586	49.82	6.00E-06	754.4	168.4	9.09E-05	7.06E-05
		C	552	48.34	6.00E-06	732.0	180.0	9.09E-05	6.85E-05
		D	613	46.06	6.00E-06	697.5	84.5	9.09E-05	7.99E-05
		E	524	41.99	6.00E-06	635.8	111.8	9.09E-05	7.49E-05
		F	535	35.68	6.00E-06	540.3	5.3	9.09E-05	9.00E-05
		G	281	22.00	6.00E-06	333.2	52.2	9.09E-05	7.66E-05
		T 1.5	890	41.24	6.00E-06	624.6	-265.4	9.09E-05	1.29E-04
		T 3	683	37.16	6.00E-06	562.7	-120.3	9.09E-05	1.10E-04
		T6	646	29.45	6.00E-06	446.0	-200.0	9.09E-05	1.32E-04
							129.7	average	9.09E-05
								std dev	2.41E-05
123	12	A	616	64.80	6.00E-06	601.1	-14.9	5.57E-05	5.70E-05
		B	562	71.31	6.00E-06	661.4	99.4	5.57E-05	4.73E-05
		C	566	73.17	6.00E-06	678.7	112.7	5.57E-05	4.64E-05
		D	539	72.35	6.00E-06	671.1	132.1	5.57E-05	4.47E-05
		E	543	67.71	6.00E-06	628.0	85.0	5.57E-05	4.81E-05
		F	572	58.77	6.00E-06	545.1	-26.9	5.57E-05	5.84E-05
		G	320	31.45	6.00E-06	291.7	-28.3	5.57E-05	6.10E-05
		T 1.5	796	71.02	6.00E-06	658.8	-137.2	5.57E-05	6.72E-05
		T 3	686	63.50	6.00E-06	589.0	-97.0	5.57E-05	6.48E-05
		T6	509	49.69	6.00E-06	460.9	-48.1	5.57E-05	6.15E-05
							76.7	average	5.57E-05
								std dev	8.32E-06

Test #	Model Avg. Period (HRS)	Sampler	C2 Net Measured Concentration $\mu\text{g}/\text{m}^3$	C1 bLs Avg. Test Conc. $\mu\text{g}/\text{m}^3$	Q1 bLs ER $\text{g}/\text{s}\cdot\text{m}^2$	bLs Avg. Conc. $\mu\text{g}/\text{m}^3$	Q2 bLs ER $\text{g}/\text{s}\cdot\text{m}^2$	ER to Match Measured Concentration $\text{g}/\text{s}\cdot\text{m}^2$	
131	3	A	1020	81.78	6.00E-06	860.3	-159.7	6.31E-05	7.48E-05
		B	818	87.78	6.00E-06	923.5	105.5	6.31E-05	5.59E-05
		C	802	88.06	6.00E-06	926.4	124.4	6.31E-05	5.46E-05
		D	718	86.96	6.00E-06	914.8	196.8	6.31E-05	4.95E-05
		E	716	80.83	6.00E-06	850.3	134.3	6.31E-05	5.32E-05
		F	859	70.01	6.00E-06	736.5	-122.5	6.31E-05	7.36E-05
		G	475	38.53	6.00E-06	405.3	-69.7	6.31E-05	7.40E-05
		T 1.5	1049	88.28	6.00E-06	928.7	-120.3	6.31E-05	7.13E-05
		T 3	860	79.18	6.00E-06	832.9	-27.1	6.31E-05	6.52E-05
		T6	619	62.89	6.00E-06	661.6	42.6	6.31E-05	5.91E-05
							104.3	average	6.31E-05
								std dev	9.78E-06
132	3	A	430.7	23.3	6.00E-06	418.6	-12.1	1.08E-04	1.11E-04
		B	454	37.5	6.00E-06	673.4	219.4	1.08E-04	7.27E-05
		C	898	43.6	6.00E-06	783.7	-114.3	1.08E-04	1.24E-04
		D	685	45.5	6.00E-06	817.9	132.9	1.08E-04	9.03E-05
		E	540	46.1	6.00E-06	828.1	288.1	1.08E-04	7.03E-05
		F	1061	46.1	6.00E-06	828.4	-232.6	1.08E-04	1.38E-04
		G	872	46.1	6.00E-06	828.4	-43.6	1.08E-04	1.14E-04
		T 1.5	940	45.2	6.00E-06	812.7	-127.3	1.08E-04	1.25E-04
		T 3	790	40.6	6.00E-06	729.6	-60.4	1.08E-04	1.17E-04
		T6	628	32.1	6.00E-06	576.9	-51.1	1.08E-04	1.17E-04
							-1.0	average	1.08E-04
								std dev	2.26E-05

Test #	Model Avg. Period (HRS)	Sampler	C2 Net Measured Concentration $\mu\text{g}/\text{m}^3$	C1 bLs Avg. Test Conc. $\mu\text{g}/\text{m}^3$	Q1 bLs ER $\text{g}/\text{s}\cdot\text{m}^2$	bLs Avg. Conc. $\mu\text{g}/\text{m}^3$	Q2 bLs ER $\text{g}/\text{s}\cdot\text{m}^2$	ER to Match Measured Concentration $\text{g}/\text{s}\cdot\text{m}^2$	
133	3	A	980	27.0	6.00E-06	485.2	-494.8	1.08E-04	2.18E-04
		B	685	43.7	6.00E-06	786.0	101.0	1.08E-04	9.40E-05
		C	1355	51.2	6.00E-06	920.0	-435.0	1.08E-04	1.59E-04
		D	665	53.6	6.00E-06	964.6	299.6	1.08E-04	7.44E-05
		E	593	53.9	6.00E-06	968.4	375.4	1.08E-04	6.61E-05
		F	926	53.9	6.00E-06	968.4	42.4	1.08E-04	1.03E-04
		G	765	53.9	6.00E-06	968.4	203.4	1.08E-04	8.52E-05
		T 1.5	868	53.5	6.00E-06	962.7	94.7	1.08E-04	9.73E-05
		T 3	738	48.0	6.00E-06	863.7	125.7	1.08E-04	9.22E-05
		T6	571	38.2	6.00E-06	686.5	115.5	1.08E-04	8.97E-05
							427.9	average	1.08E-04
								std dev	4.59E-05
134	3	A	729	48.3	6.00E-06	608.5	-120.5	7.55E-05	9.05E-05
		B	910	53.1	6.00E-06	668.0	-242.0	7.55E-05	1.03E-04
		C	583	53.1	6.00E-06	668.8	85.8	7.55E-05	6.58E-05
		D	508	53.1	6.00E-06	668.8	160.8	7.55E-05	5.74E-05
		E	437	53.1	6.00E-06	668.8	231.8	7.55E-05	4.93E-05
		F	791	53.1	6.00E-06	668.7	-122.3	7.55E-05	8.93E-05
		G	323	48.9	6.00E-06	615.1	292.1	7.55E-05	3.97E-05
		T 1.5	842	54.1	6.00E-06	680.3	-161.7	7.55E-05	9.35E-05
		T 3	720	48.5	6.00E-06	610.0	-110.0	7.55E-05	8.91E-05
		T6	496	38.3	6.00E-06	482.1	-13.9	7.55E-05	7.77E-05
							0.0	average	7.55E-05
								std dev	2.13E-05

Test #	Model Avg. Period (HRS)	Sampler	C2 Net Measured Concentration $\mu\text{g}/\text{m}^3$	C1 bLs Avg. Test Conc. $\mu\text{g}/\text{m}^3$	Q1 bLs ER $\text{g}/\text{s}\cdot\text{m}^2$	bLs Avg. Conc. $\mu\text{g}/\text{m}^3$	Q2 bLs ER $\text{g}/\text{s}\cdot\text{m}^2$	ER to Match Measured Concentration $\text{g}/\text{s}\cdot\text{m}^2$	
135	12	A	408	43.2	6.00E-06	336.2	-71.8	4.67E-05	5.67E-05
		B	410	58.4	6.00E-06	454.6	44.6	4.67E-05	4.22E-05
		C	478	65.8	6.00E-06	512.8	34.8	4.67E-05	4.36E-05
		D	456	70.4	6.00E-06	548.6	92.6	4.67E-05	3.89E-05
		E	436	73.5	6.00E-06	572.8	136.8	4.67E-05	3.56E-05
		F	724	74.6	6.00E-06	581.4	-142.6	4.67E-05	5.82E-05
		G	432	63.6	6.00E-06	495.4	63.4	4.67E-05	4.08E-05
		T 1.5	612	66.5	6.00E-06	518.2	-93.8	4.67E-05	5.52E-05
		T 3	518	59.6	6.00E-06	464.4	-53.6	4.67E-05	5.21E-05
		T6	344	46.7	6.00E-06	363.6	19.6	4.67E-05	4.42E-05
							29.9	average	4.67E-05
								std dev	8.11E-06
141	3	A	416	31.3	6.00E-06	243.8	-172.2	4.67E-05	6.52E-05
		B	367	56.3	6.00E-06	438.1	71.1	4.67E-05	3.07E-05
		C	756	69.5	6.00E-06	540.9	-215.1	4.67E-05	3.78E-05
		D	396	77.3	6.00E-06	601.5	205.5	4.67E-05	3.07E-05
		E	509	80.8	6.00E-06	628.2	119.2	4.67E-05	3.78E-05
		F	660	83.1	6.00E-06	646.2	-13.8	4.67E-05	4.77E-05
		G	985	84.9	6.00E-06	660.5	-324.5	4.67E-05	6.96E-05
		T 1.5	592	69.3	6.00E-06	538.9	-53.1	4.67E-05	5.13E-05
		T 3	513	62.2	6.00E-06	483.7	-29.3	4.67E-05	4.95E-05
		T6	378	48.9	6.00E-06	380.4	2.4	4.67E-05	4.64E-05
							-409.7	average	4.67E-05
								std dev	1.32E-05

Test #	Model Avg. Period (HRS)	Sampler	C2 Net Measured Concentration $\mu\text{g}/\text{m}^3$	C1 bLs Avg. Test Conc. $\mu\text{g}/\text{m}^3$	Q1 bLs ER $\text{g}/\text{s}\cdot\text{m}^2$	bLs Avg. Conc. $\mu\text{g}/\text{m}^3$	Q2 bLs ER $\text{g}/\text{s}\cdot\text{m}^2$	ER to Match Measured Concentration $\text{g}/\text{s}\cdot\text{m}^2$	
142	3	A	206	29.5	6.00E-06	173.8	-32.2	3.53E-05	4.18E-05
		B	467	46.1	6.00E-06	271.1	-195.9	3.53E-05	6.08E-05
		C	447	53.4	6.00E-06	313.9	-133.1	3.53E-05	5.03E-05
		D	165	57.1	6.00E-06	336.2	171.2	3.53E-05	1.73E-05
		E	140	59.5	6.00E-06	350.3	210.3	3.53E-05	1.41E-05
		F	202	61.1	6.00E-06	359.7	157.7	3.53E-05	1.98E-05
		G	120	61.0	6.00E-06	359.1	239.1	3.53E-05	1.18E-05
		T 1.5	363	39.2	6.00E-06	230.9	-132.1	3.53E-05	5.55E-05
		T 3		35.7					
		T6	219	28.4	6.00E-06	167.2	-51.8	3.53E-05	4.62E-05
							233.2	average	3.53E-05
								std dev	1.94E-05
143	3	A	412	63.8	6.00E-06	603.9	191.9	5.68E-05	3.87E-05
		B	381	68.5	6.00E-06	648.0	267.0	5.68E-05	3.34E-05
		C	287	69.2	6.00E-06	654.7	367.7	5.68E-05	2.49E-05
		D	768	69.2	6.00E-06	654.9	-113.1	5.68E-05	6.66E-05
		E	126	68.8	6.00E-06	650.9	524.9	5.68E-05	1.10E-05
		F	706	66.5	6.00E-06	628.7	-77.3	5.68E-05	6.37E-05
		G	676	42.2	6.00E-06	399.1	-276.9	5.68E-05	9.61E-05
		T 1.5	821	64.4	6.00E-06	609.5	-211.5	5.68E-05	7.65E-05
		T 3	727	58.1	6.00E-06	550.0	-177.0	5.68E-05	7.50E-05
		T6	628	46.1	6.00E-06	436.3	-191.7	5.68E-05	8.17E-05
							303.9	average	5.68E-05
								std dev	2.79E-05

Test #	Model Avg. Period (HRS)	Sampler	C2 Net Measured Concentration $\mu\text{g}/\text{m}^3$	C1 bLs Avg. Test Conc. $\mu\text{g}/\text{m}^3$	Q1 bLs ER $\text{g}/\text{s}\cdot\text{m}^2$	bLs Avg. Conc. $\mu\text{g}/\text{m}^3$	Q2 bLs ER $\text{g}/\text{s}\cdot\text{m}^2$	ER to Match Measured Concentration $\text{g}/\text{s}\cdot\text{m}^2$	
144	3	A	622	58.8	6.00E-06	805.3	183.3	8.22E-05	6.35E-05
		B	695	58.2	6.00E-06	796.5	101.5	8.22E-05	7.17E-05
		C	863	56.4	6.00E-06	772.7	-90.3	8.22E-05	9.18E-05
		D	536	53.9	6.00E-06	737.7	201.7	8.22E-05	5.97E-05
		E	519	49.4	6.00E-06	676.0	157.0	8.22E-05	6.31E-05
		F	468	40.7	6.00E-06	557.5	89.5	8.22E-05	6.90E-05
		G	177	8.3	6.00E-06	113.3	-63.7	8.22E-05	1.28E-04
		T 1.5	835	51.5	6.00E-06	705.1	-129.9	8.22E-05	9.73E-05
		T 3	684	45.8	6.00E-06	627.7	-56.3	8.22E-05	8.95E-05
		T6	521	35.6	6.00E-06	487.5	-33.5	8.22E-05	8.78E-05
							359.4	average	8.22E-05
								std dev	2.12E-05
145	12	A	587	103.7	6.00E-06	542.3	-44.7	3.14E-05	3.40E-05
		B	622	120.9	6.00E-06	632.2	10.2	3.14E-05	3.09E-05
		C	705	128.2	6.00E-06	670.4	-34.6	3.14E-05	3.30E-05
		D	625	129.5	6.00E-06	677.1	52.1	3.14E-05	2.90E-05
		E	544	125.3	6.00E-06	655.6	111.6	3.14E-05	2.60E-05
		F	553	111.4	6.00E-06	582.8	29.8	3.14E-05	2.98E-05
		G	199	64.9	6.00E-06	339.7	140.7	3.14E-05	1.84E-05
		T 1.5	821	127.3	6.00E-06	665.8	-155.2	3.14E-05	3.87E-05
		T 3	718	113.8	6.00E-06	595.4	-122.6	3.14E-05	3.78E-05
		T6	538	89.0	6.00E-06	465.6	-72.4	3.14E-05	3.63E-05
							-85.1	average	3.14E-05
								std dev	6.10E-06

Test #	Model Avg. Period (HRS)	Sampler	C2 Net Measured Concentration $\mu\text{g}/\text{m}^3$	C1 bLs Avg. Test Conc. $\mu\text{g}/\text{m}^3$	Q1 bLs ER $\text{g}/\text{s}\cdot\text{m}^2$	bLs Avg. Conc. $\mu\text{g}/\text{m}^3$	Q2 bLs ER $\text{g}/\text{s}\cdot\text{m}^2$	ER to Match Measured Concentration $\text{g}/\text{s}\cdot\text{m}^2$	
151	3	A	947	29.1	6.00E-06	315.2	-631.8	6.51E-05	1.96E-04
		B	380	55.0	6.00E-06	596.6	216.6	6.51E-05	4.14E-05
		C	750	68.7	6.00E-06	744.6	-5.4	6.51E-05	6.55E-05
		D	447	78.3	6.00E-06	849.1	402.1	6.51E-05	3.43E-05
		E	1055	86.1	6.00E-06	933.6	-121.4	6.51E-05	7.35E-05
		F	688	90.8	6.00E-06	985.2	297.2	6.51E-05	4.54E-05
		G	984	91.9	6.00E-06	996.3	12.3	6.51E-05	6.43E-05
		T 1.5	569	73.1	6.00E-06	792.5	223.5	6.51E-05	4.67E-05
		T 3	447	64.7	6.00E-06	702.2	255.2	6.51E-05	4.14E-05
		T6	351	49.5	6.00E-06	536.7	185.7	6.51E-05	4.26E-05
							833.9	average	6.51E-05
								std dev	4.76E-05
152	3	A	842	38.4	6.00E-06	463.1	-378.9	7.24E-05	1.32E-04
		B	398	50.9	6.00E-06	613.7	215.7	7.24E-05	4.69E-05
		C	581	55.9	6.00E-06	674.6	93.6	7.24E-05	6.23E-05
		D	423	58.6	6.00E-06	706.8	283.8	7.24E-05	4.33E-05
		E	374	60.1	6.00E-06	724.5	350.5	7.24E-05	3.74E-05
		F	864	60.8	6.00E-06	733.5	-130.5	7.24E-05	8.52E-05
		G	921	54.9	6.00E-06	661.9	-259.1	7.24E-05	1.01E-04
		T 1.5	656	51.4	6.00E-06	619.5	-36.5	7.24E-05	7.66E-05
		T 3	531	45.8	6.00E-06	552.8	21.8	7.24E-05	6.95E-05
		T6	423	36.2	6.00E-06	436.7	13.7	7.24E-05	7.01E-05
							174.2	average	7.24E-05
								std dev	2.85E-05

Test #	Model Avg. Period (HRS)	Sampler	C2 Net Measured Concentration $\mu\text{g}/\text{m}^3$	C1 bLs Avg. Test Conc. $\mu\text{g}/\text{m}^3$	Q1 bLs ER $\text{g}/\text{s}\cdot\text{m}^2$	bLs Avg. Conc. $\mu\text{g}/\text{m}^3$	Q2 bLs ER $\text{g}/\text{s}\cdot\text{m}^2$	ER to Match Measured Concentration $\text{g}/\text{s}\cdot\text{m}^2$	
153	3	A	813	40.1	6.00E-06	756.3	-56.7	1.13E-04	1.22E-04
		B	655	40.6	6.00E-06	766.0	111.0	1.13E-04	9.68E-05
		C	630	40.6	6.00E-06	766.5	136.5	1.13E-04	9.31E-05
		D	656	40.5	6.00E-06	765.3	109.3	1.13E-04	9.71E-05
		E	630	40.1	6.00E-06	756.0	126.0	1.13E-04	9.44E-05
		F	702	37.3	6.00E-06	704.6	2.6	1.13E-04	1.13E-04
		G	288	15.2	6.00E-06	287.5	-0.5	1.13E-04	1.13E-04
		T 1.5	923	38.1	6.00E-06	718.4	-204.6	1.13E-04	1.46E-04
		T 3	774	34.1	6.00E-06	643.0	-131.0	1.13E-04	1.36E-04
		T6	542	26.8	6.00E-06	506.0	-36.0	1.13E-04	1.21E-04
							56.8	average	1.13E-04
								std dev	1.83E-05
154	3	A	498	58.0	6.00E-06	827.9	329.9	8.56E-05	5.15E-05
		B	623	58.0	6.00E-06	828.1	205.1	8.56E-05	6.44E-05
		C	769	58.0	6.00E-06	828.1	59.1	8.56E-05	7.95E-05
		D	493	58.0	6.00E-06	828.1	335.1	8.56E-05	5.10E-05
		E	414	58.0	6.00E-06	828.1	414.1	8.56E-05	4.28E-05
		F	546	56.9	6.00E-06	811.7	265.7	8.56E-05	5.76E-05
		G	1130	21.2	6.00E-06	301.9	-828.1	8.56E-05	3.21E-04
		T 1.5	690	59.0	6.00E-06	842.6	152.6	8.56E-05	7.01E-05
		T 3	556	52.9	6.00E-06	754.8	198.8	8.56E-05	6.31E-05
		T6	389	41.8	6.00E-06	597.1	208.1	8.56E-05	5.58E-05
							1340.3	average	8.56E-05
								std dev	8.32E-05

Test #	Model Avg. Period (HRS)	Sampler	C2 Net Measured Concentration $\mu\text{g}/\text{m}^3$	C1 bLs Avg. Test Conc. $\mu\text{g}/\text{m}^3$	Q1 bLs ER $\text{g}/\text{s}\cdot\text{m}^2$	bLs Avg. Conc. $\mu\text{g}/\text{m}^3$	Q2 bLs ER $\text{g}/\text{s}\cdot\text{m}^2$	ER to Match Measured Concentration $\text{g}/\text{s}\cdot\text{m}^2$	
155	12	A	576	202.2	6.00E-06	628.1	52.1	1.86E-05	1.71E-05
		B	660	228.7	6.00E-06	710.2	50.2	1.86E-05	1.73E-05
		C	689	233.5	6.00E-06	725.3	36.3	1.86E-05	1.77E-05
		D	578	233.4	6.00E-06	724.8	146.8	1.86E-05	1.49E-05
		E	565	226.0	6.00E-06	701.9	136.9	1.86E-05	1.50E-05
		F	751	214.2	6.00E-06	665.2	-85.8	1.86E-05	2.10E-05
		G	597	148.3	6.00E-06	460.7	-136.3	1.86E-05	2.41E-05
		T 1.5	825	251.7	6.00E-06	781.9	-43.1	1.86E-05	1.97E-05
		T 3	726	220.6	6.00E-06	685.1	-40.9	1.86E-05	1.97E-05
		T6	543	164.7	6.00E-06	511.4	-31.6	1.86E-05	1.98E-05
							84.7	average	1.86E-05
								std dev	2.83E-06

VITA

Jacqueline Elaine Price

Education

Master of Science. August 2004. Department of Biological & Agricultural Engineering.
Texas A&M University

Emphasis: Agricultural Air Quality Engineering & Science

Bachelor of Science. May 2002. Department of Industrial Engineering.
Texas A&M University

Professional License

Engineer-In-Training (EIT) No. 34397 – State of Texas

Honors

Texas A&M Academic Excellence Award; Tau Beta Pi (National Engineering); Alpha Epsilon (Agricultural Engineering); Gamma Sigma Delta (Agricultural); Alpha Pi Mu (Industrial Engineering)

Correspondence can be sent to:

Department of Biological and Agricultural Engineering, Texas A&M University
College Station, TX 77843-2117

Papers and Presentations

Price, J.E., R.E. Lacey, B.W. Shaw, and C.E. Parnell, Jr. Preliminary Ammonia Emission Rates from Cattle Feedlots. Accepted. *2004 Annual International Meeting of the American Society of Agricultural Engineers*. Ottawa, ON, Canada. August 2004.

Price, J.E., R.E. Lacey, B.W. Shaw, and C.B. Parnell, Jr. 2004. Uncertainty Associated With Particulate Matter Concentration Measurements From Agricultural Operations. *Proceedings of the 2004 Beltwide Cotton Conference*. San Antonio, TX

Hynes, J., J.R. Lindner, K.E. Dooley, and J.E. Price. 2003. Patterns of engagement and performance for female and male students in an online course. *Proceedings of the 30th Annual National Agricultural Education Research Conference*. Orlando, Florida.

Price, J.E. and R.E. Lacey. 2003. Uncertainty Associated with the Gravimetric Sampling of Particulate Matter. *Proceedings of the 2003 Annual International Meeting of the American Society of Agricultural Engineers*. Las Vegas, Nevada, Paper No. 034116.

Lacey, R.E., J.E. Price, and J.M. Peschel. 2003. A Mini-Robot Sumo Competition to Teach Mechatronics to Engineering Undergraduates. *Proceedings of the 2003 Annual International Meeting of the American Society of Agricultural Engineers*. Las Vegas, Nevada, Paper No. 033131.